



Pro gradu -tutkielma
Teoreettinen fysiikka

Particle physics models with four generations

Hanna Grönqvist
2012

Ohjaaja: Prof. Katri Huitu
Tarkastajat: Prof. Katri Huitu
Prof. Paul Hoyer

HELSINGIN YLIOPISTO
FYSIKAN LAITOS

PL 64 (Gustaf Hällströmin katu 2)
00014 Helsingin yliopisto

Contents

I	Preliminaries	5
1	Motivation	7
1.1	Historical overview – the ‘discovery’ of the standard model	7
1.2	Problems of the standard model solved by a fourth generation	10
1.2.1	Naturalness	12
1.2.2	Flavor democracy – a solution to the naturalness problem	14
1.2.3	Electroweak Precision Data	15
1.3	Unitarity constraints on the fourth generation	17
2	The Standard Model	21
2.1	Quantum chromodynamics	21
2.1.1	Gauge fixing and Faddeev–Popov ghosts	22
2.1.2	Renormalization and asymptotic freedom	24
2.2	Local $SU(2)$ and $U(1)$ symmetries	25
2.2.1	Isospin symmetry	25
2.2.2	Quantum electrodynamics	26
2.3	Spontaneous symmetry breaking	26
2.3.1	The Higgs mechanism	27
2.4	The Glashow–Weinberg–Salam model	29
2.5	Quark and lepton mixing	31
2.5.1	The quark sector	31
2.5.2	Beyond the SM: mixing in the lepton sector	33
II	The minimal four–generation model	39
3	Phenomenology of the fourth family	41
3.1	Mixing of the fourth family with the first three ones	41
3.1.1	Sources for constraints	41
3.1.2	Possible parameter space	43
3.2	Higgs production and partial decay widths	47
3.2.1	Higgs production at hadron colliders	47
3.2.2	Branching fractions	51
3.2.3	Searches for the Higgs <i>and</i> the fourth family	53

4	Experimental searches	57
4.1	Search strategies – SM4 quarks	57
4.1.1	General event topologies	57
4.1.2	Pair production of fourth family quarks	58
4.1.3	Single production of fourth family quarks	59
4.1.4	Current experimental bounds	64
4.2	Searches for fourth generation leptons	66
4.2.1	Neutrinos and Higgs at the LHC	67
4.2.2	Searches at future lepton colliders	68
4.2.3	Existing experimental constraints	70
4.3	Higgs searches	71
4.3.1	Higgs searches at Tevatron	71
4.3.2	Higgs searches at the LHC	72
5	Experimental exclusion of the minimal SM4	75
III	The two Higgs doublet model	79
6	Theory of the 2HDM	81
6.1	Why add another doublet?	81
6.2	The scalar potential and the field content	82
6.3	Flavor conservation	83
6.4	Yukawa couplings of the type II 2HDM	84
7	4F2HDM phenomenology	85
7.1	Higgs production and decay in the 2HDM–II	85
7.1.1	Production and decay of the neutral pseudoscalar A^0	86
7.1.2	Production and decay of the light neutral Higgs h^0	88
7.1.3	The charged Higgs	89
7.2	Searches for the 4F2HDM at the LHC	91
7.2.1	Fourth generation quarks masses	91
8	Conclusions	95
	Appendices	97
A	Definitions of electroweak observables	99
B	The Goldstone model	101
C	Mathematical description of neutrino oscillations	105
D	Oblique electroweak parameters	107
E	Feynman diagrams for production of fourth family particles	113
F	Form factors for A^0, h^0 branching ratios	117
	Bibliography	119

Part I

Perliminaries

Chapter 1

Motivation

In this chapter we will shortly review the historical development of the Standard Model of elementary particle physics. The aim of the historical overview is to give an idea as to how the current theory was born, from theoretical predictions and experimental verification with many unexpected discoveries leading to reformulations and expansions of the theory. With this section we wish to show the reader that there have been unexpected events along the way: that there might still be many surprises in store for us and that it might be premature to think that our current view of particle physics is complete.

In the second part of this chapter we list some shortcomings of the current model, called the ‘standard model’, and give some arguments in favor of adding a fourth family of particles. Ideas presented in this section will be considered in some detail later on in the text.

1.1 Historical overview – the ‘discovery’ of the standard model

The observable matter of the universe consists of atoms that are made up of protons, neutrons and electrons. All of these particles were discovered in the 1930’s, and at the time they were deemed to be elementary constituents, just as had been thought of atoms before that. Before this the photon had also been found, the photon being the quantum of the electromagnetic field that ‘binds’ the electron to the atomic nucleus. The force binding the protons and neutrons of the nucleus was thought to be mediated by a particle called the ‘pi-meson’, as suggested by Yukawa [1]. When Pauli predicted the existence of one more particle, the electron neutrino, as a solution to a problem (missing energy in beta decays) [2], it appeared that a complete picture of particle physics had been established.

The situation changed when the muon was discovered some years later, in 1937 [3, 4]. The muon seemed identical to the electron, but with 200 times its mass. It was also very puzzling that this new particle seemed to be produced by strong interactions but its interactions with matter were electromagnetic. A famous physicist, Rabi, then made a comment conveying the amazement at this surprise, cited many times since: ‘Who ordered that?’ [5].

Ten years later the charged pion, predicted by Yukawa, was found [6, 7, 8]. At the same time another meson was discovered, too [9]. Later it became clear that this was similar to Yukawa’s particle, but neutral, and so it became known as the ‘neutral pion’ [10]. These new pieces fit into a beautifully simple theory where electromagnetic interactions are mediated by photons, strong interactions by π -mesons and weak interactions are described by the Fermi four-fermion interaction; all nuclei are bound states of protons and neutrons, atoms bound states of nuclei and electrons and

the matter fields classified as leptons (electron and its neutrino), mesons (the pions) and baryons (consisting of protons and neutrons).

The beginning of a new decade, the 50's, opened a new 'era' of elementary particle physics [5, 11]: In 1951, cloud chamber observations showed a new neutral particle (Λ), which decayed into a proton and a negative pion; in 1952-1953 the negatively charged Ξ and the charged Σ -particles were detected in cosmic rays at high altitudes. All of these (later called hyperons) were heavier than the known nucleons and exhibited an unusual feature: they were produced relatively often in nuclear collisions, but then they decayed with long life-times of $\mathcal{O}(10^{-10}) - \mathcal{O}(10^{-8})$ s, suggesting that they were produced in strong interactions but decayed through weak ones. These particles, called 'strange' and always produced in pairs led to the discovery of the strange quark [12, 13, 9]. A theoretical explanation was given both by Nakano and Nishijima [14] in Japan, and independently Gell-Mann [15] in the USA. As a part of this explanation they introduced a new quantum number called 'strangeness', related to other, already established, quantum numbers.

In the following years there was a great accumulation of data on baryon and meson resonances as a consequence of the completion and running of several particle accelerators. By the mid-1960's it was realized that the contemporary theory did not suffice as an explanation for the many new particles that were being discovered. The idea of quarks as the constituents of mesons and baryons was put forward by Gell-Mann [16] and Zweig [17] in 1964. Further the notion of 'color charge' was introduced in 1964 by Greenberg [18] and in 1965 by Nambu and Han [19]. Since leptons were observed to have a specific pattern, emanating from the discovery of the muon and muon neutrino [20], a fourth quark was predicted in 1964 by Bjorken and Glashow [21], an idea that was further worked on by Glashow, Iliopoulos and Maiani [22] in 1970. It was recognized that the fourth quark allowed for a theory with flavor conserving neutral currents, but not flavor changing ones (called the 'GIM' mechanism), as explained by two generations related through Cabibbo mixing [23]. This model was consistent with observations and the fourth quark, called 'charm', was found in 1974 [24, 25, 26, 27]. By this time a renormalizable gauge theory had been developed [28, 29, 30, 31], based on the two 'generations' of particles observed thus far, the first generation being the u and d quarks, the electron and its neutrino and the second generation consisting of the c and s quarks, the muon and its neutrino.

A quantum field theory of strong interactions was formulated in 1973, first suggested by Fritzsch, Gell-Mann and Leutwyler [32]. Quarks were deemed to be real particles (as opposed to mere mathematical tool) carrying a charge of their own – the 'color' charge. In this theory of color interactions, called quantum chromodynamics (QCD), the massless quanta of the color field were named gluons. A very peculiar feature of the theory was discovered not long afterwards – a property later called 'asymptotic freedom', needed to describe observed properties of the proton [33, 34, 35, 36, 37].

As had been the case for the theory based on just one family of particles, the theory based on two families suddenly experienced severe problems with the experimental discovery of the tau lepton in 1975 [38]. Two years later, in 1977, a fifth quark, named 'bottom', was discovered [39, 40]. The search for a sixth quark went on for 18 years and it was only when the Fermilab accelerator Tevatron reached sufficiently high energies that the unexpectedly heavy top quark was found in 1995 [41, 42], with a mass much larger than that of the bottom quark.

The last particle of the third generation, the tau neutrino was finally found in 2000 [43].

This brief review of the 'discovery' of particle physics is meant to show the reader that there has been an abundance of surprises in the history of particle physics. Especially, the discovery of particles belonging to a new generation has already on two occasions, in the case of the second and the third families, come as a surprise. When the history of new and unexpected discoveries is taken

into account, it might well be that, even though the situation has been ‘stable’ for many years, we still do not know the whole story.

That there are only three families of particles is an idea that has been generally accepted for some time. The origin of this idea lies in the precision tests made at LEP, showing with high statistical significance that the number of light neutrinos is three. This ‘has led to the prevalent, if rather optimistic, belief that ... the number of sequential lepton and quark families has also been determined to be 3’ [44]. But then again ‘this belief hinges on the notion that a heavy sequential Dirac neutrino ($m_\nu \gg m_Z/2$) belonging to a possible fourth generation would necessarily imply an unnaturally large hierarchy among the Yukawa couplings of different neutrinos with the Higgs boson’ [44]. In sections to come, we will see that the masses of elementary particles are described through the particles’ Yukawa interactions with a field called the Higgs field. ‘Unnaturally large hierarchy’ among the couplings here refers to the fact that the known particles have very different masses. ‘Though the naturalness argument is intuitively rather appealing, it is basically a philosophical outlook and hence is not beyond debate’ [44].

A further similar, more specific argument for the three families of particles is that one would not expect a neutrino to be so heavy as to not be seen in the LEP measurements of the Z boson. This argument has been countered by a wise comment: “the necessarily heavy neutrino mass, $m_{\nu_4} > m_Z/2$, would be surprising, but without a theory of neutrino masses we are not really in a position to judge” [45].

1.2 Problems of the standard model solved by a fourth generation

Although the standard model [46, 28, 31] with three generations (to be denoted ‘SM3’) has been immensely successful in describing the strong and electroweak interactions of elementary particles there are still some issues that it does not cover in a satisfactory way. Many physicists today believe that the SM3 is not the ‘ultimate’ theory, but rather an effective theory which is applicable at low energies only. In this sense the SM is thought to be just the *low energy limit* of a more fundamental, underlying theory. A variety of ‘beyond the standard model’ (BSM) theories have been proposed to take the role of this underlying, more extensive theory. Such BSM models are *e.g.* theories including supersymmetry or extra dimensions or even string theory and grand unified theories. A possible way to extend the standard model, so that it might better explain observed phenomena is to add a sequential fourth chiral family to the three already known families of elementary particles. This is a very simple and perhaps a very ‘natural’ way to extend the SM, and it is the topic of this thesis. This model will henceforth be referred to as ‘SM4’.

The motivation for the development of the various BSM models is the fact that some of the theoretical aspects of the SM are not well understood, seem to be lacking a fundamental explanation or are not yet experimentally verified. Another problem is that there are some experimentally observed phenomena that exhibit some tension with the SM predictions. Amongst these open issues are for example :

1. Origin of mass
2. Quark-lepton symmetry
3. Family replication and number of families
4. Masses and mixing pattern of fermions
5. Violation of parity
6. Baryon asymmetry of the universe
7. Large number of arbitrary parameters

The origin of mass is a question of fundamental importance to particle physics. As we will later see (in Section 2.3), the masses of all particles are thought to arise from their interactions with a scalar field. These interactions are called ‘Yukawa interactions’ and the scalar field is called the ‘Higgs field’. The SM predicts some of the properties of the Higgs particle, the quantum of the Higgs field, but it does not predict its mass. Short-lived particles that live such a short time that they cannot be directly seen, are instead indirectly observed in detectors through their decay products. A motivation for SM4 is that the presence of a massive fourth generation would affect the Higgs boson cross sections and decay channels.

At the moment there is some tension between the SM fit to and the lower bound on the Higgs boson mass as measured by LEP II. It is not known whether the two anomalies giving rise to this tension arise from unknown physics or if they are just due to systematic errors. If these anomalies are removed, the SM fit improves, but then the predicted Higgs mass falls into a region already excluded by LEP giving a contradiction. When the anomalies are present, then the SM fit is bad and this situation is not satisfactory either. Interestingly, if a fourth family is added, then the fit

gets better, giving a reason to study such a model. [47] We come later (in Chapter 5) to the issue of an observed 125 GeV boson at the LHC.

A further thing about the fourth family and the origin of mass is that, in addition to the effect the fourth generation particles have on the Higgs field, they could also be the initiators of electroweak symmetry breaking themselves. This would be possible if the Yukawa couplings of the fourth generation particles were found to be very big because then they could dynamically break the electroweak symmetry [48].

The idea that there are three SM families has been widely accepted for a long time. This belief is based on SLAC [49, 50] and LEP [51, 52, 53, 54] data of the width of the Z boson peak. As noted in Ref. [54]: “In the standard electroweak model the Z boson is expected to decay with comparable probability into all species of fermions that are kinematically allowed. The decay rate of the Z into light, neutral, penetrating particles such as neutrinos, that would otherwise escape detection, can be measured through an increase in the total width Γ_Z ”. The visible width from experimentally measured decay channels can be subtracted to give the ‘invisible’ width, that of the neutrino channels. The results of the measurements at electron–positron colliders is that there are only three light ($m_\nu \ll m_Z/2$) neutrinos [55]:

$$\text{Number of light neutrino types : } 2.9840 \pm 0.0082 \text{ at 95\% C.L.} \quad (1.1)$$

with ‘C.L.’ standing for confidence level (or limit).

The generally accepted conclusion drawn from these results was that there could thus only exist three generations of particles in the SM. Yet, as already mentioned in the previous section, this conclusion relies upon the thought that a heavy fourth neutrino would not be ‘natural’, and that its presence (along with the other, probably heavy, particles of the fourth generation) would lead to ‘unnaturally’ large differences in the masses of all the elementary particles. But in fact an unnatural hierarchy is not inevitable for the existence of a heavy fourth neutrino: actually the most natural scenario can be implemented in a four family model [44]. This is the case if there are three (nearly) massless neutrinos and a heavy neutrino, as given by the democratic mass matrix in the hypothesis of *flavor democracy* (see Section 1.2.2). This hypothesis is in agreement with a very simple conclusion of the Z width (1.1): that there are *at least three generations*.

As it is, the SM does not give a theoretical prediction for the number of families. Each SM family is independently anomaly-free and therefore the number of families is completely unrestricted in the sense of theoretical consistency of the model. The only restriction coming from the SM is an upper limit given by the asymptotic freedom of Quantum Chromodynamics (QCD) [35], which requires the number of generations to be less than or equal to eight. There are also some other hints of an upper limit, namely some considerations that seem to disfavor a fifth sequential family. If one assumes flavor democracy, then a fifth family would lead to four massless or nearly massless neutrinos and one heavy one but this contradicts (1.1), and is therefore improbable. One would also expect $m_t \ll m_{t'} \ll m_{t''}$, where m_t is the top quark mass ($m_t \sim 175$ GeV) and t' and t'' refer to the top type quarks of the fourth and fifth generation respectively. In this scenario $m_{t'}$ is already close to the unitarity limit, and therefore the theory is no longer trustworthy for energies as high as $m_{t''}$. [56]

Finally, we note that a fourth family could give an explanation to one of the open questions in cosmology, concerning the ratio of matter to antimatter in the observable universe. A fourth family could contribute with a factor up to $\mathcal{O}(10^{10})$ [57] or possibly from $\mathcal{O}(10^{13})$ to $\mathcal{O}(10^{15})$ [58] to the baryon asymmetry of the universe, thus giving the observed amount of baryons to antibaryons in the universe, a ratio that that SM3 predicts to be much too small.

1.2.1 Naturalness

As far as has been experimentally found to date, there exists three families or generations of particles. In the standard model, to be reviewed in the next chapter, the elementary particles are grouped into *doublets* of the $SU(2)$ gauge group.

$$i^{\text{th}} \text{ generation : quarks } \begin{pmatrix} u_i \\ d_i \end{pmatrix} \quad \text{and} \quad \text{leptons } \begin{pmatrix} \ell_i \\ \nu_i \end{pmatrix} , \quad (1.2)$$

with

$$u_i = \{u, c, t\} , \quad d_i = \{d, s, b\} , \quad \ell_i = \{e, \mu, \tau\} , \quad \nu_i = \{\nu_e, \nu_\mu, \nu_\tau\} , \quad (1.3)$$

for $i = 1, 2, 3$. The quarks of a family form one doublet and the leptons another.

The masses of all particles are created in the same way – through the Higgs mechanism. One might think that this would imply that all masses are of the same order of magnitude, but this turns out not to be the case. From experiments we know that [59]

$$\begin{pmatrix} m_u \approx 2.3 \text{ MeV} \\ m_d \approx 4.8 \text{ MeV} \end{pmatrix} , \quad \begin{pmatrix} m_c \approx 1.3 \text{ GeV} \\ m_s \approx 95 \text{ MeV} \end{pmatrix} , \quad \begin{pmatrix} m_t \approx 173 \text{ GeV} \\ m_b \approx 4 \text{ GeV} \end{pmatrix} , \quad (1.4)$$

$$\begin{pmatrix} m_e \approx 2.3 \text{ MeV} \\ m_{\nu_e} < 225 \text{ eV} \end{pmatrix} , \quad \begin{pmatrix} m_\mu \approx 1,275 \text{ GeV} \\ m_{\nu_\mu} < 0.19 \text{ MeV} \end{pmatrix} , \quad \begin{pmatrix} m_\tau \approx 173 \text{ GeV} \\ m_{\nu_\tau} < 18.2 \text{ MeV} \end{pmatrix} . \quad (1.5)$$

Eqs. (1.4), (1.5) show that the masses of each generation increase, the first generation being the lightest one, the third the heaviest one. The mass gap between sequential generations is often called the *flavor problem*.

The large mass differences are surprising, since one might think that since the masses are generated at the electroweak breaking scale ($v \approx 246 \text{ GeV}$) that they would all be proportional to this scale. This would be plausible since the masses m_f of particles are given by their Yukawa couplings [1] λ_f , related to the electroweak breaking scale by

$$m_f = \lambda_f \frac{v}{\sqrt{2}} . \quad (1.6)$$

This shows that the only ‘natural’ mass scale would be the one given by the top quark, since $\lambda_t \sim \mathcal{O}(1)$. But from this point of view the masses of the other particles would seem ‘unnatural’. This is what is often called the *naturalness problem*. The standard model does not provide a satisfactory motivation for the differences in the Yukawa couplings.

Dynamical symmetry breaking

A sequential fourth generation might prove to be a solution to this problem [48]. Non-perturbative *dynamics* of the system may cause a breaking of symmetry, leading to large differences in scales. The fourth generation is an option for quarks with masses close to the unitarity breaking scale $m_{q_4} \sim 550 \text{ GeV}$ (with Yukawa couplings $\lambda_{q_4} \sim 2.5$). In this scenario a heavy quark *condensate* $\langle \bar{q}_4 q_4 \rangle$ could be responsible for the dynamical symmetry breaking.

Dynamical symmetry breaking is exhibited *e.g.* in the Nambu–Jona–Lasinio (NJL) model [60, 61]. In this model the dynamics of heavy fourth generation quarks is described by a four-fermion interaction

$$\frac{g^2}{\Lambda^2} (\bar{q}_L q_R) (\bar{q}_R q_L) , \quad (1.7)$$


where g is the coupling and Λ the cut-off scale at which new physics enters the game. When g is above some critical value g_c the condensation occurs. The subscripts R, L are used to denote right-handed and left-handed fields, respectively.

Fine-tuning

What is the cut-off scale Λ , the energy scale signaling the domain of new physics?

A modern point of view is that theories, such as the standard model, are but effective theories of some more fundamental, underlying ones. The effective theories describe the low-energy regime, say energies below a threshold M , whereas the fundamental theory is seen for $E > M$. The threshold M is physical in the sense that the whole physical spectrum is contained in $E < M$. [62]

In order to study the concept of naturalness, let us consider a scalar theory with quartic vertices, that is, a theory with an interaction Lagrangian of the type $\mathcal{L}_{\text{int}} \sim \lambda \phi^4$, as in Ref. [62]. Upon renormalization, the mass of such a field acquires a counterterm as shown in Fig. 1.1 at one-loop order.



$$\delta m^2 = \lambda \int^\Lambda \frac{d^4 k}{(2\pi)^4} \frac{1}{k^2} \sim \frac{\lambda}{16\pi^3} \int^\Lambda dk^2 \sim \frac{\lambda}{16\pi^3} \cdot \Lambda^2$$

Figure 1.1: Mass renormalization of a scalar field with quartic interactions.

The renormalized (‘dressed’) mass m of the scalar is then

$$m^2 = m_0^2 + \alpha \lambda \frac{\Lambda^2}{16\pi^2} , \quad (1.8)$$

where m_0 is the bare mass, α is a (positive or negative) constant of order one. We note that the mass has a quadratic dependence on the cut-off scale Λ . If we consider Λ to be a fundamental mass unit, then

$$\frac{m_0^2}{\Lambda^2} = \frac{m^2}{\Lambda^2} - \alpha \frac{\lambda}{16\pi^2} . \quad (1.9)$$

Plugging in some typical values into this expression (1.9), *e.g.* $m = 100$ GeV and $\Lambda = M_P \sim 10^{19}$ GeV shows that, in order to get the divergence canceled out, the ratio m_0^2/Λ^2 has to be adjusted to more than 30 orders of magnitude. This amounts to extreme ‘fine-tuning’ of the theory – a feature that is not desirable in a theory.

In order to avoid this kind of fine-tuning of $m_{q_4}^2/\Lambda^2$ in the NJL model with dynamical symmetry breaking, the ‘dynamical mass’ $m_{q'}$ should not be much smaller than $\Lambda/2$. The cutoff scale Λ , the mass m_{q_4} and the electroweak breaking scale $v = 246$ GeV are related by the approximate formula

$$v^2 \approx \frac{3m_{q_4}^2}{4\pi^2} \cdot \ln \frac{\Lambda^2}{m_{q_4}^2} . \quad (1.10)$$

An appropriate value for v is given by *e.g.* $m_{q_4} \approx 750$ GeV and $\Lambda \sim 2m_{q_4}$, but m_{q_4} as low as 500 GeV might also be acceptable. [63] For such ‘low’ fourth generation quark masses Eq.(1.10) gives the TeV-scale as the scale for new physics.

1.2.2 Flavor democracy – a solution to the naturalness problem

The *flavor democracy* hypothesis or the *democratic mass matrix model* was proposed [64] more than thirty years ago as a solution to some of the problems of the standard model. For three SM families this approach leads to a number of ‘false’ predictions, such as a low mass for the t -quark [65], but in the case of four families flavor democracy seems fitting since it gives three exactly massless neutrinos and a heavy neutrino without requiring a large hierarchy among the Yukawa couplings of the fermions of different types [66]. This is the foundation of the hypothesis: the idea that all fermions of a particular type have equal Yukawa couplings with the Higgs field before the diagonalization of the mass matrix. The three exactly massless neutrinos obtain small masses from the slight breaking of democracy.

In order to familiarize ourselves with the ideas of flavor democracy let us consider three different bases [66, 65]:

- standard Model basis $\{f^0\}$,
- mass basis $\{f^m\}$ and
- weak basis $\{f^W\}$.

In the three family SM quarks are grouped into the following multiplets before symmetry breaking:

$$\begin{pmatrix} u_L^0 \\ d_L^0 \end{pmatrix}, u_R^0, d_R^0; \quad \begin{pmatrix} c_L^0 \\ s_L^0 \end{pmatrix}, c_R^0, s_R^0; \quad \begin{pmatrix} t_L^0 \\ b_L^0 \end{pmatrix}, t_R^0, b_R^0. \quad (1.11)$$

For one family all bases are equal and the Yukawa interaction of, for example, the d -quark mass reads

$$\mathcal{L}_Y^{(d)} = \lambda_d (\bar{u}_L \bar{d}_L) \begin{pmatrix} \phi^+ \\ \phi^0 \end{pmatrix} d_R + \text{h.c.}, \quad (1.12)$$

where λ_d is the Yukawa coupling and $(\phi^+, \phi^0)^T$ is the SM Higgs doublet where only the second, neutral component ϕ^0 has a nonzero vacuum expectation value $\langle \phi^0 \rangle_0 = v = 246$ GeV (the Higgs mechanism will be discussed later on, in Section 2.3). The interaction (1.12) leads to a mass term for the d -quark :

$$\mathcal{L}_m^{(d)} = m_d \bar{d} d, \quad (1.13)$$

with $m_d = \lambda_d \cdot v / \sqrt{2}$.

For n generations the Yukawa couplings form an $n \times n$ matrix λ_{ij} and the Yukawa-term in the SM Lagrangian is a sum over all the flavors. For the down-type quark this interaction reads :

$$\mathcal{L}_Y^{(d)} = \sum_{i,j=1}^n \lambda_{ij}^d (\bar{u}_{Li}^0 \bar{d}_{Li}^0) \begin{pmatrix} \phi^+ \\ \phi^0 \end{pmatrix} d_{Ri}^0 + \text{h.c.}, \quad (1.14)$$

where the quark fields are in the SM basis. Eq. (1.14) gives the mass terms

$$\mathcal{L}_m^{(d)} = \sum_{i,j=1}^n m_{ij}^d \bar{d}_i^0 d_j^0, \quad (1.15)$$

where $d_1 = d$, $d_2 = s$ etc and $m_{ij}^d = \lambda_{ij}^d v / \sqrt{2}$. As will be discussed further on, a bi-unitary transformation diagonalizes the mass matrix of a given type of fermions and makes the transition from the SM basis to the mass basis.

The basic idea of flavor democracy is that the mass matrix M is fully ‘democratic’ in the sense that all of its entries have the same value $M_{ij} = \lambda v / \sqrt{2} \ \forall i, j$. Such a matrix has two eigenvalues: a three-fold degenerate eigenvalue $\Lambda_1 = 0$ and the nonzero $\Lambda_2 = 4$. For the generic case of n generations one gets an $n \times n$ mass matrix M^f instead of the 4×4 of SM4. The superscript f refers to the type of fermion considered (up, down, charged lepton, neutrino).

If the model has approximate flavor democracy among the Yukawa couplings then M^f can be written in terms of the fully democratic matrix described above and a small, democracy-breaking term $\lambda M'_f$ as [66]

$$M^f = Y^f (M^0 + \lambda M'_f) , \quad (1.16)$$

where Y^f is interpreted as the common Yukawa coupling of fermions of type f and the parameter λ is introduced for bookkeeping purposes (as is usually done in perturbative quantum mechanics). λ is assumed to be real and to take values between 0 and 1. The matrix M' has entries $\mathcal{O}(1)$, and since the first three eigenvalues of the fully democratic mass matrix are zero, M' gives the first three generation particles their ‘small’ masses – the deviation of the model from perfect democracy [67, 68, 44].

Again, in the generic case of n generations the first $n-1$ eigenvalues of M are equal to zero while one is equal to n so a large hierarchy among the masses of a given species f does not necessarily require a similar hierarchy among the elements of the mass matrix [66, 65].

In order to be able to work with the flavor democracy hypothesis one needs to make the following assumptions [65]:

1. Before spontaneous symmetry breaking all fermions with the same quantum numbers are indistinguishable so the Yukawa couplings within each type of fermions should be equal:

$$\lambda_{ij}^d \simeq \lambda^d , \quad \lambda_{ij}^u \simeq \lambda^u , \quad \lambda_{ij}^\ell \simeq \lambda^\ell \quad \text{and} \quad \lambda_{ij}^\nu \simeq \lambda^\nu . \quad (1.17)$$

This assumption leads to $n-1$ massless particles and one massive particle with $m^f = n \cdot \lambda^f v / \sqrt{2}$ for n generations and $f = u, d, \ell, \nu$.

2. Because there is only one Higgs doublet giving Dirac masses to all four types of fermions it would seem natural that the Yukawa couplings of different types of fermions be nearly equal:

$$\lambda^d \simeq \lambda^u \simeq \lambda^\ell \simeq \lambda^\nu . \quad (1.18)$$

3. A natural value for λ is the $SU(2)$ gauge coupling constant g_W . If this were true then $m_4 = 2\sqrt{2}g_W v \approx 450$ GeV. On the other hand, if $\lambda = 1$ then $m_4 \approx 700$ GeV, which is close to the upper limit posed on quark masses by partial wave unitarity (discussed in Section 1.3).

A prediction of the first and second assumptions is that, taking into account the actual masses of the third SM family, namely $m_{\nu_\tau} \ll m_\tau < m_b \ll m_t$, *the fourth SM family should exist* [65].

1.2.3 Electroweak Precision Data

During the last two decades precision tests have been made at CERN, Fermilab and SLAC. The results have provided increasingly precise tests of the SM, so that the SM is now confirmed at the level of virtual quantum effects. The tests also probe the mass scale of the Higgs boson. Even though in many cases the agreement between experiment and theory is excellent, there are some observables of the electroweak precision data (EWPD) that have some tension with the SM predictions. These

discrepancies may be due to various errors in the measurements, or possibly signals of new physics beyond the standard model. Interestingly, it seems that the adding of a fourth generation might amount to a better agreement with the data. The situation is, however, far from clear.

B physics

Measurements of the b -quark CP -asymmetries, often called B - CP asymmetries have shown several indications of new physics. During the last years the amount of available data has accumulated and at the same time the accuracy of some important theoretical calculations has improved. These developments make it increasingly apparent that several of the results are difficult to reconcile with SM3 (see *e.g.* [47, 69, 70, 71]) and provide a test for models going beyond the SM (BSM models).

The problem of the B - CP asymmetries from a phenomenological point of view is that the CKM picture of CP -violation does not explain all of the experimentally observed phenomena. As will be discussed later on, in the SM CP -violation is encoded in a few CP violating phases of the quark mixing matrix, called the CKM matrix. Phenomena not explained by the CKM model are [72] (see Appendix A for explanations of the parameters) ¹:

1. *The large difference in direct CP asymmetries is difficult in the SM framework:* the direct CP asymmetry is measured to be [75]

$$\Delta A_{CP} = A_{CP}(B^- \rightarrow K^- \pi^0) - A_{CP}(\bar{B}^0 \rightarrow K^- \pi^+) = (14.4 \pm 2.9)\% . \quad (1.20)$$

Naively this quantity would be expected to vanish but on the other hand it is difficult to draw any conclusions from the value (1.20), since the associated hadronic decays are not fully understood.

2. *The need for a non-standard CP -phase* has recently been brought up [76, 77] in the study of $B_s \rightarrow \psi\phi$ by CDF [78] and DØ [79] at Fermilab.

Some of the above anomalies may be explained by a fourth generation. The heavy up-type quark of the fourth generation generate a new source of electroweak penguin contribution since the amplitudes do not obey the decoupling theorem and hence grow as $m_{t'}^2$. This might help to explain two of the anomalies in $b \rightarrow s$ transitions and this also helps in explaining the difference in CP asymmetries ΔA_{CP} . [72]

Z -pole anomaly

In addition to the above listed discrepancies in B physics there is a Z -pole observable with a large anomaly that has been mentioned in the literature [69]: the $Z \rightarrow \bar{b}b$ front-back asymmetry $A_{FB}^{b\bar{b}}$ (A.3), which differs by about 3σ from the SM prediction (3.2σ at 99.9% C.L. in 2011 [80], 2.8σ in 2006 [81]).

This deviation could be a signal for new physics but there are a few issues that suggest caution [69]:

¹ A few years ago there was another parameter that would have been added to this listing; namely the $\sin 2\beta$ parameter (see Eq. (A.2)). In 2008 the SM prediction was approximately $2 - 3 \sigma$ larger than the directly measured value (see *e.g.* [71]). Recent measurements have shifted the parameter towards the SM prediction, and the discrepancy has vanished. In 2012 the PDG [59] reported the result [73]

$$\beta = 0.07_{-0.08}^{+0.06} , \quad (1.19)$$

of the HFAG collaboration, which is in agreement with the SM prediction $\beta = 0.018 \pm 0.001$ [74].

1. the direct determination of \mathcal{A}_b (A.5) from the front-back left-right asymmetry A_{LRFB} (A.4), with a deviation of only 0.7σ is consistent with the SM but when \mathcal{A}_b is determined from $\mathcal{A}_b = 4A_{FB}^b/3A_\ell$, with A_ℓ the leptonic asymmetry, disagrees by 3.5σ at 99.95% C.L.,
2. there is no hint of an R_b anomaly to match the \mathcal{A}_b one, so fine-tuning of the left and right-handed $Z\bar{b}b$ couplings is required as well as an extremely large shift in the right-handed coupling,
3. $Z \rightarrow \bar{b}b$ measurements are known to be difficult.

Another thing to keep in mind is that the deviation could be due to a statistical fluctuation or subtle systematic error. If the explanation were systematic error A_{FB}^b should be omitted from the SM fit. In this case the global fit, which is poor with A_{FB}^b included, becomes excellent, but at the same time the predicted value of m_H gets low values in direct conflict with the search limit 114.4 GeV (95% C.L.) [82].

The effective leptonic mixing angle $x_W^\ell = \sin^2 \theta_W^\ell$, extracted from the hadronic asymmetry measurements A_{FB}^c and Q_{FB} agrees with x_W^ℓ extracted from A_{FB}^b but deviates from the SM fit (the leptons do not mix in the SM, as we will see). When all measurements are combined, they differ from the SM fit at 99.5% but on the other hand these are the only measurements that raise the predicted value of m_H toward the range required by the search limit. It follows that the data favors new physics whether the A_{FB}^b anomaly is genuine or not. In any case an important consequence is that the evidence from the SM fit favoring a light Higgs boson becomes less credible. [69]

1.3 Unitarity constraints on the fourth generation

At the quantum level conservation of probability is guaranteed by the unitarity of the scattering matrix \mathbf{S} , which is generally written as $\mathbf{S} = \mathbf{1} + i\mathbf{T}$ with \mathbf{T} the matrix describing the interactions of the system. The expression for \mathbf{T} can be deduced from a given Lagrangian, and its eigenvalues give information about the spectrum of fermion masses. More specifically, the largest eigenvalue of \mathbf{T} is used to compute the lowest ‘critical’ value of the mass of fermions. The expression ‘critical mass’ is used here to signify the value of mass $(m_f)_{\text{crit}}$ beyond which the electroweak interactions are no longer weak, but strong, signaling the breakdown of perturbation theory (the perturbative regime holds for fermions with mass $m_f \lesssim (m_f)_{\text{crit}}$). At the energy scale of a possible fourth generation the color interactions usually denoted as ‘strong interactions’ may actually be weak compared to the electroweak interactions, due to the asymptotic freedom of QCD. Hence it is conceivable that weak interactions dominate at the scale of fourth generation masses and that these new particles may be bound together by the $SU(2) \times U(1)$ gauge bosons, giving ‘quarkonia’ and ‘leptonia’ bound by W , Z , H . The long-distance behavior of these states would nevertheless be explained by QCD, since the color interactions are known to become strong at small energies, but since the small-distance (high-energy) behavior is dominantly described by the electroweak interactions, these are the ones to study when investigating the validity of perturbation theory, the series expansion in powers of the coupling. Perturbation theory is applicable as long as terms of high orders are subleading and do not overtake the lower-order ones. [83]

A tool used to study unitarity is called ‘partial wave analysis’ – a method which we shall now briefly review. This method can be used to bound the masses of a possible fourth generation. It has also been used to deduce an upper limit on the Higgs boson mass [84].

Partial wave analysis

A generic scattering amplitude \mathcal{A} may be written in terms of ‘partial waves’ :

$$\mathcal{A} = 16\pi \sum_{\ell=0}^{\infty} (2\ell+1) P_{\ell}(\cos \theta) a_{\ell} \quad , \quad (1.21)$$

where the $P_{\ell}(\cos \theta)$ are Legendre polynomials and a_{ℓ} gives the spin- ℓ partial wave (see *e.g.* [85]). We recall that the differential cross section of a $2 \rightarrow 2$ scattering is simply

$$\frac{d\sigma}{d\Omega} = \frac{1}{64\pi^2 s} |\mathcal{A}|^2 \quad , \quad (1.22)$$

which, together with equation (1.21) gives the total cross section

$$\sigma = \frac{8\pi}{s} \sum_{\ell, \ell'=0}^{\infty} (2\ell+1)(2\ell'+1) a_{\ell} a_{\ell'} \int_{-1}^{+1} d\cos \theta P_{\ell}(\cos \theta) P_{\ell'}(\cos \theta) \quad (1.23)$$

$$= \frac{16\pi}{s} \sum_{\ell=0}^{\infty} (2\ell+1) |a_{\ell}|^2 \quad , \quad (1.24)$$

where, going from (1.23) to (1.24) the orthogonality property of the Legendre polynomials has been used. We note that the cross section of Eq. (1.24) is a sum of positive definite terms. On the other hand, by the optical theorem, the cross section is proportional to the imaginary part of the amplitude in the $\theta = 0$ direction :

$$\sigma = \frac{1}{s} \Im [\mathcal{A}(\theta = 0)] \quad , \quad (1.25)$$

which together with (1.24) gives

$$|a_{\ell}|^2 = \Im(a_{\ell}) \implies [\Re(a_{\ell})]^2 + \left[\Im(a_{\ell}) - \frac{1}{2} \right]^2 = \frac{1}{4} \quad , \quad (1.26)$$

which is nothing but the equation for a circle of radius $\frac{1}{2}$ – the ‘unitarity circle’ – centered at $(0, \frac{1}{2})$ in the complex a_{ℓ} plane. The real part of the partial wave a_{ℓ} lies thus in the region

$$\Re(a_{\ell}) < \frac{1}{2} \quad \forall \ell \quad . \quad (1.27)$$

Limits on fermion masses

In the high-energy limit $\sqrt{s} \gg m_f$ the amplitudes of $2 \rightarrow 2$ processes simplify, and since this is also the case of current experiments (notably at the LHC) this is the limit upon which we focus. In this high-energy limit the tree-level amplitudes of certain $2 \rightarrow 2$ processes, such as [86]

$$f\bar{f} \longrightarrow f\bar{f}, W^+W^-, ZZ, ZH, HH \quad (1.28)$$

tend toward the constant value of $G_F m_f^2$. When m_f is very large the constant $G_F m_f^2$ may become of the order of unity, signaling the saturation of the tree-level unitarity of the \mathbf{S} -matrix. When the \mathbf{S} -matrix is saturated already at tree level, this implies that the higher-order corrections need to be relatively large, which in turn implies that the coupling is relatively strong and that one is working at the limit of the validity of perturbation theory.

This is also seen from the point of view of partial-wave analysis. As noted above, the most stringent bound on the mass of new fermions is given by the largest eigenvalue of the \mathbf{T} matrix. In the partial wave analysis presented above, the $\ell = 0$ partial wave is computed from

$$a_0 = \frac{1}{32\pi} \int_{-1}^{+1} d\cos\theta \mathbf{T} \quad . \quad (1.29)$$

For quarks (leptons) the smallest critical mass comes from the spin-0 (spin-1) matrix, giving the following tree-level results [83]

$$m_q < \frac{4\sqrt{2} \cdot \pi}{G_F} \frac{1}{5 + \sin^2 \theta_C} \times \frac{1}{N} \quad \text{and} \quad (1.30)$$

$$m_\ell < \frac{4\sqrt{2} \cdot \pi}{G_F} \frac{1}{1 + \sin^2 \theta_C} \times \frac{1}{N} \quad , \quad (1.31)$$

when the particles of a doublet are assumed degenerate: $m_1 = m_2 = m$ with m_1, m_2 the masses of the particles of an $SU(2)$ doublet. Here G_F is the Fermi constant, θ_C is the Cabibbo angle and N is the number of nearly degenerate doublets, ‘nearly degenerate’ meaning that the mass difference of the particles in a given doublet is much smaller than the masses themselves. The doublets of the three-generation SM are *not* nearly degenerate, so for a degenerate fourth family $N = 1$. In the absence of mixing between doublets, *i.e.* for $\theta = 0$, these limits read :

$$m_q \lesssim 550 \text{ GeV} \quad \text{and} \quad m_\ell \lesssim 1200 \text{ GeV} \quad . \quad (1.32)$$

Chapter 2

The Standard Model

The standard model of elementary particle physics is a gauge theory – a theory based upon the *local*, continuous symmetries of the system, ‘local’ meaning that the parameters of the transformation depend on the space–time coordinates. Symmetry transformations have a mathematical description in terms of group theory, and more specifically *continuous symmetries* are described by *Lie groups*. Each Lie group has an associated Lie algebra, a vector space over some field and where an operator called the Lie bracket has been defined. The standard model is based upon the symmetry group (the *gauge group*) $SU(3) \times SU(2) \times U(1)$, where each group of this direct product is associated with a symmetry of the system. $SU(3)$ is the *color* group, $SU(2)$ and $U(1)$ the isospin and hypercharge symmetry groups. The theory of quantum chromodynamics (QCD) [36, 37, 34, 87] is based upon the gauge group $SU(3)$ whereas the Glashow–Weinberg–Salam (GWS) [46, 31, 28, 22] theory of electroweak interactions is based on $SU(2) \times U(1)$. The $SU(2) \times U(1)$ symmetry is broken *spontaneously* by the presence of a scalar field, separating the interactions into weak and electromagnetic ones. This spontaneous symmetry breaking (SSB) generating *masses* for the standard model particles is called the *Higgs mechanism* [88, 89, 90] and the associated scalar field is called the *Higgs field*.

In the following we give a brief review of the salient features of this theory that in elementary particle physics is called the standard model. We start by presenting the theory of strong interactions before going on to the electroweak theory and the breaking of the $SU(2) \times U(1)$ symmetry and the generation of mass.

2.1 Quantum chromodynamics

The theory that describes the strong interactions that bind together nuclear matter is called quantum chromodynamics (QCD) – from the Greek word ‘chromo’ meaning *color*. The gauge group $SU(3)$ of the theory is often called the ‘color group’, with $N_c = 3$ the number of colors (the number of degrees of freedom in the fundamental representation) for the case of QCD. The quanta of the gauge field, the ‘gluons’, live in the adjoint representation of the gauge group and hence there are $N_c^2 - 1 = 8$ of them.

The Lagrangian density of a system must respect the relevant symmetries, for QCD this means that the Lagrangian is required to be invariant under $SU(3)$. The Yang–Mills Lagrangian for a non-abelian theory with the Dirac field ψ reads

$$\mathcal{L}_{\text{QCD}} = \mathcal{L}_{\text{Dirac}} + \mathcal{L}_{YM} = \bar{\psi}(i\not{D} - m)\psi - G^{a\mu\nu}G_{\mu\nu}^a \quad , \quad (2.1)$$

where $G_{\mu\nu}^a$ is the field strength tensor

$$G_{\mu\nu}^a = \partial_\mu A_\nu^a - \partial_\nu A_\mu^a + gf^{abc} A_\mu^b A_\nu^c \quad , \quad (2.2)$$

with A_μ^a the gauge field with color index a and Lorentz index μ and g is a constant that is eventually identified with the gauge coupling. The f^{abc} are the (completely antisymmetric) structure constants of the $SU(3)$ algebra :

$$[t^a, t^b] = if^{abc} t^c \quad . \quad (2.3)$$

The t^a are the generators of the algebra.

The notation can be abbreviated writing

$$G_\mu \equiv G_\mu^a t^a \quad \text{and} \quad A_\mu \equiv A_\mu^a t^a \quad , \quad (2.4)$$

where summation over a is implied.

A specific representation of the group is given by the Gell-Mann matrices $\lambda^a \equiv t^a/2$, after the Nobel-prize winning physicist Murray Gell-Mann. The action of the covariant derivative D^μ on ψ in (2.1) reads

$$D^\mu \psi(x) = [\partial^\mu - igA^\mu(x)] \psi(x) \quad , \quad (2.5)$$

where we have used the Feynman slash notation

$$\not{D} \equiv \gamma^\mu D_\mu \quad , \quad (2.6)$$

for γ^μ generators of the Clifford algebra in four dimensions. Matter fields transform in the fundamental representation whereas gauge fields transform in the adjoint (antifundamental) representation.

From the Lagrangian (2.1) and the identities (2.2), (2.4), (2.3) we see that invariance under $SU(3)$ implies that the spinors ψ transform as (see *e.g.* [91])

$$\psi(x) \rightarrow V(x) \psi(x) \quad , \quad (2.7)$$

where $V(x) = e^{igt^a \alpha^a(x)}$, $\alpha^a(x)$ being a space-time dependent vector whose a^{th} component is multiplied by the corresponding Lie algebra generator. The gauge field transforms as

$$A_\mu \rightarrow V(x) \left(A_\mu + \frac{i}{g} \partial_\mu \right) V^\dagger(x) \quad . \quad (2.8)$$

2.1.1 Gauge fixing and Faddeev–Popov ghosts

Let us for a moment discuss the quantization of a non-abelian field theory in the path integral formalism.

The generating functional of a QFT with a Yang–Mills Lagrangian $\mathcal{L}_{YM} \equiv \mathcal{L}_{YM}(A_\mu^a) = -\frac{1}{4}(F_{\mu\nu}^a)^2$ is written as a functional integral over the gauge field A_μ^a

$$\mathcal{Z} \sim \int \mathcal{D}A \exp \left(i \int d^4x \mathcal{L} \right) \quad (2.9)$$

$$\sim \int \mathcal{D}A e^{iS[A_\mu^a]} \quad , \quad (2.10)$$

up to a normalization factor. Here the action S is

$$S[A_\mu^a] \equiv \int dt L(A_\mu^a) = \int dt d^3\mathbf{x} \mathcal{L}(A_\mu^a) \quad , \quad (2.11)$$

with L the spatial integral of the Lagrangian density \mathcal{L} . Since \mathcal{L} is invariant under a (non-abelian) gauge transformation, and gauge transformations are continuous, there is an infinite number of directions in configuration space along which the Lagrangian is unchanged. The choice of direction in configuration space – the gauge choice – should *not* affect the physics of the system, so these ‘redundant’ degrees of freedom corresponding to the different gauges need to be integrated out of (2.11), since the dynamics is given by the action (or the Lagrangian) through the equations of motion. This procedure of choosing direction in phase space is often called *gauge fixing*.

A clever way to fix the gauge, proposed by Faddeev and Popov [92], is to insert the identity in disguise into the functional integral (2.10)

$$1 = \int \mathcal{D}\alpha(x) \delta(G(A)) \det\left(\frac{\delta G(A^\alpha)}{\delta \alpha}\right) . \quad (2.12)$$

This equation enforces a *gauge-fixing condition* $G(A) = 0$ at every spacetime point x . In (2.12) A^α is the gauge field transformed by a *finite* gauge transformation

$$A_\mu^\alpha \equiv (A^\alpha)_\mu^{at^a} = e^{i\alpha^a t^a} \left(A_\mu^b t^b + \frac{i}{g} \partial_\mu \right) e^{-i\alpha^c t^c} , \quad (2.13)$$

with the t^a generators of the adjoint representation of $SU(3)$, satisfying

$$(t^b)_{ac} = i f^{abc} . \quad (2.14)$$

For the determinant in (2.12) it is convenient to write (2.13) in its infinitesimal form

$$(A^\alpha)_\mu^a = A_\mu^a + \frac{1}{g} \partial_\mu \alpha^a + f^{abc} A_\mu^b \alpha^c \quad (2.15)$$

$$= A_\mu^a + \frac{1}{g} D_\mu \alpha^a , \quad (2.16)$$

where one recognizes the covariant derivative D_μ of (2.5) using (2.14). When the generalized Lorentz gauge condition $G(A) = \partial^\mu A_\mu^a(x) - \omega^a(x)$, with $\omega^a(x)$ a Gaussian weight, is chosen the result (2.16) gives

$$\frac{\delta G(A^\alpha)}{\delta \alpha} = \frac{1}{g} \partial^\mu D_\mu \quad (2.17)$$

The idea of Faddeev and Popov was to write the determinant of the left-hand side of (2.17) as a functional integral over Grassmannian (*i.e.* fermionic or anticommuting) fields c , \bar{c} , with a Gaussian integrand

$$\det\left(\frac{1}{g} \partial^\mu D_\mu\right) = \int \mathcal{D}c \mathcal{D}\bar{c} \exp\left[i \int d^4x \bar{c}(-\partial^\mu D_\mu)c\right] . \quad (2.18)$$

The fields c , \bar{c} that appear in this way are called Faddeev–Popov ghosts or simply *ghosts*. The ghosts couple to the gauge field through the minimal coupling of the covariant derivative $\bar{c} A_\mu c \in \bar{c} D_\mu c$, giving vertices with one external gauge boson and two ghosts. These ghost fields are not physical since they have no asymptotic states. They arise, however, as intermediate states in loop calculations. They are crucial to getting results that are gauge invariant and need to be taken into account when *renormalizing* QCD.

2.1.2 Renormalization and asymptotic freedom

Non-abelian gauge theories have a very interesting characteristic, which is not present in the Abelian case. It turns out that at very high energies the strength of the color interactions, as given by the QCD coupling α_s , become weak. This property is called *asymptotic freedom* [35, 37, 36, 34, 33], signaling the asymptotic tendency

$$\text{asymptotic freedom : } \alpha_s(\mu^2) \ll 1 \quad \text{when} \quad \mu^2 \gg \Lambda_{\text{QCD}}^2 \quad , \quad (2.19)$$

with $\Lambda_{\text{QCD}} \simeq 200$ MeV the QCD ‘cut-off scale’. The coupling α_s is related to the gauge coupling g through

$$\alpha_s \equiv \frac{g^2}{4\pi} \quad . \quad (2.20)$$

The property (2.19) is extracted from the dependence of the coupling on the energy scale at which it is determined. Actually, the physics of a system quite generally depends on the scale at which one studies it. For instance, at the low energies in the domain of application of Newtonian mechanics, the orbit of the Earth may at the lowest order be computed by approximating the motion of the Earth around the sun as a classical two-body problem of pointlike particles. However, when ‘zooming in’ a little bit one notices that the sun is not pointlike at all, and at this *distance scale* the shape and varying density of the sun have to be taken into account. Zooming in yet more one discerns even details of the Earth, and sees that it is not a pointlike particle either, and that when wanting to do an even more comprehensive calculation you need to take the finiteness of its size into account, too. [93] (For published notes see *e.g.* [94] by the same author.)

A similar situation arises in elementary particle physics – the *physics of the system depends upon the energy scale considered*. It is well known that some loops diagrams lead to divergences (see *e.g.* [95]) in quantum field theories. Whenever the divergences come from a finite number of subdiagrams they can be ‘absorbed’ into a finite number of so-called *counterterms*. The procedure of identifying the divergences and grouping them into counterterms is called *renormalization*. This renders the physical observables finite, since the infinities are canceled by the counterterms. In doing so, however, one needs to introduce an arbitrary scale μ that is called the *renormalization scale*. The finite, *renormalized*, quantities then depend upon this scale, as does for example the coupling ‘constant’ α_s that is in fact scale-dependent $\alpha_s \equiv \alpha_s(\mu^2)$ and not a constant at all.

The dependence of the gauge coupling g on the renormalization scale μ is given by the β -function (also called the Callan–Symanzik function)

$$\beta(g) \equiv \frac{\partial g}{\partial \log(\mu/\mu_0)} \quad , \quad (2.21)$$

when the coupling is known at some reference scale μ_0 . For non-abelian theories the general expression at the leading order in perturbation theory reads (see *e.g.* [96])

$$\beta(g) = -\frac{g^3}{(4\pi)^3} \left(\frac{11}{3} C_2^{(A)} - \frac{4}{3} n_f C^{(r)} \right) + \mathcal{O}(g^5) \quad , \quad (2.22)$$

where $C_2^{(A)}$ is the quadratic Casimir operator for the adjoint representation, $C^{(r)}$ is the Casimir operator for the representation r and n_f is the species of fermions. When the gauge group is $SU(N)$ these are, for the fundamental (F) and adjoint (A) representations

$$C^{(F)}(N) = \frac{1}{2} \quad , \quad C_2^{(F)} = \frac{N^2 - 1}{2N} \quad \text{and} \quad C^{(A)}(N) = C_2^{(A)}(N) = N \quad . \quad (2.23)$$

For QCD with gauge group $SU(3)$ the β -function (2.22) is negative when the number of fermion species is $n_f \leq 16$, which implies that the number of families can be at most four. Since we believe that QCD indeed does exhibit asymptotic freedom the β -function should be negative, meaning that the coupling diminishes with the energy, this gives *an upper limit on the number of fermion generations*.

2.2 Local $SU(2)$ and $U(1)$ symmetries

Besides the theory of strong interactions just covered, the standard model contains the *electroweak interactions*, whose gauge group is $SU(2) \times U(1)$. According to Noether's theorem [97] to each symmetry of a system there is related a conserved current and a conserved charge. The conserved charges of the electroweak theory [98, 46, 31, 28] are the *isospin* I for $SU(2)$ [99] and *hypercharge* Y for $U(1)$ – one often sees the notation $SU(2)_I \times U(1)_Y$. This $SU(2) \times U(1)$ symmetry, is *not* an invariance of the low-energy theory, because it is *broken* by another field at what is called the *electroweak scale* $v \approx 246$ GeV. After this symmetry breaking, the isospin and hypercharge are no longer conserved separately, but combine to form just one conserved charge, the *electric charge*. In other words, the $SU(2)_I \times U(1)_Y$ symmetry group is broken down to a subgroup: $U(1)_Q$.

The field that breaks the electroweak symmetry is called the Higgs field [88, 89, 90]. It is a scalar field whose non-zero vacuum expectation value (VEV) is responsible for the breaking of the symmetry and the generation of mass of the standard model particles. The quantum associated with the field, the *Higgs boson* seems to have been found at the time of writing this report [100, 101].

2.2.1 Isospin symmetry

As already noted in Section 1.2.1, the particles of the standard model come in *doublets*. A general fermion doublet $\Psi(x)$ is of the form $\Psi(x) = (\psi_1(x), \psi_2(x))^T$, with ψ_1, ψ_2 complex fields. Under the $SU(2)$ isospin symmetry group such a doublet transforms as (see *e.g.* [102])

$$\Psi(x) \rightarrow \Psi'(x) = e^{-i\alpha^a(x)t^a} \Psi(x) \quad , \quad (2.24)$$

where the t^a are generators of $SU(2)$ and the parameters $\alpha^a(x)$ are local. The Pauli matrices σ^a give a specific representation of the group such that $t^a = \sigma^a/2$. In order for the Dirac Lagrangian

$$\mathcal{L}_{\text{Dirac}} = \bar{\psi}(x) (i\gamma^\mu \partial_\mu - m) \psi(x) \quad (2.25)$$

to be invariant under the transformation (2.24), the partial derivative ∂_μ must be replaced by the covariant derivative D_μ , given in (2.5). The covariant derivative transforms as the Dirac field (this is the meaning of a 'covariant' derivative)

$$(D_\mu \Psi(x))' = e^{-i\alpha^a(x)t^a} D_\mu \Psi(x) \quad , \quad (2.26)$$

so the gauge field should transform as

$$A_\mu'^a t^a = U(\alpha) A_\mu^a t^a U^{-1}(\alpha) - \frac{i}{g} [\partial_\mu U(\alpha)] U^{-1}(\alpha) \quad , \quad (2.27)$$

where $U(\alpha) = \exp(-i\alpha^a(x)t^a)$.

Now we are ready to add the Yang–Mills term for the gauge field to get the complete Lagrangian

$$\mathcal{L} = \mathcal{L}_{\text{YM}} + \mathcal{L}_{\text{Dirac}} = -\frac{1}{2} \text{Tr}(F^{\mu\nu} F_{\mu\nu}) + \bar{\psi}(x) (i\gamma^\mu D_\mu - m) \psi(x) \quad , \quad (2.28)$$

where we see interactions between the matter fields and the gauge bosons appearing from the minimal coupling in the covariant derivative.

2.2.2 Quantum electrodynamics

After the breaking of the $SU(2)_I \times U(1)_Y$ symmetry of the electroweak theory the remaining invariant subgroup is $U(1)$. This is however not the same $U(1)$ group as the original one; originally, the $U(1)_Y$ symmetry has the associated quantum number that is the hypercharge, whereas the relevant quantum number after the breaking is the *electric charge* so the one may use the notation $U(1)_Q$. The electric charge Q is in fact a linear combination of the quantum numbers of the two broken symmetries, namely

$$Q = I^3 + \frac{Y}{2} \quad , \quad (2.29)$$

with I^3 the third generator of the $SU(2)$ isospin algebra $[I^i, I^j] = i\epsilon^{ijk}I^k$ (the structure constants of $SU(2)$ are the components of the completely antisymmetric tensor with three indices).

The remaining $U(1)_Q$ group gives rise to an Abelian gauge theory called Quantum electrodynamics (QED), describing the electric and magnetic interactions of matter. It may be derived from the free Dirac equation, as done above for the $SU(2)$ gauge theory, simply by replacing the partial derivative in the Dirac term with a covariant one and by also inserting a Yang–Mills term for the gauge field into the Lagrangian. The only difference to the treatment of Eqs. (2.24)–(2.28) is that since QED is based on an Abelian gauge group, there is no commutator algebra for the generators (the generators commute) and the transformation matrix that is called $U(\alpha)$ in (2.27) simplifies

$$U_{\text{QED}}(\alpha) = \exp(-i\alpha(x)) \quad . \quad (2.30)$$

The vector $\alpha^a(x)$ is now just one real parameter α , reflecting the fact that only one degree of freedom is enough to uniquely determine $U(1)$ transformations. The associated Lagrangian reads

$$\mathcal{L}_{\text{QED}} = \mathcal{L}_{\text{Dirac}} + \mathcal{L}_\gamma \quad (2.31)$$

$$= \bar{\psi}(x) (i\gamma^\mu D_\mu - m) \psi(x) - \frac{1}{4} F^{\mu\nu} F_{\mu\nu} \quad (2.32)$$

$$= -\frac{1}{4} F^{\mu\nu} F_{\mu\nu} + \bar{\psi}(x) (i\gamma^\mu \partial_\mu - m) \psi(x) - e \bar{\psi}(x) \gamma_\mu \psi(x) A^\mu(x) \quad , \quad (2.33)$$

where, in going from (2.31) to (2.32) Eqs. (2.25),(2.28) have been used as has the definition of the covariant derivative (2.5) in the last equality. The covariant derivative (2.5) simplifies for an Abelian theory:

$$D_\mu \psi(x) = (\partial_\mu + ieA_\mu) \psi \quad , \quad (2.34)$$

where the parameter $\alpha = \alpha(x)$ of (2.5) actually is the electric charge e ($e \neq e(x)$), appearing in (2.33) (we have written e instead of Q , as is often done). An important thing to note about the Lagrangian (2.33) is that a mass term for the gauge field A_μ is missing. This is so because such a term would break the gauge symmetry and is thus forbidden. The last term in (2.33) gives the coupling of the electromagnetic field to matter. It arises from the minimal coupling of the covariant derivative and may also be written as a current J_μ coupling to the gauge field A_μ

$$e \bar{\psi}(x) \gamma_\mu \psi(x) A^\mu(x) \equiv J_\mu(x) A^\mu(x) \quad , \quad (2.35)$$

with J_μ the *Noether current* [97].

2.3 Spontaneous symmetry breaking

As long as the $SU(2)$ and $U(1)$ gauge theories presented in the previous section 2.2 do not include mass terms

$$\sim m_A^2 A^\mu A_\mu \quad (2.36)$$

for the gauge mediators the theories work well: they are gauge invariant and renormalizable but as soon as one attempts to introduce conventional mass terms for the gauge bosons the theory loses these characteristics. Experimentally, however, it is known that some of the gauge bosons observed in nature are indeed massive, so there has to be some other means of mass generation besides the *ad hoc* addition of terms like (2.36).

The Goldstone model reviewed in Appendix B provides such a means of mass generation, through the appearance of massless bosons that can be interpreted as longitudinal degrees of freedom of the gauge fields. The Goldstone model is the basis for another model where spontaneous symmetry breaking appears – the *Higgs model*, a field theory which is invariant under $U(1)$ gauge transformations. The ‘Higgs field’ of this model breaks the $SU(2)_I \times U(1)_Y$ symmetry of the combined weak and electromagnetic interactions of the electroweak theory down to the remaining $U(1)_Q$ of QED.

2.3.1 The Higgs mechanism

The Goldstone theorem (see the Appendices, B) is evaded in gauge theories since the proof of the theorem requires all of the usual axioms of quantum field theory to be valid: manifest Lorentz covariance, positivity of norms and so on. This is a problem because there is no possible gauge-fixing condition for which a given gauge theory would obey all of the axioms of usual field theories. For example: in covariant gauges states of negative norm (longitudinal photons) arise whereas in axial gauges Lorentz covariance is not manifest. As it turns out, both of these problems are solved in the physical spectrum of the theory, where massive vector particles arise without ruining the renormalizability of the theory, as first suggested by Anderson [103, 104]. Englert and Brout [90] and independently Higgs [89, 105] carried out the generalization to relativistic fields. Finally, the renormalizability of gauge field theories in the presence of spontaneous symmetry breaking was shown by ‘t Hooft [30].

Abelian case

The Higgs model is a field theory invariant under $U(1)$ gauge transformations, obtained from the Goldstone model (see Appendix B) by replacing the partial derivatives by covariant ones (2.34) and introducing a Yang-Mills term $F_{\mu\nu}F^{\mu\nu}$ into (B.8) :

$$\mathcal{L} = (D_\mu \phi)^\dagger (D^\mu \phi) - \mu^2 \phi^\dagger \phi - \lambda (\phi^\dagger \phi)^2 - \frac{1}{4} F_{\mu\nu} F^{\mu\nu} , \quad (2.37)$$

with ϕ the ‘Higgs field’. The ground state of the system corresponds to a minimum of the ‘potential’

$$\begin{aligned} V(\phi) &= \mu^2 \phi^\dagger \phi + \lambda (\phi^\dagger \phi)^2 \\ &= \mu^2 |\phi|^2 + \lambda |\phi|^4 . \end{aligned} \quad (2.38)$$

For $\lambda > 0$, which is required for V to have a minimum, two situations arise. For $\mu^2 > 0$ the origin $|\phi|^2 = 0$ is the point where the state of lowest energy is obtained; here both $\phi(x)$ and $A_\mu(x)$ vanish. The ground state is clearly invariant (under the gauge group $U(1)$) and is unique. If, on the other hand, $\mu^2 < 0$ then the potential has the form of a ‘mexican hat’ whose minimum is at

$$|\phi| = \sqrt{-\frac{\mu^2}{2\lambda}} \equiv \frac{v}{\sqrt{2}} . \quad (2.39)$$

The vacuum is now given by any of the points on the ring of radius $v/\sqrt{2}$ in the complex ϕ -plane. (The numerical value of v is ~ 246 GeV in the SM.)

In this case the point $|\phi| = 0$ is unstable and any value of ϕ such that Eq. (2.39) is satisfied gives a ground state. The number of ground states is infinite. These states are not invariant under the gauge transformations $\phi(x) \rightarrow \exp(-i\alpha(x)) \cdot \phi(x)$, since such a transformation actually takes one from one ground state to another, the ground states all being of the form

$$\phi_{vac} = \frac{v}{\sqrt{2}} e^{i\Lambda} , \quad (2.40)$$

Λ being a real parameter, but otherwise arbitrary. All of the points on the ring of minima are equivalent since any of the points can be obtained from any other by applying a $U(1)$ transformation. Since this is the most interesting case, we will assume $\mu^2 < 0$ in the following.

Eq. (2.39) implies that the field operator $\phi \equiv \phi(x)$ develops a vacuum expectation value (*vev*)

$$|\langle 0|\phi|0\rangle| = \frac{v}{\sqrt{2}} . \quad (2.41)$$

Writing the complex ϕ in terms of two real fields ϕ_1 and ϕ_2

$$\phi = \frac{1}{\sqrt{2}} (\phi_1 + i\phi_2) \quad (2.42)$$

one is free to chose

$$\langle 0|\phi_1|0\rangle = v \quad \text{and} \quad \langle 0|\phi_2|0\rangle = 0 . \quad (2.43)$$

This amounts to choosing one vacuum out of the infinitely many possibilities. Making such a specific choice breaks the $U(1)$ symmetry of the Lagrangian.

Shifting the fields

$$\phi'_1 = \phi_1 - v \quad \text{and} \quad \phi'_2 = \phi_2 \quad (2.44)$$

and replacing (2.44) into (2.37) it appears that ϕ'_2 corresponds to the massless Goldstone boson because:

$$\begin{aligned} |D_\mu \phi|^2 &= |(\partial_\mu - igA_\mu)\phi|^2 \\ &= \frac{1}{2}(\partial_\mu \phi'_1 + gA_\mu \phi'_2)^2 + (\partial_\mu \phi'_2 - gA_\mu \phi'_1)^2 - gvA^\mu(\partial_\mu \phi'_2 + gA_\mu \phi'_1) + \frac{g^2 v^2}{2} A^\mu A_\mu \end{aligned} \quad (2.45)$$

The last term can be interpreted as a mass term for A_μ , a term that would vanish if the *vev* of the Higgs field (2.41) were zero: *The nonzero value of (2.41) is responsible for the mass of the gauge boson.*

The mixed term

$$gvA^\mu \partial_\mu \phi'_2 \quad (2.46)$$

couples the fields A_μ and ϕ'_2 and makes the interpretation of Eq. (2.45) less clear. This possible problem can be fixed using the *unitary gauge*, in which the term (2.46) disappears. The unitary gauge amounts to a redefinition of the fields ϕ and A_μ :

$$\begin{aligned} \phi(x) &\longrightarrow \exp(-i\xi(x)/v) \phi(x) = \frac{1}{\sqrt{2}}(v + \eta(x)) \\ A_\mu(x) &= B_\mu(x) + \frac{1}{gv} \partial_\mu \xi(x) . \end{aligned} \quad (2.47)$$

Now the Lagrangian (2.37) may be written

$$\begin{aligned}\mathcal{L} &= \frac{1}{2} [\partial_\mu \eta - ig B_\mu (v + \eta)]^2 - \frac{\mu^2}{2} (v + \eta)^2 - \frac{\lambda}{4} (v + \eta)^4 - \frac{1}{4} (\partial_\mu B_\nu - \partial_\nu B_\mu)^2 \\ &= \mathcal{L}_0 + \mathcal{L}_1 ,\end{aligned}\tag{2.48}$$

with \mathcal{L}_0 the free Lagrangian density for a *massive* vector field B_μ with mass $M = gv$ and a scalar meson η with mass $m = \sqrt{2}\mu$ and

$$\mathcal{L}_1 = \frac{1}{2} g^2 B_\mu B^\mu \eta (2v + \eta) - \lambda v^2 \eta^3 - \frac{1}{4} \lambda \eta^4\tag{2.49}$$

the interaction Lagrangian. The *would-be-Goldstone boson* $\xi(x)$ has disappeared from the Lagrangian and the massless gauge field A_μ and the scalar field ξ have combined to form a massive vector field B_μ .

Non-abelian case

The generalization of the above mechanism to a case with a non-Abelian gauge field is straightforward. In the Lagrangian (2.37) one just uses the covariant derivative (2.5) instead of (2.34) and the field strength tensor (2.2).

2.4 The Glashow–Weinberg–Salam model

Having familiarized ourselves with the local $SU(2)$ and $U(1)$ symmetries and the spontaneous breaking of such, we are ready to review the $SU(2) \times U(1)$ model of electroweak interactions, also called the Glashow–Weinberg–Salam model after its founders [46, 31, 28, 22]. We will use $U(1)_Y$ and $U(1)_Q$ to denote the groups whose conserved charges are the weak hypercharge and electric charge, respectively ($SU(2)$ will be written without any indices since there should be no risk for ambiguity here).

Gauge and scalar sectors

The gauge and scalar sectors of the model read (see *e.g.* [62]):

$$\mathcal{L} = -\frac{1}{4} F^{a\mu\nu} F_{\mu\nu}^a - \frac{1}{4} B^{\mu\nu} B_{\mu\nu} + D^\mu \phi^\dagger D_\mu \phi - V(\phi^\dagger \phi) ,\tag{2.50}$$

where $F_{\mu\nu}^a$ is the $SU(2)$ field strength tensor (given as $G_{\mu\nu}^a$ in (2.5)) whose index $a = 1, 2, 3$ runs over the number of generators of the group, $B_{\mu\nu}$ reading

$$B_{\mu\nu} = \partial_\mu B_\nu - \partial_\nu B_\mu ,\tag{2.51}$$

is the field strength tensor that is invariant under $U(1)_Y$ and ϕ in (2.50) is the Higgs field. The derivative D_μ is invariant under both $SU(2)$ and $U(1)_Y$, so it has the minimal substitution terms of both these groups :

$$D_\mu \phi = \partial_\mu \phi - ig A_\mu^a \frac{\sigma^a}{2} \phi - i \frac{g'}{2} y_\phi B_\mu \phi ,\tag{2.52}$$

where $g, g'/2$ are the $SU(2), U(1)_Y$ gauge coupling constants, respectively, and $y_\phi = +1$ is the hypercharge of the neutral Higgs field ϕ^0 (when $\phi = (\phi^+, \phi^0)^T / \sqrt{2}$). Invariance of (2.50) under

$SU(2) \times U(1)_Y$ gives the infinitesimal transformations of the fields :

$$\begin{aligned}\delta A_\mu^a &= -\frac{1}{g}\partial_\mu \alpha^a + \varepsilon^{abc}\alpha^b A_\mu^c, \\ \delta B_\mu &= -\frac{2}{g}\partial_\mu \beta, \\ \delta \phi &= -i\alpha^a \frac{\sigma^a}{2}\phi - iy_\phi \beta \phi,\end{aligned}\tag{2.53}$$

where α^a ($a = 1, 2, 3$), β are the parameters of the $SU(2)$, $U(1)_Y$ transformations. (The choice $\alpha^1 = \alpha^2 = 0$ and $\alpha^3 = 2\beta = \theta$ corresponds to the QED $U(1)$ transformation $\delta\phi^+ = -i\theta\phi^+$, $\delta\phi^0 = 0$.) Taking the scalar potential (2.38) with $\mu^2 = -m^2$ the ground state of ϕ is at

$$\langle\phi\rangle = \begin{pmatrix} 0 \\ \frac{v}{\sqrt{2}} \end{pmatrix},\tag{2.54}$$

with v given in (2.39). The gauge field mass matrix is obtained from the matrix of the covariant derivative (2.52), which in the ground state $\langle\phi\rangle$ reads

$$\langle D_\mu \phi \rangle = \begin{pmatrix} -ig\frac{v}{\sqrt{2}} \cdot \frac{A_\mu^1 - A_\mu^2}{2} \\ +i\frac{v}{\sqrt{2}} \cdot \frac{gA_\mu^3 - g'B_\mu}{2} \end{pmatrix}.\tag{2.55}$$

The masses of the gauge bosons come from the terms quadratic in the gauge field and linear in the Higgs field, and more precisely, of the vev of this term: $\langle D^\mu \phi^\dagger D_\mu \phi \rangle$. Computing the matrix product reveals the mass eigenstates :

$$W_\mu^\pm = \frac{A_\mu^1 \mp iA_\mu^2}{\sqrt{2}}, \quad M_W = \frac{1}{2}gv,\tag{2.56}$$

$$Z_\mu^0 = \frac{gA_\mu^3 - g'B_\mu}{\sqrt{g^2 + g'^2}}, \quad M_Z = \frac{1}{2}\sqrt{g^2 + g'^2}v,\tag{2.57}$$

$$A_\mu = \frac{g'A_\mu^3 + gB_\mu}{\sqrt{g^2 + g'^2}}, \quad M_A = 0.\tag{2.58}$$

Only the photon A_μ is massless after the breaking of the $SU(2) \times U(1)_Y$ symmetry – the remaining symmetry group is $U(1)_Q$ of QED. Both neutral bosons A_μ and Z_μ are superpositions of the same generators – they depend on the same basis vectors and the mixing angle between them is called the Weinberg angle :

$$\sin \theta_W = \frac{g'}{\sqrt{g^2 + g'^2}}, \quad \cos \theta_W = \frac{g}{\sqrt{g^2 + g'^2}}, \quad \tan \theta_W = \frac{g'}{g}.\tag{2.59}$$

Substituting (2.59) into (2.57),(2.58) gives the Z boson and the photon in terms of the generators and θ_W :

$$Z_\mu = \cos \theta_W A_\mu^3 - \sin \theta_W B_\mu,\tag{2.60}$$

$$A_\mu = \sin \theta_W A_\mu^3 + \cos \theta_W B_\mu.\tag{2.61}$$

The masses of the gauge bosons and the Weinberg mixing angle can be grouped together to a parameter traditionally denoted as ρ :

$$\rho = \frac{M_W^2}{M_Z^2 \cos^2 \theta_W},\tag{2.62}$$

which upon substitution of (2.56),(2.57) and (2.59) gives the (tree-level) result :

$$\rho = 1 , \quad (2.63)$$

an important prediction of the standard model, and a good test for various BSM models.

Matter sector

The spontaneous breaking of $SU(2) \times U(1)_Y$ gives masses to fermions as well as gauge bosons. This happens through the so-called Yukawa couplings of the Higgs field to the fermion fields (again, see for example [62]):

$$\mathcal{L}_{Yuk} = \lambda_e \bar{\psi}_\ell \tilde{\phi} e_R + \lambda_\nu \bar{\psi}_\ell \phi N_R + \lambda_d \bar{\psi}_q \phi d_R + \lambda_u \bar{\psi}_q \tilde{\phi} u_R + \text{h.c.} , \quad (2.64)$$

where e, N stand for the charged and neutral lepton fields, respectively, u, d are quarks of up-type and down-type and

$$\tilde{\phi} \equiv i\sigma_2 \phi^* = \begin{pmatrix} \phi^{0*} \\ -\phi^- \end{pmatrix} . \quad (2.65)$$

The masses are obtained when the scalar ϕ takes its vacuum expectation value:

$$\mathcal{L}_m^f = \langle \mathcal{L} \rangle = \lambda_e \frac{v}{\sqrt{2}} \bar{e}_L e_R + \lambda_\nu \frac{v}{\sqrt{2}} \bar{\nu}_L N_R + \lambda_d \frac{v}{\sqrt{2}} \bar{d}_L d_R + \lambda_u \frac{v}{\sqrt{2}} \bar{u}_L u_R + \text{h.c.} \quad (2.66)$$

The right-handed neutrino N_R does not exist in the SM, so the above term $\lambda_\nu \frac{v}{\sqrt{2}} \bar{\nu}_L N_R$ is only hypothetical. The issue of neutrino mass will be discussed at a later time, in Section 2.5.2. The masses of the established SM particles are :

$$m_e = -\lambda_e \frac{v}{\sqrt{2}} , \quad m_d = -\lambda_d \frac{v}{\sqrt{2}} , \quad m_u = -\lambda_u \frac{v}{\sqrt{2}} . \quad (2.67)$$

2.5 Quark and lepton mixing

Of the almost twenty free parameters of the SM ten are related to the quark sector: six give the quark masses and four parametrize the mixing between flavors, encoded in the Cabibbo – Kobayashi – Maskawa (CKM) mixing matrix [23, 106]. This mixing is a result of the quark mass eigenstates being different from the interaction eigenstates. The two eigenstates form bases that are related to each other by a unitary transformation and the CKM matrix represents this transformation that connects the two bases.

It appears that the same is true in the lepton sector: there are experimental observations suggesting that there is mixing in the lepton sector, too. This is an issue that is problematic in the SM, because in the SM framework lepton number is assumed to be a conserved quantity, prohibiting the change of leptons of one flavor into another. This question, which is closely related to the problem of neutrino mass, is the topic of the second part of this section.

2.5.1 The quark sector

In the standard $SU(2) \times U(1)$ electroweak theory the charged current Lagrangian density, in the basis of the weak interaction eigenstates, reads

$$\mathcal{L}_W = -\frac{g}{\sqrt{2}} \bar{U}_L^I \gamma^\mu D_L^I W_\mu^+ + \text{h. c.} \quad (2.68)$$

the vectors U_L^f (D_L^f) are left-handed up- (down-) quark interaction eigenstates of flavor f [107]. The Lagrangian (2.68) is diagonal in flavor space thanks to the absence of a flavor space-tensor; hence the charged current interactions are diagonal in the interaction basis. The $SU(2)_L \times U(1)_Y$ symmetry being broken by the Higgs field (Section 2.3.1) implies a distinction between the interaction and mass bases. In the interaction basis the mass matrix $M_{ij} \equiv v\Lambda_{ij}$, arising from (see *e.g.* [62])

$$\mathcal{L}_{\text{Yukawa}}^q = \Lambda_{ij}^d \bar{\psi}_{q_i} \phi d_j + \Lambda_{ij}^u \bar{\psi}_{q_i} \tilde{\phi} u_j \quad , \quad (2.69)$$

with $\Lambda_{ij}^{u,d}$ the matrix of Yukawa interactions of up and down quarks, respectively. Here ϕ is the Higgs field and $\tilde{\phi} \equiv i\sigma_2 \phi$ with σ_2 the second Pauli matrix and $\psi_{q_i} = (u_{L,i}, d_{L,i})^T$. In general M is non-diagonal, but it can always be diagonalized by a bi-unitary transformation (see *e.g.* Ref. [108])

$$M^{\text{diag}} = V_L M V_R^\dagger \quad (2.70)$$

The mass eigenstates $D_{L,R}$ satisfy $\bar{D}_L M_D^{\text{diag}} D_R = \bar{D}_L^I M_D D_R^I$, M_D being the mass matrix of the down-type quarks, so

$$D_L = V_L D_L^I \quad \text{and} \quad D_R = V_R D_R^I . \quad (2.71)$$

The charged current interaction (2.68) is then

$$\mathcal{L}_W = -\frac{g}{\sqrt{2}} \bar{U}_L \gamma^\mu V_L^\dagger D_L W_\mu^+ + \text{h. c.} , \quad (2.72)$$

whence one can deduce that V_L^\dagger is the quark mixing matrix. In a generic n generation case $V_L^\dagger \in U(n)$, containing n^2 parameters. Of these $\frac{1}{2}n(n-1)$ can be chosen as real angles and $\frac{1}{2}n(n+2)$ are phases (see *e.g.* Ref. [109]). Of the phases, $2n-1$ ones can be eliminated by a bi-unitary transformation

$$V_L^\dagger \rightarrow V = P_U V_L^\dagger P_D^* , \quad (2.73)$$

with P_u, P_D unitary diagonal matrices. The number of physically meaningful phases is therefore $\frac{1}{2}(n-1)(n-2)$. The matrix V thus obtained is the CKM matrix for three generations [23, 106]

$$V_{CKM} = \begin{pmatrix} V_{ud} & V_{us} & V_{ub} \\ V_{cd} & V_{cs} & V_{cb} \\ V_{td} & V_{ts} & V_{tb} \end{pmatrix} . \quad (2.74)$$

The elements of the CKM matrix are given by experiment. There are in principle two ways to determine the matrix elements. Charged weak decays depend on these already at tree level, so *e.g.* a measurement of a decay rate gives direct information on the corresponding CKM elements (*cf.* *e.g.* [110] and references therein). This has the advantage of allowing for the matrix elements to be extracted independently of the number of generations. On the other hand processes involving flavor-changing neutral currents (FCNCs) provide strong constraints on the CKM elements, since such processes are forbidden at tree level. The absence of such currents at tree level is due to a cancellation that is called the *GIM mechanism* [22]. FCNC processes are, however, present in loops in so called *penguin* and *box* diagrams. [111]

The different matrix elements are determined from the processes given in Table 2.1.

The current values found in literature are [55]

$$V_{CKM} \simeq \begin{pmatrix} |V_{ud}| \simeq 0.97425 \pm 0.00022 & |V_{us}| \simeq 0.2252 \pm 0.0009 & |V_{ub}| \simeq (3.89 \pm 0.44) \times 10^{-3} \\ |V_{cd}| \simeq 0.230 \pm 0.011 & |V_{cs}| \simeq 1.023 \pm 0.036 & |V_{cb}| \simeq (40.6 \pm 1.3) \times 10^{-3} \\ |V_{td}| \simeq (8.4 \pm 0.6) \times 10^{-3} & |V_{ts}| \simeq (38.7 \pm 2.1) \times 10^{-3} & |V_{tb}| \simeq 0.88 \pm 0.07 \end{pmatrix} . \quad (2.75)$$

The most striking feature of Eq. (2.75) is that the diagonal elements V_{ud} , V_{cs} , V_{tb} are clearly dominant.

Matrix element	Direct measurement from
V_{ud}	nuclear β decay
V_{us}	semi-leptonic K decay
V_{ub}	semi-leptonic B decay
V_{cd}	semi-leptonic D decay
V_{cs}	(semi-) leptonic D decay
V_{cb}	semi-leptonic B decay
V_{tb}	(single) t quark production

Table 2.1: Measurements allowing for determination of CKM matrix elements [55].

2.5.2 Beyond the SM: mixing in the lepton sector

Measurements of neutrinos produced in the sun, the atmosphere, accelerators and reactors show that neutrinos *oscillate*, that is, they change flavor in time. The oscillations are not possible if the neutrinos were massless (see Appendix C), so the oscillations provide direct proof of neutrinos being massive. In the SM neutrinos are massless, and experiments have put some upper limits on the masses, the most stringent being that of the electron anti-neutrino [55]

$$m_{\bar{\nu}_e} < 2.3 \text{ eV} \quad \text{at 95\% C.L.} \quad (2.76)$$

Furthermore, since the oscillations are just neutrinos of one flavor changing into ones of another flavor, the experimental results imply that there is *mixing in the lepton sector*, just as for the quarks. The mixing, however, poses a problem for the standard model, since it violates lepton number conservation, which is presumed in the SM. In fact, a recent study [112] gives the 90% C.L. upper limit of 2.4×10^{-12} on the branching ratio of the $\mu^+ \rightarrow e^+ \gamma$ decay, constituting the most stringent limit on the existence of this decay to date and constraining the mixing in the lepton sector.

In what follows the issues of neutrino mass and mixing will be discussed in some detail. A mathematical treatment of oscillations is given in the appendices C.

Experimental evidence for neutrino oscillations

As noted above, in several experiments neutrinos are seen to change flavor between the time of production and the time of their observation. This phenomenon, known as *neutrino oscillations* has been discussed in the literature as early as in the 1950's and 60's [113, 114] as was the issue of mixing in the lepton sector [115, 116]. Measurements made during the last ten years have striven to shed light on this. Among the results of such measurements are [117]:

- Solar ν_e 's oscillate to ν_μ or ν_τ with a statistical significance of more than 7σ [118, 119].
- Reactor-produced $\bar{\nu}_e$ are reported to disappear :
 - In 2008 the KamLAND experiment ¹ reported its first observations of $\bar{\nu}_e$ disappearance at distances of ~ 180 km and a distortion of their energy spectrum. The two pieces of evidence combined give a statistical significance of more than 3σ C.L. [120].

¹Kamioka Liquid-scintillator Anti-Neutrino Detector, <http://kamland.lbl.gov/>

- In 2012 the Daya Bay reactor neutrino experiment ² measured the mixing between the first and third generations and found it to be nonzero at a statistical significance of 5.2 standard deviations [121] (see Table 2.3). The distances from the reactor to the detectors of the experiment vary between 470m and 1678m.
- Measurements show that ν_μ disappear (it is likely that they convert to ν_τ [122]) at a significance of more than 15σ [119];
 - K2K ³ has reported the disappearance of ν_μ 's at distances of 250 km and a distortion of the energy spectrum of the neutrinos at a C.L. of $2.5 - 4\sigma$ [123].
 - LSND ⁴ has reported evidence for $\bar{\nu}_\mu \rightarrow \bar{\nu}_e$. This measurement has recently been confirmed by MiniBooNE ⁵ [124].

In light of experimental evidence, the SM clearly needs to be extended, so that the observed phenomena may be explained. A possible solution to the mixing is the inclusion of a mixing matrix, called the PMNS matrix [113, 114, 115, 116], in the lepton sector – analogously to the CKM mixing of the quark sector. But before getting to the mixing, the problem of neutrino mass needs to be discussed. We say ‘the problem of neutrino mass’ because the SM lacks right-handed neutrinos, and therefore the usual Dirac-mass terms, originating in the Yukawa couplings of the neutrinos with the Higgs field, are prohibited.

Neutrino mass

The lepton fields of the SM are arranged into $SU(2)$ doublets:

$$\begin{pmatrix} \ell \\ \nu_\ell \end{pmatrix}, \quad (2.77)$$

with ℓ the charged lepton of a given family, ν_ℓ the neutral one. Each field has quantum numbers of the $SU(2) \times U(1)$ theory: the weak hypercharge Y and the isospin I_3 , whose linear combination gives the electric charge according to Eq. (2.29). The hypercharge has couplings to the weak current, whereas the isospin couples to both neutral and charged currents. The SM leptons and their quantum numbers are listed in Table. 2.2, above the dashed line. Below the dashed line are the two neutrinos that are missing in the SM, the right-handed neutrino and the left-handed antineutrino. The lack of these prevents the neutrinos from having Dirac mass terms. Note that since the $SU(2) \times U(1)$ quantum numbers of these fields are zero, they do not interact with the gauge bosons of the electroweak theory, but are *sterile*.

The seesaw mechanism

Dirac mass terms can be introduced in the SM Lagrangian if the fields ν_R and $\bar{\nu}_L$ are added to the matter content of the theory (as is done in Table 2.2). There is, however, the possibility of another mass term, applicable for *neutral* lepton fields. This is called the ‘Majorana mass’ term [126]. Majorana neutrinos, just as SM ones, are described by two-component spinors. In the SM neutrinos

²A neutrino-oscillation experiment designed to measure the mixing angle θ_{13} using anti-neutrinos produced by the reactors of the Daya Bay Nuclear Power Plant; <http://dayabay.ihep.ac.cn/twiki/bin/view/Public/>

³From KEK to Kamioka - Long baseline neutrino oscillation experiment, <http://neutrino.kek.jp/>.

⁴Liquid Scintillator Neutrino Detector, Los Alamos National Laboratory, <http://www.nu.to.infn.it/exp/all/lsnd/>.

⁵Mini Booster Neutrino Experiment, <http://www.nu.to.infn.it/exp/all/boone/index.html>, <http://www-boone.fnal.gov/>.

N	N_x	Particle states	I_3	Y	Q
+1	L	$\begin{pmatrix} e_L \\ \nu_L \end{pmatrix}$	-1/2	-1	-1
+1	L		+1/2	-1	0
-1	R	$\begin{pmatrix} \bar{e}_R \\ \bar{\nu}_R \end{pmatrix}$	+1/2	+1	+1
-1	R		-1/2	+1	0
+1	R	e_R	0	-2	-1
-1	L	\bar{e}_L	0	+2	+1

+1	R	ν_R	0	0	0
-1	L	$\bar{\nu}_L$	0	0	0

Table 2.2: Lepton charges. N denotes fermion number, N_x left- or right-handedness, I_3 the third isospin component, Y and Q stand for hypercharge and electric charge, respectively. The fields above the dashed line are those of the SM, the fields below this line are not included in the SM. Table from Ref. [125]

are massless and described by Weyl spinors (a Dirac spinor is composed of two Weyl spinors) – a mass term may be added by including ν_R and $\bar{\nu}_L$ to the theory, as noted above. In the Majorana case the neutrino fields are described by two-component spinors, too, but there is no need to include the fields ν_R and $\bar{\nu}_L$, since a Majorana particle is its own antiparticle; the two components ν_L , $\bar{\nu}_R$ suffice. This has the consequence that Majorana particles have only half the number of degrees of freedom compared to Dirac ones.

In the most general case neutral lepton fields can have both of the mass terms mentioned above :

$$\mathcal{L}_{\text{Dirac}} = -m_D \bar{\nu}_L \mathcal{N}_R + \text{h.c.} \quad (2.78)$$

$$\mathcal{L}_{\text{Majorana}} = -\frac{1}{2} M \bar{\mathcal{N}}_L^c \mathcal{N}_R + \text{h.c.} , \quad (2.79)$$

where we denote the right-handed neutrino by N_R instead of ν_R , following the notation of [62]. Here m_D , M are the Dirac and Majorana masses, respectively and the superscript c stands for charge conjugation. The Dirac mass m_D arises from $SU(2) \times U(1)$ breaking and is of the order of the electroweak scale. The symmetry factor 1/2 in (2.79) accounts for the ‘degeneracy’ of the Majorana neutrino being its own antiparticle. Both mass terms (2.78),(2.79) can be generated by the so-called ‘Seesaw mechanism’, where the mass term is of the form (see *e.g.* [62])

$$\mathcal{L} = -\frac{1}{2} (\bar{\nu}_L (\mathcal{N}^c)_L) \begin{pmatrix} 0 & m_D \\ m_D & M \end{pmatrix} \begin{pmatrix} (\nu^c)_R \\ \mathcal{N}_R \end{pmatrix} + \text{h.c.} \quad (2.80)$$

The eigenvalues of this matrix are

$$m_{1,2} = \sqrt{\frac{1}{4}M^2 + m_D^2} \mp \frac{1}{2}M , \quad (2.81)$$

which in the limit $M \gg m_D$ gives

$$m_1 \sim \frac{m_D^2}{M} , \quad m_2 \sim M . \quad (2.82)$$

The mixing angle θ depends on the mass eigenvalues [127]

$$\tan \theta = \frac{m_1}{m_D} = \frac{m_D}{m_2} = \sqrt{\frac{m_1}{m_2}} \quad (2.83)$$

and in the present limit it reads

$$\tan \theta \sim \frac{m_D}{M} . \quad (2.84)$$

When m_D is fixed and M is increased, the mixing angle tends to zero and the two different neutrino states decouple. The Dirac mass is usually set proportional to the SM mass scale, whereas M is associated with the scale of BSM physics. We recall that the LEP bounds presented previously imply that $m_{\nu'} \gtrsim m_z/2$ while the argument of naturalness restricts the Yukawa coupling of the neutrino to be $\mathcal{O}(1)$. This restricts the Dirac component of the fourth generation neutrino mass to $m_D \simeq \mathcal{O}(100 - 500)$ GeV, which in turn implies that the mixing angle is approximately confined into the range [128]:

$$0.1 \lesssim \tan \theta \lesssim 1 . \quad (2.85)$$

For more than one generation, the above considerations are generalized in a straightforward manner (see *e.g.* [62]). In the general n generation scenario, the mass matrix M is of size $n \times n$ and complex. An arbitrary $M \in \text{GL}(N, \mathbb{C})$ is not necessarily positive definite but the operator MM^\dagger is. Hence there exists a matrix $U \in U(N)$ such that [108]

$$MM^\dagger = U m_D^2 U^\dagger , \quad (2.86)$$

with $m_D^2 = \text{diag}(m_1^2, \dots, m_N^2)$, where m_i^2 are the eigenvalues of MM^\dagger . One can just as well use another matrix $V \in U(N)$ to perform the diagonalization

$$m_D = U^\dagger M V . \quad (2.87)$$

A similar unitary matrix appears in the mass term for the charged leptons [127], we denote this by U_ℓ . The product of the charged and neutral lepton matrices then becomes the analogue of the CKM matrix for the leptons, called the PMNS matrix [113, 114, 115, 116] :

$$U_{\text{PMNS}} \equiv U_\ell^\dagger U . \quad (2.88)$$

The PMNS matrix

In order to investigate the leptonic mixing matrix, let us define weak and mass eigenfields ν_W and ν_M by

$$\nu_W \equiv \begin{pmatrix} \nu_e \\ \nu_\mu \\ \nu_\tau \end{pmatrix} \quad \text{and} \quad \nu_M \equiv \begin{pmatrix} \nu_1 \\ \nu_2 \\ \nu_3 \end{pmatrix} . \quad (2.89)$$

The states that are physically observed are the ones taking part in interactions, that is, the states ν_W . The two different bases in (2.89) are related by

$$\nu_W = U \nu_M . \quad (2.90)$$

with $U \in U(3)$ for three generations (see also Section 2.5.1 and Appendix C).

The Majorana case differs from the Dirac one in that the Majorana condition $\nu = \nu^c$ does not allow a certain number of phases to be absorbed into neutrino phases. Only N phases, equal to the

number of charged leptons which are Dirac particles, can be absorbed into charged lepton phases, giving $\frac{1}{2}N(N-1)$ unabsorbed phases. [127]

There are several ways to parametrize the 3×3 unitary matrix for three generations, depending on whether the particles are Dirac or Majorana. One of these, perhaps the best known, is the Cabibbo – Kobayashi – Maskawa (CKM) representation [23, 106]

$$U_{\text{PMNS}} = \begin{pmatrix} c_{12}c_{13} & s_{12}c_{13} & s_{13}e^{-i\delta} \\ -s_{12}c_{23} - c_{12}s_{23}s_{13}e^{i\delta} & c_{12}c_{23} - s_{12}s_{23}s_{13}e^{i\delta} & s_{23}c_{13} \\ s_{12}s_{23} - c_{12}c_{23}s_{13}e^{i\delta} & -c_{12}s_{23} - s_{12}c_{23}s_{13}e^{i\delta} & c_{23}c_{13} \end{pmatrix} \times \begin{pmatrix} 1 & & \\ & e^{i\frac{\alpha_{21}}{2}} & \\ & & e^{i\frac{\alpha_{31}}{2}} \end{pmatrix} \quad (2.91)$$

where $c_{ij} \equiv \cos \theta_{ij}$, $s_{ij} \equiv \sin \theta_{ij}$, the angles $\theta_{ij} \in [0, \pi/2]$, the Dirac CP violating phase $\delta \in [0, \pi/2]$ and α_{21} , α_{31} are the two Majorana CP violating phases [55]. The current values for the parameters $\sin \theta_{ij}$ are shown in Table 2.3. The value of the parameter δ is yet unknown.

Parameter	Best fit $\pm 1\sigma$
$\sin^2 \theta_{12}$	$0.312^{+0.017}_{-0.015}$
$\sin^2 \theta_{23}$	0.51 ± 0.06 0.52 ± 0.06
$\sin^2 \theta_{13}$	$0.092 \pm 0.016(\text{stat}) \pm 0.005(\text{syst})$

Table 2.3: Values of the neutrino mixing angles, with the statistical (stat) and systematical (syst) errors given separately for $\sin^2 \theta_{13}$. For $\sin^2 \theta_{23}$ the upper (lower) row corresponds to normal (inverted) neutrino mass hierarchy. $\sin^2 \theta_{12}$ and $\sin^2 \theta_{23}$ values from Ref. [129], $\sin^2 \theta_{13}$ from Ref.[121].

Part II

The minimal four-generation model

Chapter 3

Phenomenology of the fourth family

In this part we consider adding a sequential fourth generation of elementary particles to the standard model, *sequential* meaning that the fourth family has the same structure as the first three families. This means adding one quark and one lepton doublet to the SM :

$$\text{quark doublet } \begin{pmatrix} t' \\ b' \end{pmatrix}, \quad \text{lepton doublet } \begin{pmatrix} \ell' \\ \nu'_\ell \end{pmatrix}, \quad (3.1)$$

such that the particles of (3.1) have the same quantum numbers as their counterparts in the first three families (the t' quark is the fourth family ‘equivalent’ to the u, c, t quarks of the first, second and third families, respectively, and so on). In the Introduction appealing features of this extension were considered; in this chapter we will focus on the phenomenological implications of and the experimental constraints on a fourth family.

3.1 Mixing of the fourth family with the first three ones

As already discussed (see Section 2.5.1), the phenomenon of mixing in the quark sector is well established in the SM. Apparently also the neutrinos ‘mix’ among themselves, as observed in the neutrino oscillations presented above (Section 2.5.2). It may seem natural that since the first three families mix among themselves, that a sequential fourth generation would do so too. The mixing of the fourth family is constrained by both theoretical and experimental considerations, as we shall see, but it is not ruled out by the already measured CKM matrix elements. The task of measuring with better precision these parameters and determining the number of fermion families is one of the goals of the LHC [63, 130]) and further at the ILC [131].

In this section we will often use the notation ‘CKM3’ and ‘CKM4’ to denote the 3×3 and 4×4 mixing matrices of the three-generation and four-generation models, respectively.

3.1.1 Sources for constraints

CKM Unitarity

The 3×3 CKM submatrix is well tested by a variety of processes, as discussed previously (see Section 2.5.1 and especially Table 2.1). The unitarity of the CKM matrix constrains the elements of each row and column :

$$\sum_{j=1}^4 |V_{ij}^2| = 1 \quad \text{for fixed } i, \quad \sum_{i=1}^4 |V_{ij}^2| = 1 \quad \text{for fixed } j. \quad (3.2)$$

When the currently measured values of the 3×3 matrix are taken into account, the unitarity constraint (3.2) allows to deduce some of the mixing parameters [132]:

$$1^{\text{st}} \text{ row} : |V_{ub'}|^2 = 1 - |V_{ud}|^2 - |V_{us}|^2 - |V_{ub}|^2 \simeq 0.0008 \pm 0.0011 \quad (3.3)$$

$$2^{\text{nd}} \text{ row} : |V_{cb'}|^2 = 1 - |V_{cd}|^2 - |V_{cs}|^2 - |V_{cb}|^2 \simeq -0.003 \pm 0.027 \quad (3.4)$$

$$1^{\text{st}} \text{ column} : |V_{t'd}|^2 = 1 - |V_{ud}|^2 - |V_{cd}|^2 - |V_{td}|^2 \simeq -0.001 \pm 0.005 . \quad (3.5)$$

Requiring Eqs. (3.3)–(3.5) to be valid at 1σ one finds

$$|V_{ub'}| \lesssim 0.04 , \quad |V_{cb'}| \lesssim 0.17 , \quad |V_{t'd}| \lesssim 0.08 . \quad (3.6)$$

All of these are larger than the smallest elements of the CKM matrix, namely $|V_{ub}|$ and $|V_{td}|$ (see Eq. (2.75)).

Oblique electroweak corrections

Global fits to electroweak precision data serve to constrain the mixing between third and fourth family quarks. The dominant constraint comes from nondecoupling oblique corrections, denoted by the parameters S, T, U (see Appendix D).

Two of the electroweak (EW) precision observables have a quadratic dependence on the masses of the fourth generation fermions and therefore serve to constrain the SM4: the ρ parameter [133, 134, 135] correction through the oblique parameter T [136, 137] and the $Z\bar{b}b$ vertex correction (Fig. 3.1)

$$R_b = \frac{\Gamma(Z \rightarrow \bar{b}b)}{\Gamma(Z \rightarrow \text{hadrons})} . \quad (3.7)$$

This quantity is highly relevant in the study of the fourth generation because, as shown in Fig. 3.1, the $Z \rightarrow \bar{b}b$ partial decay width has corrections from fourth-generation quark loops, in addition to the oblique corrections [86]. This dependence differs from what is expected at 1-loop order in the SM [45]

$$\delta\rho, \delta R_b|_{\text{SM}} \propto G_F m_t^2 , \quad (3.8)$$

$$\delta\rho, \delta R_b|_{\text{SM4}} \propto |V_{t'b}|^2 \cdot (m_t^2 - m_{t'}^2) , \quad (3.9)$$

evaluated from the nondecoupling vertex correction from the $t + W$ diagrams. The correction of (3.9) is the one arising from 3–4 CKM mixing.

These relations serve to constrain the free parameters of the fourth generation, since they both have been measured with good precision. Specifically, the value of the rho-parameter is known to be very close to one [59]:

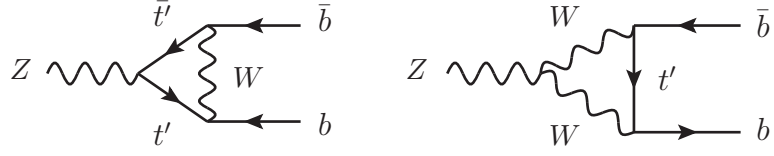
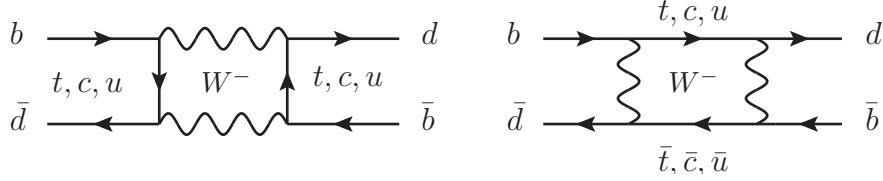
$$\rho = 1.0004_{-0.0004}^{+0.0003} , \quad (3.10)$$

as obtained from global fits to electroweak precision data.

If the mass splitting of the fourth quark doublet is large ($m_{b'}^2 \gg m_{t'}^2$) then there are also large corrections proportional to $|V_{t'b}|^2 m_{b'}^2$. [45]

Flavor changing neutral currents

Also processes including flavor changing neutral currents (FCNCs) constrain new-physics models. This is so because FCNCs are absent at tree level in the SM, thanks to the unitarity of the CKM matrix and the inclusion of just one Higgs doublet (the case of two Higgs doublets will be discussed

Figure 3.1: One-loop correction to the $Zb\bar{b}$ –vertex from t' .Figure 3.2: Box diagrams for B_d mixing.

further on) and no new gauge bosons [138]. From experiments it is also known that the FCNCs are suppressed, so BSM models should have this property in order to be valid options for new physics.

When the CKM matrix is enlarged from 3×3 to 4×4 , the 3×3 submatrix loses its unitary nature, as can be seen in Eq. (3.2). This allows for new FCNC processes, which must be in agreement with data in order for the four-generation model to be a possible extension to the SM. The amplitudes of FCNC processes, such as B_d or K mixing (see Fig. 3.2 for the former) depend on the CKM matrix elements, and so measurements of the cross section of a given process gives information about the matrix elements when all other parameters appearing in the amplitude are known. This is an especially good method for observables that have been measured with high precision.

Higgs mass

Measurements of the Higgs mass – the regions that have been excluded by LEP and Tevatron, and the unitarity limit – constrain mixing of the third and fourth generations. As discussed above, part of the fits' dependence on the third–fourth generation mixing angle θ_{34} comes from the nondecoupling fermion corrections to the oblique parameters, and especially T . The T parameter is furthermore related to the Higgs mass: a positive value of T pushes m_H to higher values, and so there is a dependence of the CKM4 entries on the Higgs mass. [139]

3.1.2 Possible parameter space

The elements of the mixing matrix as well as the mixing angles themselves have been analyzed in several studies during the last few years. However, there is some controversy in the choice of parameters that are allowed to vary when searches for the best fits are made. The choice of free parameters affects the bounds set on the mixing angles, and thus the bounds resulting from various studies often differ. Interestingly, sometimes neglecting some of the observables (such as hadron asymmetry) when doing the fits leads to an improvement in its quality for some observable, but at the same time the fit gets worse when another observable is considered instead.

In this section we attempt to review some of the results, emphasizing the choice of data that is fitted and which variables are left free or possibly left out completely. We note that in light of recent results concerning the Higgs boson (see Chapter 5) some of the results below are already dated, but will be presented for the sake of academic interest nevertheless.

Quite sizeable mixings seem to be allowed in a study [111] that takes its experimental constraints from

- (i) tree-level CKM3 elements in such a way as to restrict the CKM4 elements using

$$|V_i| - 2\Delta V_i < |V_{\text{CKM4},i}| < |V_i| + 2\Delta V_i, \quad (3.11)$$

where the V_i are the experimental values as given by the PDG [55], the errors being ΔV_i ,

- (ii) the unitarity of the CKM matrix,

- (iii) the following FCNC processes: K, D, B_d and B_s –mixing, the decay $b \rightarrow s\gamma$ (see Fig. 3.2 for the Feynman diagrams for B_d –mixing).

The choice for free and fixed parameters is:

- (iv) the CP violating phases δ_{13}, δ_{14} and δ_{24} are left unconstrained,
- (v) $m_{t'}$ is varied from 300 to 650 GeV, such that the fourth generation quark masses are related through

$$m_{b'} = m_{t'} - 55 \text{ GeV} . \quad (3.12)$$

Furthermore, some simplifying assumptions are made concerning the QCD corrections below, and any correlations with the lepton mixing matrix are neglected.

This choice of input parameters and experimental constraints seems to favor small mixing of the fourth generation with the other ones, but larger mixings are not excluded – in fact, there seems to be a region of parameter space where sizeable mixing is allowed. The mixing angles θ_{14}, θ_{24} and θ_{34} are shown in Table 3.1, for both conservative and aggressive bounds.

Parameter	Conservative bound	Aggressive bound
θ_{14}	≤ 0.0535	≤ 0.0364
θ_{24}	≤ 0.144	≤ 0.104
θ_{34}	≤ 0.737	≤ 0.736

Table 3.1: Allowed mixing angles, resulting from the analysis of Ref. [111]. The conservative bounds assume $\chi^2/\text{d.o.f.} < 2$, while for the aggressive constraints $\chi^2/\text{d.o.f.} < 0.5$ is required (see Eq. (A.1) for the definition of χ^2).

New FCNC processes and the following two kinds of experimental constraints are taken into account in the analysis of Ref. [138]:

- (i) the measured values of CKM3, using conservative bounds (conservative meaning in this case that the bounds are related to the experimental values that take the largest uncertainties into account, and that the orthonormality constraints on the rows and columns of the CKM3 matrix are not taken into account),

(ii) current bounds for FCNC processes.

When left–right symmetry is assumed (meaning that D_L and D_R in (2.71) are equal), the largest allowed mixings of the fourth generation may be computed, giving a CKM4 matrix :

$$V = \begin{pmatrix} 0.974 & -0.227 & 0.003 & -2.0 \times 10^{-3} \\ 0.227 & 0.973 & -0.040 & 2.1 \times 10^{-2} \\ 0.007 & 0.044 & 0.920 & -0.39 \\ -3.7 \times 10^{-4} & -3.6 \times 10^{-3} & 0.39 & 0.92 \end{pmatrix}. \quad (3.13)$$

It is worth noting that the large value of V_{tb} largely violates the ordinary 3×3 unitarity condition of the known mixing matrix. As is seen from Eq. (2.75), this element has not yet been measured with very good precision and the error ΔV_{tb} in (2.75) is quite large so the present situation allows for $0.90 \leq V_{tb} \leq 0.94$. This is in part due to the insufficient statistics on the production rate of heavy quarks and also to the small branching ratios of FCNC processes. The branching ratios are small not just because the matrix elements are small but because semileptonic top quark decays are enhanced by the same matrix elements. The LHC should allow for more precise measurements of the characteristics of heavy quarks, since these are expected to be produced in large numbers. It may be possible to reach a sensitivity of 10^{-5} or 10^{-6} for FCNC processes at the LHC, in which case the proposed matrix (3.13) may be verified or discarded. [138]

The two above reviewed studies are controversial when the experimental constraints are taken to be those of electroweak precision data (EWPD) [45]. The analysis is based upon *global* fits to the EWPD, instead of focusing on just one observable. The global fits to the data need furthermore to be *reevaluated* entirely – it is not sufficient to use the magnitude of shifts from the values of parameters in the SM fit. In this way the minimum of χ^2 may be at values that are significantly different from the SM fit and furthermore effects arising from statistical fluctuations and systematic uncertainties are smaller. [45] Global fits, when reevaluated using the same parameter set that the LEP electroweak working group [81], namely varying four SM parameters :

$$m_t, \Delta\alpha_5, \alpha_s \text{ and } m_H, \quad (3.14)$$

such that m_H may vary freely between 10 GeV and 1 TeV. In (3.14) $\Delta\alpha_5$ is the five flavor hadronic contribution to the renormalization of the electromagnetic coupling at the Z -pole (note that $m_t > m_Z$ so only five flavors contribute) and α_s is the strong coupling ‘constant’. The parameter $\Delta\alpha_5$ is the dominant uncertainty in $\alpha(m_Z)$. Differing from the LEP EWWG, the W width is neglected, since its precision is poor and this parameter has only a small effect on the results.

Setting the fourth generation quark masses to satisfy (3.12) and choosing $m'_\nu = 100$ GeV, $m'_\ell = 145$ GeV, the global fits give results as shown in Fig. 3.3 and Table 3.2. Table 3.2 shows that the limit on $|s_{34}|$ behaves as $m_{t'}^{-1}$ for $m_{t'} \gg m_t$. For these fits the Higgs boson mass is $m_H = 790 \pm 30$ GeV and the correction from the fourth generation to the oblique parameter T : T_4 is 0.47 ± 0.01 at 95% confidence level. In all the cases studied in [45] $|V_{tb}| \simeq |V_{t'b'}| \simeq |\cos \theta_{34}| \geq 0.94$ and for $m_{t'} \geq 500$ GeV $|\cos \theta_{34}| \geq 0.99$, meaning that *mixing between the third and fourth generation might well be of the order of Cabibbo mixing* of the first two families. However, mixing angles as large as those reported in [111], [138] are excluded by this analysis.

The upper limits of the mixing angles are not reported to depend sensitively on the choice of $m_{t'} - m_{b'}$, but no acceptable fits are found for larger mass differences $m_{t'} - m_{b'} \gtrsim 100$ GeV: at $|s_{34}| = 0$ the fits are poor ($\text{CL}(\chi^2) < 0.03$), and quickly become worse as $|s_{34}|$ increases. On the other hand, for smaller mass splittings, *e.g.* at the limiting case of $m_{t'} = m_{b'}$ the confidence limits

$m_{t'}$	T_4	$m_H(\text{GeV})$	$ s_{34}^{(1)} $	$ s_{34}^{(2)} \pm \Delta_{tb'}^{(2)}$	$ c_{34}^{(2)} $
300	0.46	760	0.32	0.35 ± 0.001	0.94
326	0.47	760	0.28	0.30 ± 0.002	0.95
389	0.48	760	0.21	0.23 ± 0.004	0.97
400	0.47	800	0.20	0.22 ± 0.005	0.98
500	0.48	810	0.15	0.17 ± 0.007	0.99
600	0.48	800	0.12	0.14 ± 0.010	0.99
654	0.48	820	0.11	0.13 ± 0.013	0.99
1000	0.49	820	0.07	0.11 ± 0.10	0.99

Table 3.2: 95% CL upper limits on $|s_{34}|$ at one and two loops from global fits to the EWWG data set. T_4 and m_H from the 95% CL fits are also shown, T_4 being the correction from the fourth generation to the oblique parameter T (see Appendix D). Table from Ref. [45]

of χ^2 are acceptable for $|s_{34}| = 0$ but then $m_H = 35$ GeV and then the confidence level becomes very poor, ‘unacceptable’ according to [45]: $\text{CL}(m_H > 114 \text{ GeV}) = 0.0016$.

This conclusion is supported when constraints from the Higgs boson mass are taken into account [139]. When fits are made to the data set of the EWWG and low-energy data is added, the allowed parameter space of $s_{34} \equiv \sin \theta_{34}$ as a function of m_H is as in Fig. 3.4 for different fourth generation quark masses. The upper bounds on $|\sin \theta_{34}|$ are [139]:

$$|\sin \theta_{34}| \lesssim 0.27 \quad \text{for } m_{t',b'} \simeq 350 \text{ GeV} , \quad (3.15)$$

$$|\sin \theta_{34}| \lesssim 0.17 \quad \text{for } m_{t',b'} \simeq 500 \text{ GeV} . \quad (3.16)$$

It is furthermore found that the LEP exclusion region, except for the interval between 114 and 131 GeV, rules out zero mixing $s_{34} = 0$.

Cabibbo-sized mixing between the fourth and second families may also be possible [140, 141, 72]. Regions have been found in the CKM4 parameter space that can explain possible anomalies in B meson CP measurements. These regions require large mixing of the second and fourth families as well as the third and fourth ones. In [140, 141] it was found that for $m_{t'} = 300$ GeV and $|s_{34}| = 0.22$ the 2-4 mixings

$$|V_{t's}| = 0.114 \quad \text{and} \quad |V_{cb'}| = 0.116 \quad (3.17)$$

are allowed – a conclusion that has later been confirmed [45].

However, it may be that even Cabibbo-sized mixing is disfavored as argued in more recent analyses [142, 143]. Apparently the four family model with such mixing and with the Higgs boson, t' and b' close to their unitarity bounds is strongly conflicting with electroweak data and that while the electroweak precision constraints have eased somewhat, a fourth family remains disfavored given that adding it deteriorates the global fit.

Constraints on the mixing of the leptons in the fourth family has not been studied in as much detail as the quark sector. In one study [132] bounds on the PMNS4 matrix are computed,

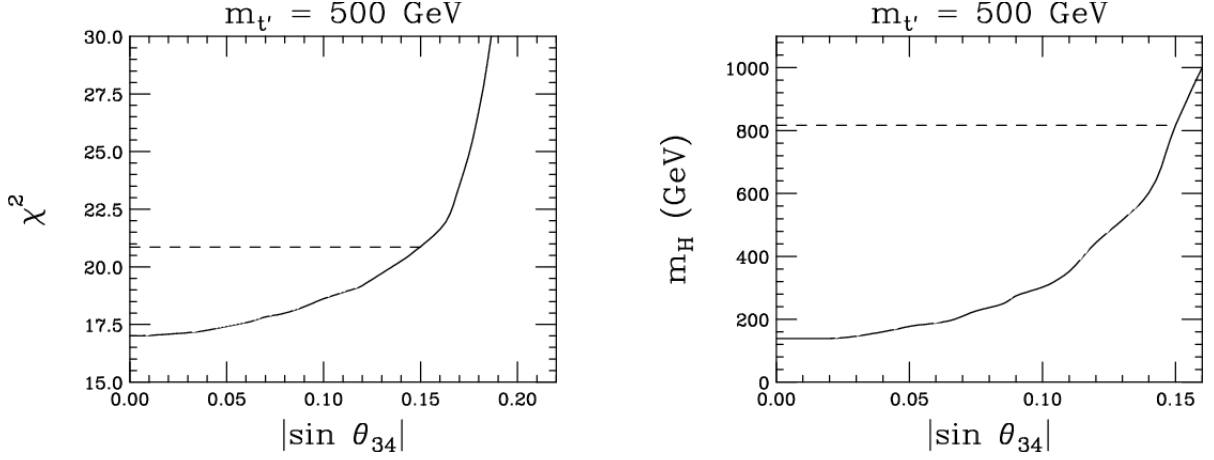


Figure 3.3: On the left the χ^2 distribution, on the right the Higgs boson mass, both as functions of $|\sin \theta_{34}|$ for the global fit to the four family model with $m_{t'} = 500$ GeV. The horizontal lines indicate the 95% confidence interval for $|\sin \theta_{34}| \leq 0.15$. Figures from Ref. [45]

taking into account constraints from lepton flavor violation both in the charged and neutral sectors – the most stringent bound coming from $\mu \rightarrow e\gamma$ decay, which has not been observed. A region of parameter space that seems to be in agreement with all experimental constraints and further has minimal contributions to the oblique parameters is reported :

$$\begin{aligned}
 m_{\ell'} - m_{\nu'} &\simeq 30 - 60 \text{ GeV} , \\
 m_{t'} - m_{b'} &\simeq \left(1 + \frac{1}{5} \ln \frac{m_H}{115 \text{ GeV}} \right) \times 50 \text{ GeV} , \\
 |V_{ub'}|, |V_{t'd}| &\lesssim 0.04 \quad \text{and} \quad |U_{e\ell'}|, |U_{\mu\ell'}| \lesssim 0.02 .
 \end{aligned} \tag{3.18}$$

Here the PMNS matrix is denoted by U (V is the CKM matrix). The upper bound on the PMNS matrix elements relating the first and fourth, as well as the second and fourth, is found to be at ~ 0.02 .

3.2 Higgs production and partial decay widths

The Higgs field, responsible for the breaking of $SU(2) \times U(1)$ electroweak gauge symmetry is one of the still open issues in particle physics, and the search for the Higgs boson a major goal at particle colliders. In addition to being of interest due to its fundamental part in the standard model, the Higgs boson could, through measurements of its properties, also provide information about BSM models. In this section we focus on the phenomenological impacts of the fourth generation on observables of the Higgs field.

3.2.1 Higgs production at hadron colliders

In high-energy pp or $p\bar{p}$ collisions the dominant Higgs production mechanism is gluon fusion, proceeding through a quark loop, as shown in Fig. 3.5. This is so because at high energies the gluon density dominates that of the quarks in the proton (see Fig. 3.6). Fig. 3.6 shows the gluon, sea and

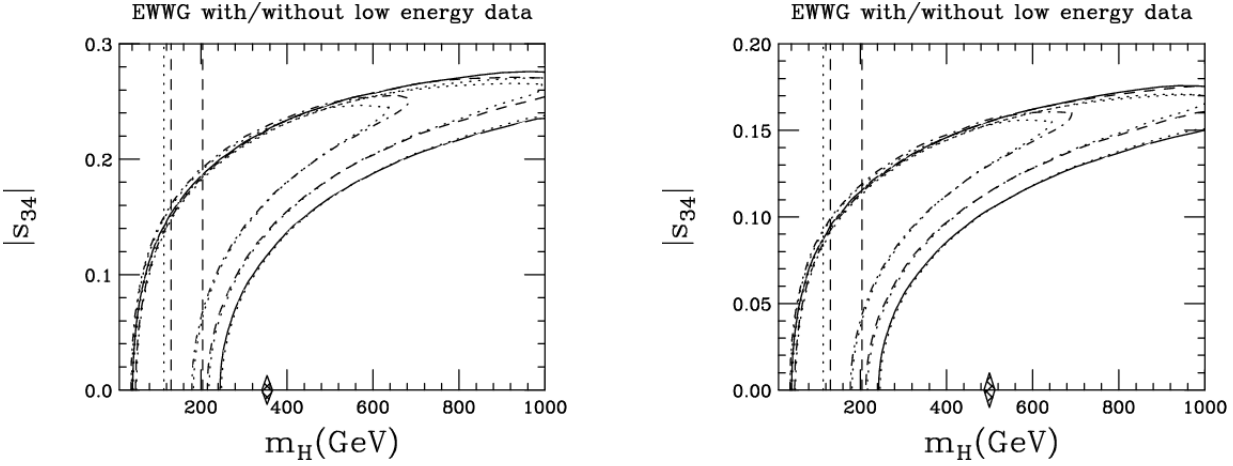


Figure 3.4: 95% CL contour plots for SM4 with $m_{t'}, m_{b'} = 354, 338$ GeV (left) and $500, 484$ GeV (right) and different $\Delta\alpha_5(m_Z)$ inputs: $\Delta\alpha_5 = 0.02758(35)$ solid, $0.02760(15)$ dashed, and $0.02793(11)$ dash-dot. The nearly identical dotted contours include the low energy data. The vertical dotted and dashed lines indicate the LEP II and Tevatron 95% exclusion regions, and the diamond on the abscissa marks the stability bound $m_H \gtrsim m_{t'}$. Figures and caption from Ref. [139].

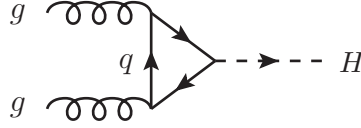


Figure 3.5: Higgs production through gluon fusion.

valence quark densities for the two energies $Q^2 = 10 \text{ GeV}^2$ (left) and 10000 GeV^2 (right) as functions of the longitudinal momentum fraction x . It should be noted that the gluon and sea distributions have been scaled down by a factor of 20, to better fit into the same graph. One sees that especially for small x the gluon density is overwhelming.

The effective Lagrangian describing the $gg\phi$ interaction, with ϕ denoting the Higgs field, reads [145]

$$\mathcal{L}_{eff} = -(\sqrt{2}G_F)^{\frac{1}{2}} m_q \frac{\alpha_s(m_H^2)}{12\pi} I G_{\mu\nu}^a G^{a\mu\nu} \phi, \quad (3.19)$$

where $\alpha_s(m_H^2)$ is the strong coupling constant evaluated at m_H^2 , the color field tensor $G_{\mu\nu}^a = \partial_\mu g_\nu^a - \partial_\nu g_\mu^a + gf^{abc}A_\mu^b A_\nu^c$ with g_μ^a the gluon field. Here, as in Section 2.1, μ is a Lorentz index and a is the index of the gauge group $SU(3)$. The parameter I in (3.19) is a function :

$$I = \sum_q I_q, \quad I_q = 3 \int_0^1 dx \int_0^{1-x} dy \frac{1 - 4xy}{1 - \frac{xy}{\lambda_q} - i\epsilon} = 3 [2\lambda_q + \lambda_q(4\lambda_q - 1)f(\lambda_q)] . \quad (3.20)$$

where the term $-i\epsilon$ in the denominator of the integrand ensures the convergence of the integral and

$$\lambda_i \equiv m_i^2/m_H^2 \quad (3.21)$$

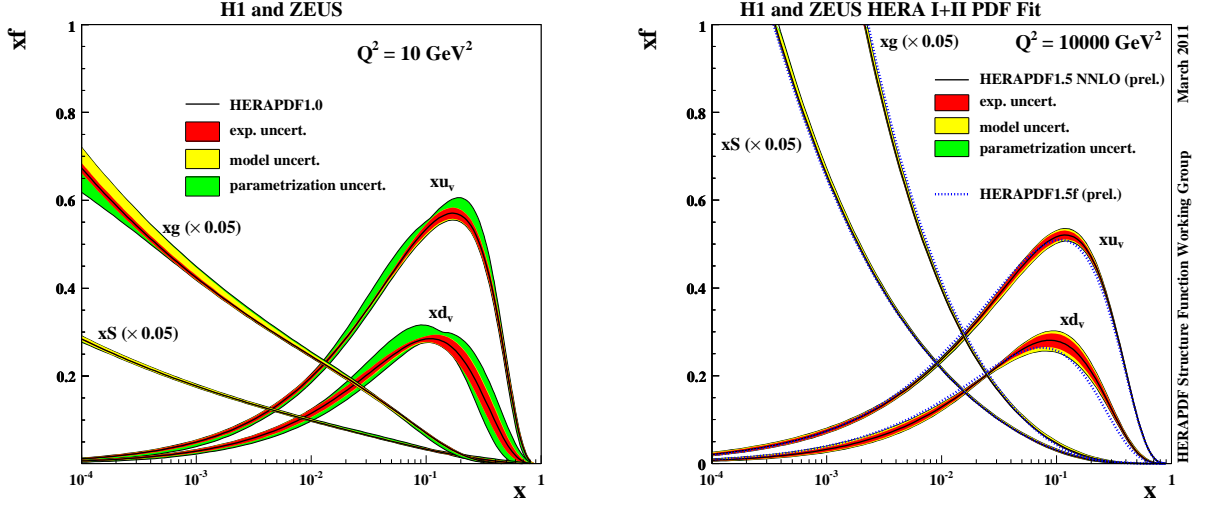


Figure 3.6: The parton distribution functions from HERAPDF1.0 at $Q^2 = 10 \text{ GeV}^2$ (left) and 10000 GeV^2 (right). The gluon and sea distributions are scaled down by a factor of 20. The experimental, model and parametrization uncertainties are shown separately. The RHS figure covers the region relevant for the hadron colliders TEVATRON and LHC. In this figure, the central values of HERAPDF1.0 NNLO are also shown. Figure and caption from Ref. [144]

and the function $f(\lambda_q)$ is

$$f(\lambda) = \begin{cases} -2 \left(\sin^{-1} \frac{1}{2\sqrt{\lambda}} \right)^2 & \text{for } \lambda > \frac{1}{4} \quad \left(\text{i.e. } m_q > \frac{m_H}{2} \right) \\ \frac{1}{2} \left(\ln \frac{\eta^+}{\eta^-} \right)^2 - \frac{\pi^2}{2} + i\pi \ln \frac{\eta^+}{\eta^-} & \text{for } \lambda < \frac{1}{4} \quad \left(\text{i.e. } m_q < \frac{m_H}{2} \right) \end{cases} \quad (3.22)$$

with $\eta^\pm = \frac{1}{2} \pm \sqrt{\frac{1}{4} - \lambda}$.

In the limit of large m_q ($\lambda_q \gg 1$) $I_q \rightarrow 1$, as seen from Eqs. (3.20), (3.22), and in the other limit, small m_q ($\lambda_q \ll 1$) $I_q \rightarrow 0$. Due to the behavior of I_q for the limiting case of heavy quarks, the top quark contribution is the most dominant one in the SM, and the heavy quarks of the fourth generation are expected to contribute significantly to (3.20), too.

The cross section for the production of a Higgs boson via gluon fusion is [145]

$$\sigma(pp \rightarrow H + \text{anything}) = \Gamma(H \rightarrow gg) \cdot \frac{\pi^2}{8m_H^3} \tau \int_\tau^1 \frac{dx}{x} g(x, m_H^2) g\left(\frac{\tau}{x}, m_H^2\right), \quad (3.23)$$

where $\tau = m_H^2/s$ and $g(x, Q^2)$ is the gluon distribution evaluated at $x = Q^2$. The partial decay rate of $H \rightarrow gg$ is

$$\Gamma(H \rightarrow gg) = \frac{G_F m_H^3}{36\sqrt{2}\pi} \left[\frac{\alpha_s(m_H^2)}{\pi} \right]^2 n_{hf}^2 \quad (3.24)$$

with n_{hf} the number of heavy quark flavors.

Substituting (3.24) into (3.25) gives

$$\sigma(pp \rightarrow H + \text{anything}) = \frac{G_F}{\sqrt{2}} \left(\frac{\alpha_s}{3\pi} \right) \frac{\pi N^2}{32} \frac{\tau}{m_H} \int_\tau^1 \frac{dx}{x} g(x, m_H^2) g\left(\frac{\tau}{x}, m_H^2\right), \quad (3.25)$$

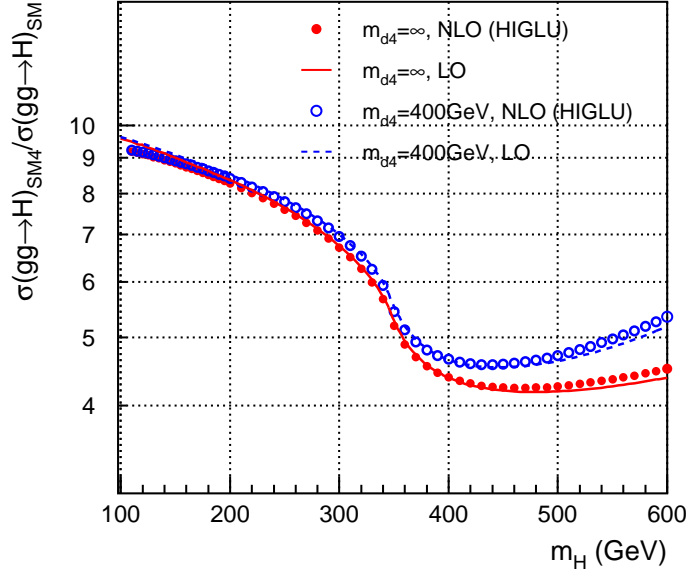


Figure 3.7: The enhancement factor of the Higgs production cross section at leading order (LO) and next-to-leading order (NLO) in a fourth generation over that of the SM as a function of m_H for two scenarios with $m_{b'} = 10$ TeV and 400 GeV. The notation used is $m_{d4} \equiv m_{b'}$. Figure from Ref. [146].

In a fourth generation with two additional heavier quarks t' and b' , the Higgs production cross section is enhanced with respect to the SM cross section due to the function I in (3.20), where the quark flavors are summed over and we already pointed out that the main contribution comes from the heaviest quarks. The ratio of the cross sections SM4 to SM is then just the ratio of their respective I :s [146]

$$R_{\sigma(gg \rightarrow H)}^{\text{SM4/SM}} \equiv \frac{\sigma(gg \rightarrow H)_{\text{SM4}}}{\sigma(gg \rightarrow H)_{\text{SM}}} = \frac{|I_b + I_t + I_{t'} + I_{b'}|^2}{|I_b + I_t|^2}. \quad (3.26)$$

The dependence of the function (3.26) on the Higgs boson mass has been computed [146] for two different $m_{b'}$ values, one of 10 TeV ('infinite mass') and the other 400 GeV, with t' fixed in both cases [132]

$$m_{t'} = m_{b'} + 50 + 10 \cdot \ln \left(\frac{m_H}{115 [\text{GeV}]} \right), \quad (3.27)$$

in order to be consistent with electroweak data. The result is shown in Fig. 3.7.

The maximal enhancement factor ~ 9 is obtained for a light Higgs boson when $I_b \rightarrow 0$ and $I_t, I_{t'}, I_{b'} \rightarrow 1$. At low m_H the enhancement factor is seen to be independent of the fourth generation quark masses (the red and blue curves in Fig. 3.7 overlap). The 'infinite mass' scenario might however not be entirely trustworthy since, as already discussed in Section 1.3, at masses beyond ~ 500 GeV [133, 134] the interactions between the heavy particles becomes strong and perturbation theory is no longer valid. But since the infinite mass scenario gives the smallest enhancement to the cross section, this just means that the exclusion limits are more conservative.

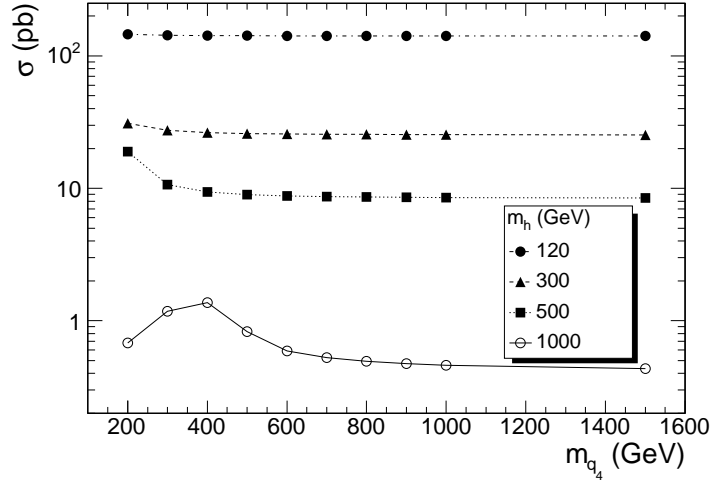


Figure 3.8: The Higgs boson production cross section for different Higgs masses as a function of the fourth generation quark mass $m_{q'}$ (the fourth generation quarks are taken to be degenerate). Figure from Ref. [148].

When the fourth generation quarks are very heavy with respect to the Higgs, $m_{q'} \gg m_H$, the Higgs coupling cancels the mass dependence of each of the three propagators of the quark loop. Hence the $gg\phi$ coupling is asymptotically independent of the masses of the fourth generation quarks. [147] This can be seen in Fig. 3.8 for the case of a degenerate fourth generation [148]. It is interesting to note that for $m_H \leq 300$ GeV the cross section seems to be independent of $m_{q'}$ (the three upmost curves in Fig. 3.8 are nearly horizontal).

3.2.2 Branching fractions

In particle detectors the Higgs will be indirectly seen from its decay products. When the number of events in the various channels is known, the branching fractions can be computed, giving in turn valuable information about the couplings. The presence of a fourth generation may affect the Higgs decays in such a way that the branching fractions differ from those predicted by the standard model. If so, this will be a measurable effect and hence the discovery of the Higgs and the measurement of its branching ratios will give information about the fourth generation and vice versa: the fourth generation also affects, through loops, Higgs pair production and the Higgs self coupling.

Higgs decay to two photons

The $H \rightarrow \gamma\gamma$ is similar to $H \rightarrow gg$ considered above (Eq. (3.24)), except that charged leptons, the W boson and the charged Higgs bosons also contribute to the loop. The effective Lagrangian, obtained from the low energy theorem, is then [145]

$$\mathcal{L}_{\text{eff}} = -\frac{\alpha}{8\pi}(\sqrt{2}G_F)^{\frac{1}{2}}IF_{\mu\nu}F^{\mu\nu}H \quad (3.28)$$

and the $H \rightarrow \gamma\gamma$ decay rate is

$$\Gamma(H \rightarrow \gamma\gamma) = \frac{G_F m_H^3}{8\sqrt{2}\pi} \left(\frac{\alpha}{\pi}\right)^2 |I|^2. \quad (3.29)$$

Here

$$I = \sum_q Q_q^2 I_q + \sum_\ell Q_\ell^2 I_\ell + I_W + I_S , \quad (3.30)$$

where Q_f denotes the charge of fermion f and the I_i , representing the quark, lepton, W boson and colorless charged scalar contributions, are

$$\begin{aligned} I_q &= 3[2\lambda_q + \lambda_q(4\lambda_q - 1)f(\lambda_q)] , \\ I_\ell &= 2\lambda_\ell + \lambda_\ell(4\lambda_\ell - 1)f(\lambda_\ell) , \\ I_W &= 3\lambda_W(1 - \lambda_W)2f(\lambda_W) - 3\lambda_W - \frac{1}{2} , \\ I_S &= -\lambda_S[1 + 2\lambda_S f(\lambda_S)] , \end{aligned} \quad (3.31)$$

with λ_i as in Eq. (3.21). For all $\lambda_i \gg 1$ Eq. (3.30) simplifies to

$$I \simeq \sum_q Q_q^2 + \frac{1}{3} \sum_\ell Q_\ell^2 - \frac{7}{4} - \frac{1}{12} . \quad (3.32)$$

The fermions and bosons contribute with opposite signs. In the other limit, that of $\lambda_i \ll 1$, only the W loop contributes and one has $I \simeq -\frac{1}{2}$.

In a fourth generation model both I_q and I_ℓ terms receive additional contributions from the fourth generation quarks q' and the charged lepton ℓ' .

Also the width $\Gamma(H \rightarrow \gamma Z)$ is affected by fourth generation quark loops. Especially the modes $gg, \gamma\gamma$ and γZ are affected at low values of m_H .

Higgs decay to weak bosons

The couplings of the Higgs boson to the weak gauge fields is [145]

$$\mathcal{L} = (\sqrt{2}G_F)^{\frac{1}{2}}(2m_W^2 HW_\mu^+ W^{-\mu} + m_Z^2 H Z_\mu Z^\mu) , \quad (3.33)$$

where the W and Z terms differ by a factor 1/2 since the Z :s are indistinguishable but the W :s are characterized by their charge. The widths of the Higgs decay into the massive gauge bosons are

$$\Gamma(H \rightarrow W^+ W^-) = \frac{G_F}{8\sqrt{2}\pi} m_H^3 (1 - 4\lambda_W)^{\frac{1}{2}} (3\lambda_W^2 - 4\lambda_W + 1) \quad \text{and} \quad (3.34)$$

$$\Gamma(H \rightarrow Z Z) = \frac{G_F}{16\sqrt{2}\pi} m_H^3 (1 - 4\lambda_Z)^{\frac{1}{2}} (3\lambda_Z^2 - 4\lambda_Z + 1) . \quad (3.35)$$

For $m_H \gg m_Z$ $\Gamma(H^0 \rightarrow ZZ)/\Gamma(H^0 \rightarrow W^+ W^-) \simeq 1/4$, which is just the symmetry factor in the Lagrangian (3.33), and for $m_H \gg m_W$ the decays into massive gauge bosons dominate over those into massless ones :

$$\frac{\Gamma(H \rightarrow \gamma\gamma)}{\Gamma(H \rightarrow W^+ W^-)} \simeq \frac{1}{4} \left(\frac{\alpha}{\pi} \right)^2 \simeq 10^{-6} . \quad (3.36)$$

Furthermore, when $m_H \gg m_W$ the decay rates for longitudinally polarized W 's dominate [146].

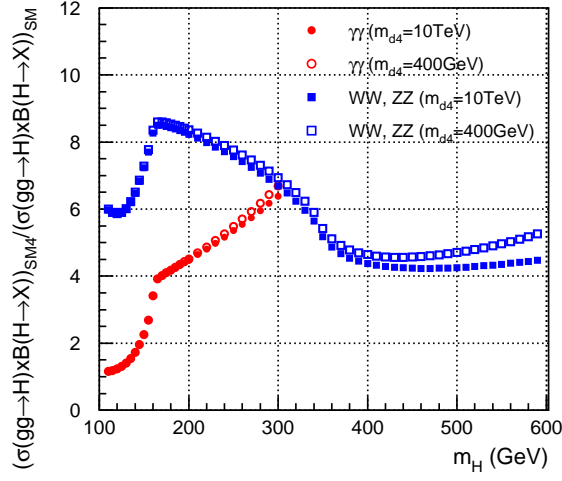


Figure 3.9: The enhancement of the product of the cross section and the branching fraction in a fourth family over the SM shown as a function of the Higgs mass for the two mass scenarios $m_{b'} \equiv m_{d4} = 10 \text{ TeV}$ and 400 GeV . Figure from Ref. [146]

The overall enhancement of the Higgs signal, the product of the production cross section and branching ratios, with respect to that of the SM

$$R^{\text{SM4}/\text{SM}} \equiv \frac{[\sigma(gg \rightarrow H) \times B(H \rightarrow X)]_{\text{SM4}}}{[\sigma(gg \rightarrow H) \times B(H \rightarrow X)]_{\text{SM}}} \quad (3.37)$$

is shown in Fig. 3.9. X stands for the decay modes $\gamma\gamma$, WW and ZZ . The drop of the enhancement factor near $m_H \approx 300 \text{ GeV}$ is due to the growth of the denominator of Eq. (3.37) since the SM cross section has a larger contribution from the top quark as m_H nears $2m_t$ [147].

The authors of Ref. [146] note that one advantage of computing $R^{\text{SM4}/\text{SM}}_{\sigma(gg \rightarrow H)}$ as in (3.37) instead of $\sigma(gg \rightarrow H)$ is that this ratio is less sensitive to higher order corrections. It is also less sensitive to other theoretical uncertainties, such as the choice of parton distribution function.

3.2.3 Searches for the Higgs and the fourth family

The assumed mixings and masses of the fourth generation are used for combined Higgs and fourth family searches at the Tevatron and the LHC. A difficulty is that the sought-after signal depends on these input parameters, that are for the time being unknown. Predictions can be made when the free parameters of the fourth family are fixed, as was done in [132]. For

$$\begin{aligned} m_{t'} &= 320 \text{ GeV} , & m_{b'} &= 260 \text{ GeV} , \\ m_{\ell'} &= 155 \text{ GeV} , & m_{\nu'} &= 100 \text{ GeV} \end{aligned} \quad (3.38)$$

the complete set of branching ratios of the Higgs as a function of m_H are shown in Fig. 3.10. Unless m_H is very large the decays into fourth generation particles will be only into the leptons, and not the quarks, a conclusion disfavored by EWPD [132]. During the last years weak boson production has shown to be the leading discovery channel for a light Higgs since loop effects on the $WW\phi$

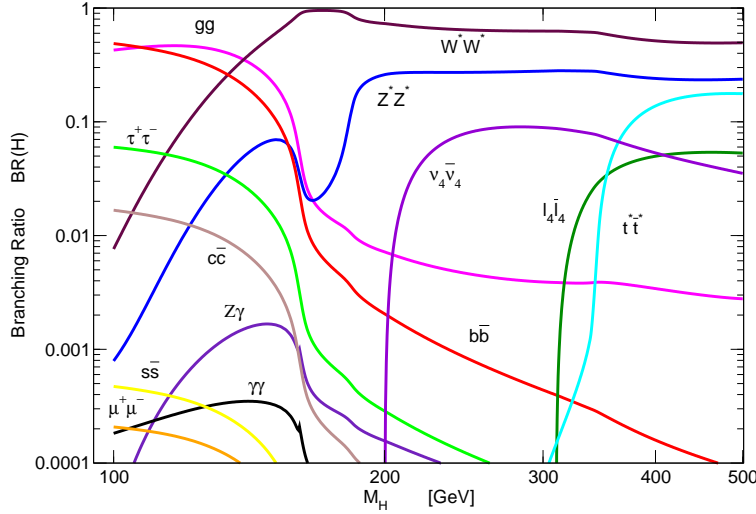


Figure 3.10: Branching ratio of the Higgs with fourth-generation effects assuming $m_\nu = 100$ GeV and $m_\ell = 155$ GeV. The loop effects to $H \rightarrow gg$ and $H \rightarrow \gamma\gamma$ are largely insensitive to the fourth-generation quark masses. The other fourth-generation masses are $m_{\nu'} = 320$ GeV, $m_{b'} = 260$ GeV. Figure and caption from [132].

couplings are so small to be ignored in the SM, but this no longer applies in a four family model. However, the decay channels $H \rightarrow \ell_4 \bar{\ell}_4$ and $H \rightarrow \nu_4 \bar{\nu}_4$ are small compared to the gauge boson decays.

New Higgs decay modes are possible if m_H is sufficiently large. Higgs decay into two heavy quarks has a production rate that is small compared with QCD production and is not a promising channel since the signal-to-background ratio is expected to be poor. Concerning decays to two heavy leptons there are two cases to consider, determined by the size of the mixing between the heavy leptons and the SM ones [132]: In a first scenario the mixing is assumed to be very small, $|U_{i4}| < 10^{-8}$, with $i = 1, 2, 3$, allowing the fourth generation neutrinos to escape the detector as missing energy. If, on the other hand, one considers a second scenario where the mixing $|U_{i4}|$ is not too small then the fourth generation neutrino will swiftly decay via a mixed charged PMNS current $U_{i4} \ell_i^\pm \nu_4 W^\mp$. The lepton flavor of the new signal

$$H \longrightarrow \nu_4 \bar{\nu}_4 \longrightarrow \ell^+ \ell^- W^+ W^- \quad (3.39)$$

relies upon the dominant PMNS element. In this case the Higgs must be heavier than 200 GeV in order for the LEP bounds on this two-body decay to be open.

If the neutrino has an electroweak scale Majorana mass the two-body decay will produce same-sign leptons half of the time:

$$H \longrightarrow \nu_4 \nu_4 \longrightarrow \ell^\pm \ell^\pm W^\mp W^\mp. \quad (3.40)$$

Analyses with relatively light fourth generation particles have been made as well [149, 150]. It has been found that precision electroweak data is in particular compatible with [149]

$$\begin{aligned} m_H &\simeq 300 \text{ GeV} , \quad m_{\nu'} \simeq 50 \text{ GeV} , \quad m_{\ell'} \simeq 100 \text{ GeV} , \\ m_{t'} + m_{b'} &\simeq 500 \text{ GeV} \text{ and } |m_{t'} - m_{b'}| \simeq 75 \text{ GeV} . \end{aligned} \quad (3.41)$$

The data seem to prefer the masses of the fourth generation to be $m_2 > m_1$ for leptons and $m_1 > m_2$ for quarks, when the doublets are $(\psi_1, \psi_2)^T$. The set of parameters (3.41) gives a minimal χ^2 of

$$\chi_{\min}^2/n_{\text{d.o.f.}} = 20.8/12 , \quad (3.42)$$

whereas $\chi_{\min}^2/n_{\text{d.o.f.}} = 23.8/13$ in the SM, so the fourth generation with masses as in (3.41) gives a slightly better fit. The quantity $\chi_{\min}^2/n_{\text{d.o.f.}}$ is the correct one to gauge the goodness of the fits in this light-fourth-family case, since the oblique parameters S, T, U are not adequate as the definition of these is valid only when all fourth generation particles are heavier than m_Z .

Chapter 4

Experimental searches

Running experiments test the standard model and physics beyond the SM. These searches – mainly done at the LHC and Tevatron – include the fourth generation. At the LHC parton interactions at $\hat{s} \sim 1$ TeV will be produced in significant rates [151] so it is well suited for the search of new, heavy particles. Specifically, such high-energy parton interactions may produce fourth generation particles of masses close to the unitarity scale ~ 500 GeV. In what follows we will review proposed search strategies and already existing bounds on the physics of a possible fourth generation. Feynman diagrams of various production processes are shown in Appendix E.

4.1 Search strategies – SM4 quarks

In this section we will review the searches proposed for finding t' and b' quarks, both in single and pair production. We start by reviewing the event topologies [151] and then present studies that were made for identifying W bosons originating from heavy quark decays in pp collisions (at the LHC) [130] or in the process $eq \rightarrow t'\nu$ (at the LHeC) [152]. It is of great interest to study both single and pair production, since the two give different information: pair production allows for precise mass measurements whereas single production gives information about the mixing of the fourth family with the others [153]. Measuring both processes allows for a more comprehensive physical picture of the fourth generation. Also, the various production mechanisms give different information about the quarks: strong production depends only on the masses of the fourth generation quarks, whereas the electroweak production and decay modes are mostly sensitive to the mass difference of the quarks and their CKM mixing [154].

4.1.1 General event topologies

For the fourth generation quark masses $\sim 400 - 600$ GeV considered throughout this report the dominant decays are into a W boson and a light quark [151]. There are several possibilities for such decays:

$$\begin{aligned} \text{(i)} \quad & Q \longrightarrow qW \\ \text{(ii)} \quad & Q \longrightarrow qWW \\ \text{(iii)} \quad & Q \longrightarrow qWWW \end{aligned} \tag{4.1}$$
$$\tag{4.2}$$

Here Q is a heavy quark (either t' or b') and q is one of the five lightest quarks (u, d, s, c, b). These different channels occur for :

- (i) This channel is especially seen for $t' \rightarrow b, s, d + W$ or $b' \rightarrow c, u + W$. When the CKM mixing matrix is such that $V_{t'b} \ll V_{cb'}$ and/or $V_{ub'}$ then this is the dominant b' decay channel.
- (ii) This is the dominant b' decay channel if the process begins by $b' \rightarrow tW$, followed by $t \rightarrow bW$. There is a similar channel for t' , open when $m_{t'} > m_{b'} + m_W$ and the b' decays through

$$b' \rightarrow Wc \text{ or } Wu \text{ such that } t' \rightarrow WWc \text{ or } WWu. \quad (4.3)$$

- (iii) This is the appropriate channel if $t' \rightarrow Wb'$ by process (i) and then b' decays as in (ii): $b' \rightarrow Wt \rightarrow WWb$.

Under certain conditions there may be important three-body decays. This is the case when the mixing between the third and fourth generations is small and the mass splitting between the t' and b' quarks is smaller than the W mass. Then the fourth generation quarks may also decay through [151]

$$(iv) \quad Q \rightarrow Q'W^* \rightarrow qWW^* \quad (4.4)$$

where W^* indicates a virtual W and Q is the heavier fourth generation quark, Q' the lighter one. If $m_{t'} > m_{b'}$ then the above chain gives $t' \rightarrow b'W^* \rightarrow tWW^* \rightarrow bWWW^*$.

What happens to the W s and the light quarks?

The light quarks form jets and the W has the following decays $W^+ (W^-) \rightarrow \ell^+ \nu_\ell (\ell^- \bar{\nu}_\ell)$ and $W^\pm \rightarrow q\bar{q}$, called *leptonic* and *hadronic* channels, respectively. Hence a W^+W^- pair can decay in three distinct ways

$$\begin{aligned} \text{leptonic :} \quad & W^+W^- \rightarrow \ell^+ \nu_\ell \ell^- \bar{\nu}_\ell \\ \text{hadronic :} \quad & W^+W^- \rightarrow q_1 \bar{q}_1 q_2 \bar{q}_2 \end{aligned} \quad (4.5)$$

$$\text{semi-leptonic :} \quad W^+W^- \rightarrow \ell^+ \nu_\ell q \bar{q} \quad . \quad (4.6)$$

The quarks of the hadronic and semi-leptonic decays give rise to jets, which are a challenge from an experimental point of view. The leptons are easier to identify.

4.1.2 Pair production of fourth family quarks

A few years ago the signal of pair produced quarks decaying weakly was analyzed [130] – the signal being $f\bar{f}W^+W^-$, with f typically a bottom or top quark. In this study the focus is on the case of the bottom quark, assuming that this ($b\bar{b}W^+W^-$) would be the dominant decay mode of a fourth generation quark that has CKM mixings with the other generations.

The t' quark is assumed to have a mass in the range 600–800 GeV, in which case its width would be approximately $60 \cdot |V_{t'b}|^2$ GeV, implying that it is possible that $\Gamma_{t'} < \Gamma_t$ if $|V_{t'b}|$ is small. The authors note that both $t'\bar{t}'$ (see Fig. E.1 (a) and (b)) and $t\bar{t}$ have the same final states and that it is imperative to have an event selection that significantly reduces the $t\bar{t}$ background since the $t\bar{t}$ cross section at the LHC is about 500 times larger than that of $t'\bar{t}'$. To this aim the following characteristics are demanded for a signal to pass the event selection :

- A lower bound $\Lambda_{\text{top5}} = 2m_{t'}$ is put on the scalar p_T sum of a number (*e.g.* five) of the hardest reconstructed objects in the detector,

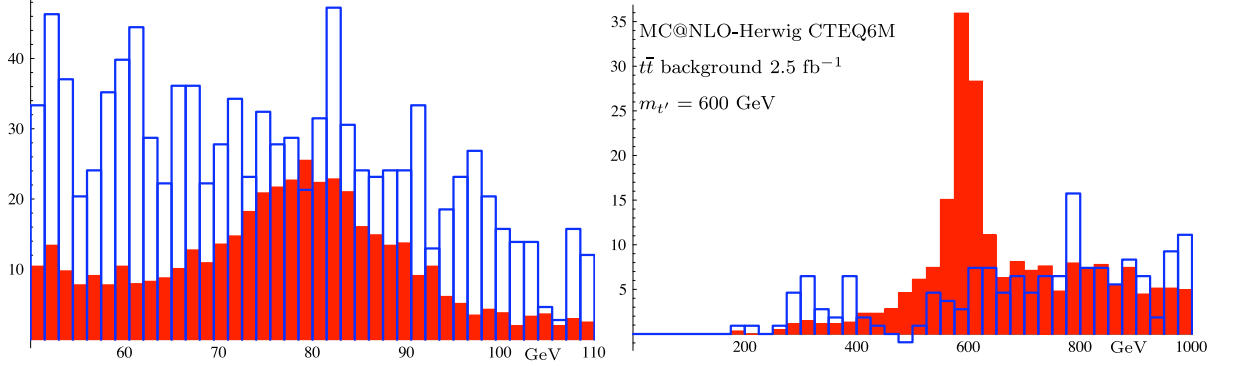


Figure 4.1: Signal (red) versus $t\bar{t}$ background (blue) resulting from simulations. LHS: W mass plot, RHS: t' mass plot. Figure from Ref. [130].

- A tagging of b jets with $p_T > \Lambda_b = m_{t'}/3$ is used and
- The fact that W 's and b 's from $t\bar{t}$ production often originate from one highly boosted t quark and are difficult to discern from one another is utilized, noting that for $t'\bar{t}'$ the W and b jets are often quite isolated. These isolated W jets can be identified using a smaller cone size than customary and then identifying the invariant mass distribution of the jets.

The authors define a W jet as a ‘non- b -tagged jet’ whose invariant mass is close to the W boson peak in the invariant mass distribution. Then the mass of the t' – the quantity that is searched for – can be reconstructed from the invariant masses of the $b - W$ jet pairs.

Different Monte Carlo-based event generators are used for the study, but the results are similar for all of these. When the event selection described above is used, the signal to background ratio is very promising, as can be seen on the RHS of Fig. 4.1.

The cross-section of pair produced fourth generation quarks has (for the case of the b' quark) been compared for LHC and Tevatron [155]. The b' quarks can be produced in much larger numbers at the LHC, as is shown in Fig. 4.2: for a b' mass of *e.g.* 300 GeV the pair production cross section at the LHC already with $\sqrt{s} = 7$ TeV is 20 times larger than at the Tevatron, so that a discovery (at 5σ significance) could be made at the LHC with ~ 30 times less data than at the Tevatron (see Fig. 4.3).

4.1.3 Single production of fourth family quarks

Having discussed the pair production of fourth generation quarks, we now turn to their single production. Single production is possible both at the LHC [153] and at the hypothetical extension of the LHC, the Large Hadron electron Collider (LHeC) [152, 156]. We will consider these both, starting with the LHC.

Single production at the LHC

The relevant production processes at the LHC are $pp \rightarrow b'(\bar{b}')jX$ and $pp \rightarrow t'(\bar{t}')jX$ (*cf.* Fig. E.4 in Appendix E), with j denoting a jet and X some hadronic final state [153]. The cross section for

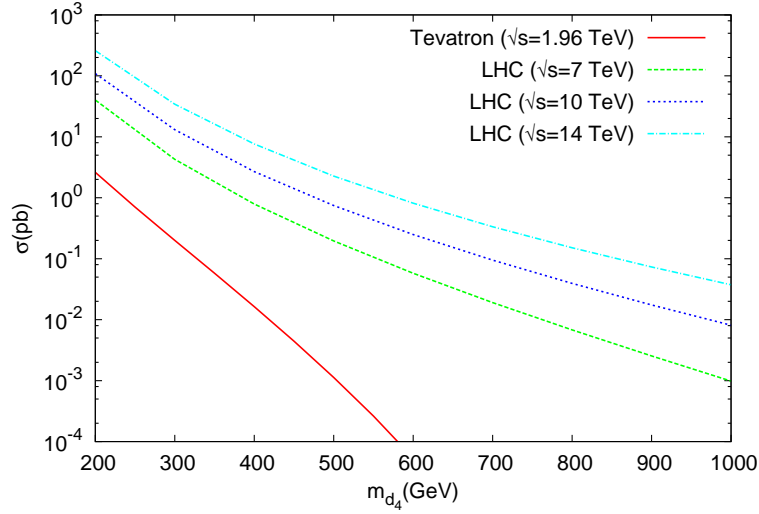


Figure 4.2: The pair production cross section of $b'\bar{b}'$ at the Tevatron and at various energies at the LHC. Figure from Ref. [155].

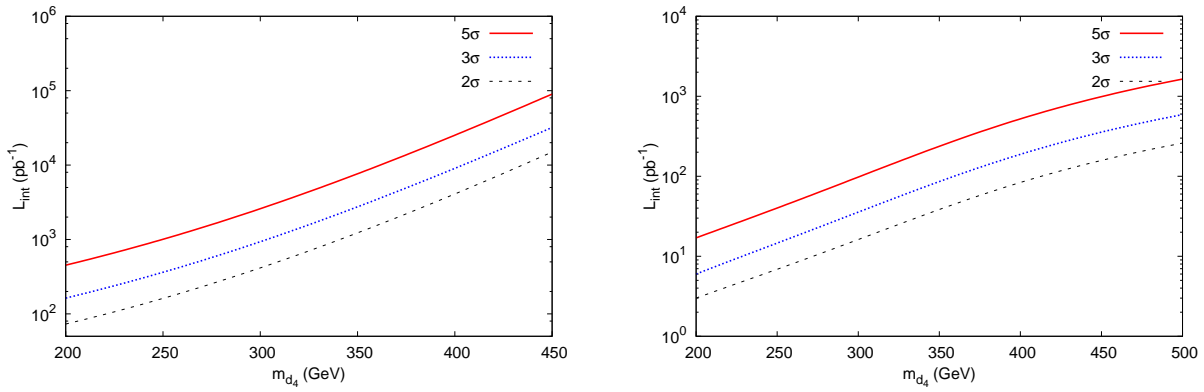


Figure 4.3: The necessary integrated luminosities for exclusion (2σ), observation (3σ) and discovery (5σ) of the b' quark at the Tevatron (left) and the LHC (right). Figures from Ref. [155].

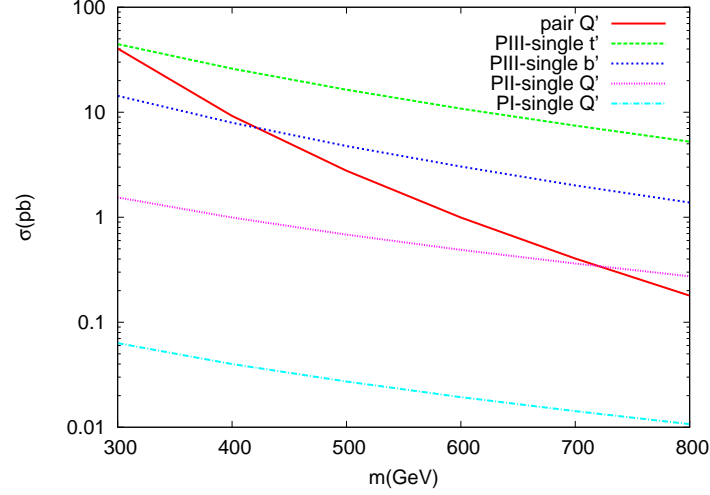


Figure 4.4: The cross sections for the single and pair production of b' and t' quarks at LHC for different parametrizations of the CKM matrix elements $V_{t'q}, V_{qb'}$. Figure from Ref. [153].

the process $pp \rightarrow q'jX$, where q' is a fourth generation quark, is

$$\sigma = \sum_{i,j} \int_{y_{\min}}^1 dy \int_y^1 \frac{dx}{x} f_{q_i/p}(x, Q^2) f_{q_j/p}(y/x, Q^2) \hat{\sigma}(ys) , \quad (4.7)$$

where the functions $f_{q/p}(x, Q^2)$ are the parton distribution functions, with $Q^2 = m_{q'}^2$ for the signal and $Q^2 = \hat{s}$ for the background and a good choice for the lower limit of the first integral is $y_{\min} = m_{q'}^2/s$.

The authors consider three different CKM parametrizations. They use the parametrizations given in Eq. (4.9) (below) for PI and PIII but choose $V_{q'i} = V_{iq'} = 0.05$ for PII. The choices are motivated by the fact that only the upper limits on the CKM matrix elements could be well predicted from the current experimental data. It is noteworthy that for a parametrization with equal strengths, $V_{q'i} = V_{iq'}$, the single production cross section becomes comparable to the pair production cross section for CKM elements $V_{t'q} = V_{qb'} = 0.25 - 0.4$ in the entire mass range considered, $m_{q'} = 300 - 800 \text{ GeV}$ (see Fig. 4.4).

If $m_{t'} > m_{b'}$, the t' decays into a W^+ and a b' , which then decays into a W^- and a t or one of the lighter quarks. On the other hand, if $m_{b'} > m_{t'}$, then one has $b' \rightarrow W^- t'$ and t' successively decaying into lighter and lighter SM quarks, seen as jets in the detector. In the case that $m_{t'} = m_{b'}$ both t' and b' decay via a charged current interaction into quarks of the first three families.

The background from the decays into $W^\pm Z$, W^+W^- , ZZZ , ZZW^\pm , W^+W^-Z , $W^+W^-W^\pm$ and Wbj , Wtj can be reduced by applying the following cuts

- invariant mass cut $m_{Wb} > 200 \text{ GeV}$,
- acceptance $p_T > 20 \text{ GeV}$ for final state jets,
- invariant mass cut $|m_{t'} - m_{W+b}| < 10 - 20 \text{ GeV}$ depending on the t' mass and similarly for the b' signal: $|m_{b'} - m_{W-t}| < 10 - 20 \text{ GeV}$.

Events with final states including a b jet or a light jet, a charged lepton (two leptons with opposite signs) and missing transverse momentum are considered as t' (b') signals. A further demand is that the invariant mass peak is found around $m_{q'}$ in the interval 300–800 GeV.

Mass (GeV)	Γ (GeV)
300	3.84
400	9.19
500	18.00
600	31.14
700	49.48
800	73.87

Table 4.1: The total decay widths of t' quark depending on its mass values, as given in Ref. [152].

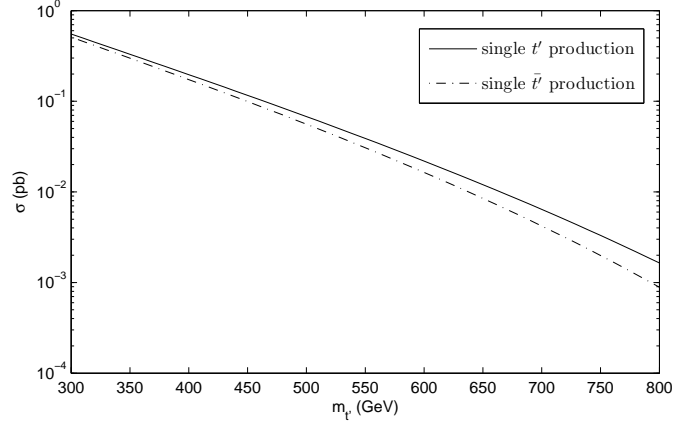


Figure 4.5: The total cross sections at the LHeC for the processes $e^+p \rightarrow t'\bar{\nu}_e$ (solid line) and $e^-p \rightarrow \bar{t}'\nu_e + X$ (dot-dashed line) with $\sqrt{s} = 1.4$ TeV. Figure from Ref. [152].

The statistical significance of b' (\bar{b}') at the integrated luminosity $L_{\text{int}} = 10^5 \text{ pb}^{-1}$ is $\mathcal{O}(10^0)$ ($\mathcal{O}(10^{-1})$) for the parametrization PI and $\mathcal{O}(0.5 \times 10^2)$ ($\mathcal{O}(10^1)$) for PII and $\mathcal{O}(0.5 \times 10^3)$ ($\mathcal{O}(0.5 \times 10^3)$) for PIII in the whole mass range. The statistical significance is a bit higher for lower mass values. For t' , \bar{t}' the corresponding values are similar for the parametrizations PI and PII but much higher for PIII, for which it is $\mathcal{O}(10^3 - 10^4)$ for \bar{t}' and $\mathcal{O}(10^3)$ for t' .

Single production at the LHeC

The Large Hadron electron Collider [157] – a hypothetical ‘extension’ of the LHC – is designed to consist of a new linear accelerator or a storage ring and the electrons from this accelerator or storage ring, having an energy of 70/140 GeV, will collide with the 7 TeV proton beam from the LHC. This allows for the study of deep inelastic scattering processes at center of mass energy of 1.4/1.9 TeV. With a design luminosity $\sim 10^{33}$ or $10^{32} \text{ cm}^{-2}\text{s}^{-1}$, the LHeC would surpass the previous ep collider, HERA at DESY. At the LHeC the fourth generation quarks are produced in the processes $ep \rightarrow t'\nu_e$ and $ep \rightarrow b'\nu_e$ (cf. Figs. E.2, E.3) for a chosen mass range of 300–800 GeV [152, 156]. The relevant CKM matrix elements used in the study of t' production [152] are $V_{t'd} = 0.063$, $V_{t's} = 0.46$ and $V_{t'b} = 0.47$, optimized for a 1σ deviation over the average values of the CKM matrix elements. For the parametrization used the t' branching fractions are the same for the whole of the mass range: $BR(t' \rightarrow W^+b) = 51\%$, $BR(t' \rightarrow W^+s) = 48\%$ and $BR(t' \rightarrow W^+d) = 0.9\%$ but the total cross sections of the t' and \bar{t}' quarks change significantly, as shown in Fig. 4.5. The total decay widths of t' are shown in Table 4.1 for the whole mass range.

For the event selection the authors propose the following cuts:

- a p_T cut to reduce the background from b quarks,
- a cut on the missing transverse momentum $p_T^{\text{miss}} > 50 \text{ GeV}$,
- a cut on the invariant mass $|m_{t'} - m_{W+b}| < 10 - 20 \text{ GeV}$, according to the mass and the decay width of the t' quark.

The statistical significance of the signal is computed (under the assumption of Poisson statistics) using

$$SS = \sqrt{2L_{\text{int}} \epsilon [(\sigma_S + \sigma_B) \ln(1 + \sigma_S/\sigma_B) - \sigma_S]} , \quad (4.8)$$

Mass (GeV)	Γ (GeV)	$W^-c(\%)$	$W^-t(\%)$	$W^-u(\%)$
300	0.18	66	30	3.9
400	0.55	52	45	3.0
500	1.22	46	52	2.7
600	2.25	43	55	2.5
700	3.72	41	57	2.4
800	5.70	40	58	2.3

Table 4.2: The total decay widths and the branching ratios of b' quark depending on its mass. Table values from Ref. [156].

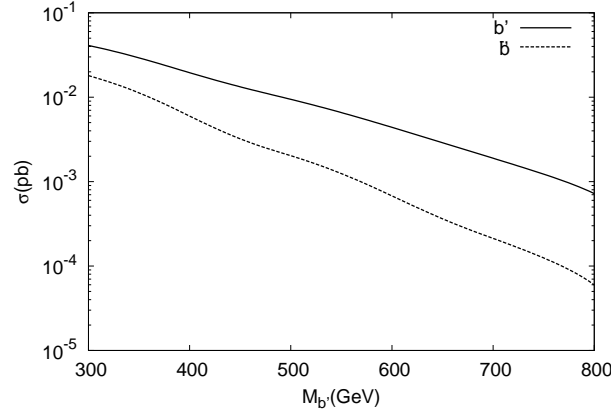


Figure 4.6: The total cross section for the process $e^- p \rightarrow b' \nu_e + X$ (solid line) and $e^+ p \rightarrow \bar{b}' \bar{\nu}_e + X$ (dashed line) with $\sqrt{s} = 1.4$ TeV. Figure from Ref. [156].

where σ_S and σ_B are the signal and background cross sections, respectively. An integrated luminosity $L_{\text{int}} = 10^4 \text{ pb}^{-1}$ is assumed, and the b -tagging efficiency is taken to be $\epsilon = 0.6$. The statistical significance (4.8) is estimated to lie approximately in the range $SS = 4113.27 - 8.35$ for $m_{t'} = 300 - 800$ GeV. For the chosen mixings and masses it could thus be possible for the LHeC to discover the t' quark up to 800 GeV.

In a similar study [156] the discovery potential of the LHeC for the single production of b' and \bar{b}' quarks was contemplated. The authors calculated the cross sections of the signal (*cf.* Fig. 4.6) and the decay widths and branching ratios (*cf.* Table 4.2) of the b' quark, using the parametrization $|V_{ub'}| = 0.028$, $|V_{cb'}| = 0.116$, $|V_{tb'}| = 0.99$, $|V_{t'b'}| = 0.99$ and assuming that $m_{b'} < m_{t'}$ with a mass splitting of $m_{t'} - m_{b'} \sim 50$ GeV.

The event selection is based upon the following demands

- transverse momentum cuts on the emitted charm quark, the lepton and missing momentum:
 $p_T^c > 20$ GeV, $p_T^\ell > 30$ GeV and $p_T^{\text{miss}} > 20$ GeV,
- a secondary vertex of the charmed jet with mass around 1 GeV,
- $|m_{b'} - m_{Wc}| < 10 - 20$ GeV according to the mass and decay width of b' .

The statistical significance of the signal can be computed from Eq. (4.8), assuming $L_{\text{int}} = 10^4 \text{ pb}^{-1}$ as in the case of the t' as well as a c -tagging efficiency of $\epsilon = 0.3$. For these values

$SS(e^+p \rightarrow W^+\bar{c}\bar{\nu}_e) = 13.2 - 2.72$ and $SS(e^-p \rightarrow W^-c\nu_e) = 6.48 - 0.5$ for $m_{b'} = 300 - 800$ GeV, rendering the observation of singly produced b' quarks possible at the LHeC, provided that the considered mass range and mixings hold.

Anomalous resonant production

The anomalous resonant production (breaking $SU(3)_c$) of the t' quark has also been considered [158]. The relevant subprocess is $gq_i \rightarrow t'$, where $q_i = u, c$ (*cf.* Fig. E.5, Appendix E). The decay products are $W^\pm b_{\text{jet}}$, as in the previous analyses, and any observation of a mass peak in the t' mass interval 300–800 GeV resulting in $W^\pm b_{\text{jet}}$ is interpreted as a signal for this type of anomalous resonant production.

The anomalous interactions are deemed to become significant at tree level due to the possible large mass of the fourth generation quarks. The t' quarks could be produced in large numbers if they have anomalous couplings that dominate over the chiral SM interactions. The strength of the anomalous coupling is taken to be $\kappa/\Lambda = \mathcal{O}(10^{-1}) \dots 1$ TeV. The decay width of t' for the different parametrizations of the CKM matrix

$$\text{PI} : |V_{Q'q}| = |V_{qQ'}| = 0.01, \quad \text{PII} : |V_{Q'q}| = |V_{qQ'}| \approx \lambda^{4-n},$$

$$\text{PIII} : |V_{t'd}| = 0.063, |V_{t's}| = |V_{cb'}| = 0.46, |V_{t'b}| = |V_{tb'}| = 0.47, |V_{ub'}| = 0.044. \quad (4.9)$$

can be seen in Fig. 4.7 for different t' masses, the CKM parametrizations (4.9) and strengths of the anomalous coupling κ/Λ . In Eq. (4.9) n is the family number.

The event selection used in [158] is based upon the following requirements:

- for leptonic decay of the W boson the criteria for the electrons or muons are: $p_T^\ell > 20$ GeV, $|\eta^\ell| < 2.5$ and $\cancel{E}_T > 20$ GeV,
- for hadronic decay of the W boson it is demanded that there are at least two jets with $p_T^j > 20$ GeV and $|\eta^j| < 2.5$,
- the b jets are in both cases required to have $p_T^{j_b} > 50$ GeV and $|\eta^{j_b}| < 2.5$.

A conclusion of this study is that for a large enough anomalous coupling with other up type quarks, t' can be discovered with early LHC data. The sensitivity to the anomalous coupling $\kappa/\Lambda = 0.1$ TeV $^{-1}$ is thought to be possible to reach at the LHC at center of mass energy $\sqrt{s} = 10$ TeV and integrated luminosity $L_{\text{int}} = 100$ pb $^{-1}$.

4.1.4 Current experimental bounds

Specific analyses where the fourth family quarks have been searched for have been made by many of the collaborations mentioned in this report. Below we will cite some of the constraints on fourth-generation parameters given in the literature. Before that, we wish to emphasize that the results of a given analysis depend on the chosen set of input parameters and their values. In experiments one often has to make assumptions about the physics in question, and the assumptions affect the final result.

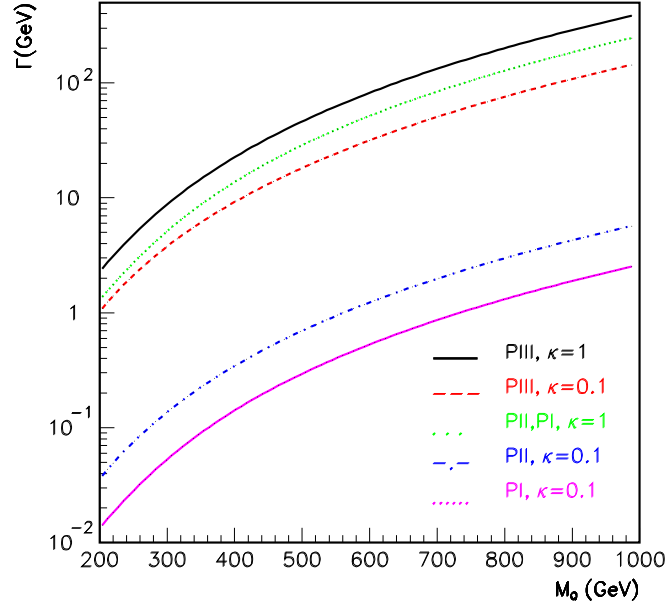


Figure 4.7: Decay width of t' as a function of its mass for different $V_{t'q}$ parametrizations and κ/Λ values. Figure from Ref. [158].

t' quark mass

Searches for a heavy up-type quark, t' , decaying into Wq , have been made by the CDF collaboration [159]. The data used for the analysis corresponds to 2.8 fb^{-1} of integrated luminosity at $\sqrt{s} = 1.96 \text{ TeV}$ in $p\bar{p}$ collisions at Tevatron, Fermilab.

The t' quark is assumed to decay to a final state with a high p_T lepton, large missing transverse energy and multiple hadronic jets having large total transverse energy. The signal is similar to that of a top pair. The transverse energy is defined as $E_T \equiv E \sin \theta$, where E is the energy deposited in a calorimeter cluster and θ is the polar angle measured from the proton beam direction. The transverse momentum is the the component of the momentum of a given track transverse to the beam line. The missing transverse energy is the magnitude of the vector defined as $-\sum_i E_T^i \hat{n}_T^i$, where \hat{n}_T^i is the transverse component of the unit vector pointing from the interaction point to the calorimeter tower i , corrected for the p_T of muons, which do not deposit all of their energy in the calorimeter as well as for tracks which point to uninstrumented regions in the calorimeter.

The highly energetic quarks of the decay undergo fragmentation, resulting in jets. The jets of an event are required to have $E_T > 15 \text{ GeV}$ and $|\eta| < 2.5$. The pseudorapidity η is defined as

$$\eta \equiv -\ln[\tan(\theta/2)] . \quad (4.10)$$

For further enhancement of the signal to background ratio a leading jet with $E_T \geq 60 \text{ GeV}$ is demanded as are some angular correlations. The main background for such events comes from electroweak processes (dominated by W +jets) and $t\bar{t}$ pair production.

Based on the results of their analysis, the CDF collaboration conclude that

$$m_{t'} \geq 311 \text{ GeV} \quad \text{at } 95\% \text{ C.L.} \quad (4.11)$$

The authors note that this result is deduced assuming that the true top mass is 175 GeV but that the top quark mass may have been affected by the presence of a heavier t' and that the conclusion should be treated with care.

If the fourth generation quarks dominantly mix with the first two generations then t' and b' will have the same signature and the Tevatron observation limit is raised to well over 400 GeV [155] and on the other hand, if a more general, wide range of mixings are considered, a reinterpretation of the CDF results give a lower bound of $m_{t'} \gtrsim 290$ GeV [160].

These results have since been improved by the CMS collaboration [161, 162], reporting

$$\begin{aligned} m_{t'} &\geq 450 \text{ GeV} \quad (\text{semileptonic channel}) , \\ m_{t'} &\geq 557 \text{ GeV} \quad (\text{dilepton channel}) . \end{aligned} \tag{4.12}$$

b' quark mass

CDF has also performed searches for new particles decaying into a Z boson and jets [163], signaling a b' quark. The data sample used has a luminosity of 1.06 fb^{-1} , collected using $Z \rightarrow ee$ and $Z \rightarrow \mu\mu$. It is assumed that the production mechanisms of the b' quark would be identical to that of the top, with pair production having the largest cross section. An assumption used for the analysis is that the branching ratio of b' to a Z and a b is 100%.

The main background for such a final state is from SM Z production with jets produced in higher order QCD processes¹. The optimal kinetic region of the four-generation model drives the focus of the searches to final states with at least 3 jets, each with a transverse energy $E_T > 30$ GeV. Topologies with large numbers of highly energetic jets in the final state allow for a better separation of the signal from the standard model Z +jet background, since the generic behavior of new signals is that the cross section decreases and the transverse energy spectra become harder as mass increases.

The result of the analysis [163], that $m_{b'} \geq 268$ GeV at 95 % C.L., has been superseded by ATLAS [164] and CMS [165] in 2012, reporting

$$m_{b'} \geq 480 \text{ GeV} \quad \text{and} \quad m_{b'} \geq 611 \text{ GeV} , \tag{4.13}$$

respectively.

4.2 Searches for fourth generation leptons

Pair production of fourth generation leptons

As discussed in Section 2.5.2, neutrinos can have either a Dirac or a Majorana mass – in the most general case both components are present. The main difference in the pair production of Dirac *vs.* Majorana neutrinos is the dependence of the cross section on the velocity β . In the case of a Dirac mass the cross section has a β -dependence $\sim \beta(3 - \beta^2)$ while in the Majorana case there is only a term $\sim \beta^3$, implying that the threshold cross section falls more rapidly in the Majorana case as in the Dirac case. [166]

¹Other sources of background may be [163]:

- single- Z production in conjunction with jets
- multi-jet events, where two jets fake leptons
- cosmic rays coincident with multi-jet events
- WZ +jets, where the W decays to jets.
- ZZ +jets, where one of the Z 's decays to jets
- WW +jets, where both W 's decay to leptons
- $t\bar{t}$ +jets

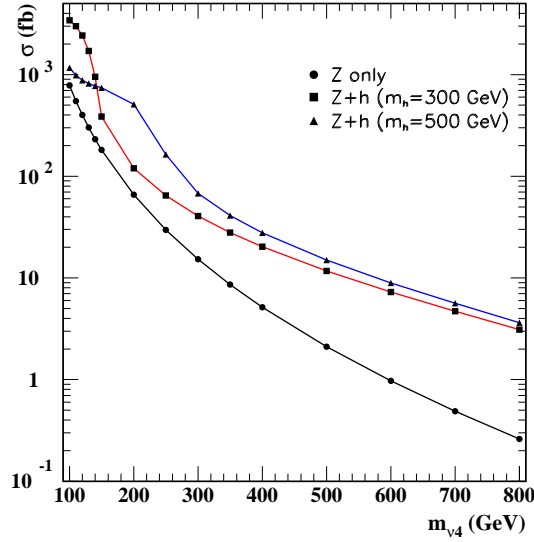


Figure 4.8: $\nu'\bar{\nu}'$ pair production cross section as a function of ν_4 mass for three scenarios: Higgsless case and cases with $Z+h$ ($m_h = 300$ GeV and $m_h = 500$ GeV). The enhancement from gluon fusion is calculated for $m_{\ell'} = m_{\nu'} = 500$ GeV. Figure from Ref. [148]

The fourth family leptons decay only through charged currents [166]

$$\ell'^{\pm} \longrightarrow \nu_{\ell} W^{\mp}, \quad \nu' \longrightarrow \ell^{\pm} W^{\mp}, \quad (4.14)$$

where $\ell = e, \mu, \tau$ and ℓ', ν' denote the fourth generation charged and neutral leptons, respectively. For $m_{\ell', \nu'} < 100$ GeV, the decay is mainly through a W : in the case of $m_{\nu'} = 100$ GeV the branching fraction is $Br(\nu' \rightarrow e^{\pm} W^{\mp}) = 90\%$ and for $m_{\nu'} < 90$ GeV it is 100%.

4.2.1 Neutrinos and Higgs at the LHC

The possible discoveries of the fourth generation neutrinos and the Higgs boson have been analyzed in Ref. [148]. The processes considered are $pp \rightarrow (Z \text{ or } H) \rightarrow \nu'\bar{\nu}' \rightarrow W\mu W\mu$, as shown in Fig. E.6 (the flavor of the final state lepton will depend on the PMNS matrix elements). The relevant cross sections are calculated for two different Higgs masses, $m_H = 300$ GeV and $m_H = 500$ GeV as is the neutrino pair production cross section as a function of the neutrino mass for the different cases (see Fig. 4.8).

The characteristics of the signal depend on the type of neutrino (Dirac or Majorana) and hence the analysis and event selection for the two cases differ. For a Majorana neutrino the decay products are two same-sign leptons half of the time and opposite-sign leptons the other half. For a Dirac neutrino the decay would always lead to opposite-sign leptons. However, in both cases two high p_T leptons are produced along with two W bosons. The event selection requirements common for both Dirac and Majorana neutrinos are:

- transverse momentum of dileptons $p_T > 15$ GeV (in the case of multiple final state leptons, the ones with the highest transverse momenta are chosen),
- at least 4 jets (originating from W bosons) with $p_T > 15$ GeV for each jet,

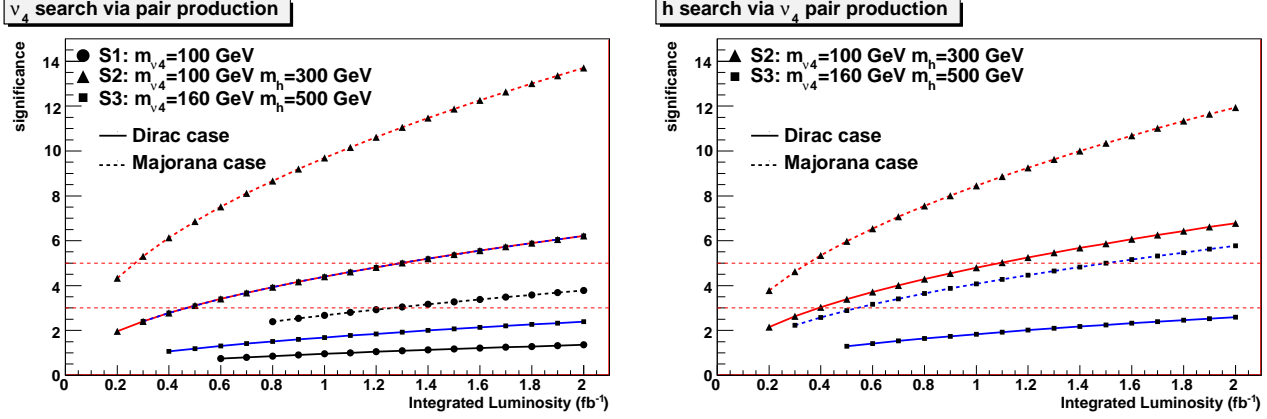


Figure 4.9: The expected signal significances (in units of standard deviations) of the fourth family neutrino searches (left) and the Higgs searches (right). Points on the curves are required to have at least three events that satisfy all the selection criteria. Here $\nu_4 = \nu'$ denotes the fourth generation neutrino. Figures from Ref. [148].

- dijet candidates for the reconstruction of W vertices should be within 20 GeV of the W mass
- rejection of events with a muon and its closest jet of $p_T > 20$ GeV that are closer than $\Delta R \equiv \sqrt{(\Delta\eta)^2 + (\Delta\phi)^2} = 0.4$ from each other.

The last criterion reduces the background due to decays of b quarks. Event selection in the case of Dirac neutrinos is more demanding than in the Majorana case and therefore further demands need to be set. In both cases the main background is from massive diboson associated dimuon production.

Fig. 4.9 shows the significance of the signals analyzed. S1 in the legend stands for the process $pp \rightarrow Z \rightarrow \nu'\bar{\nu}'$, S2 and S3 for $pp \rightarrow H \rightarrow \nu'\bar{\nu}'$ when $m_H = 300$ and 500 GeV, respectively (the authors denote the fourth generation neutrino by ν_4). Due to the enhancement of Higgs production through gluon fusion, the LHC is estimated to have the chance to simultaneously discover the Higgs boson and the fourth generation neutrinos. A 5σ significance could be reached at an integrated luminosity of $\sim 350 \text{ pb}^{-1}$ if $m_H = 300$ GeV and $m_{\nu'} = 100$ GeV.

The Higgs

The possibility of observing the Higgs boson through this channel has also been considered in other studies [167], [132], where the fourth generation neutrinos are taken to decay into W bosons and leptons: $pp \rightarrow H \rightarrow \nu'\bar{\nu}' \rightarrow \ell W \ell W$ (*cf.* Fig. E.7). The authors call this the 'silver' mode, in the sense that it could be competitive with respect to the 'golden' mode (described below) for some regions of Higgs and ν' masses. For the PMNS parametrization used the branching ratio for a discovery signal containing two muons and four jets is $\text{Br}(H \rightarrow \nu'\bar{\nu}' \rightarrow \mu^+\mu^-jjjj) = 1.22 \times 10^{-2}$ for $m_H = 300$ GeV. Comparing this with the branching ratio of the golden mode $\sim 1.12 \times 10^{-3}$ renders an enhancement factor of 11. It is assessed that this enhancement makes up for the possible inefficiencies associated with jet detection and hadronic W reconstruction.

4.2.2 Searches at future lepton colliders

Observing fourth family leptons at hadron colliders is difficult due to a large background [131]. It is therefore worthwhile to consider lepton production at lepton colliders having a sufficiently

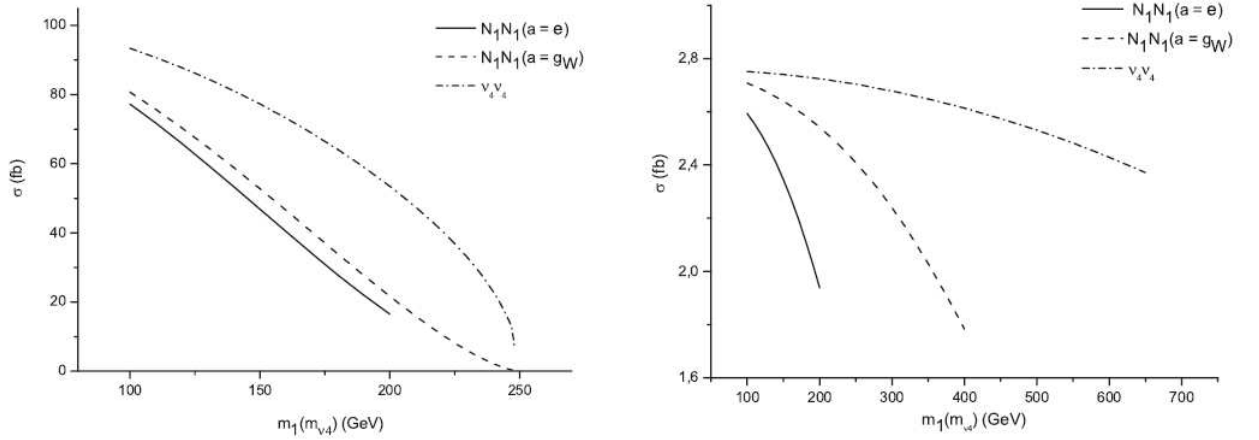


Figure 4.10: Neutrino pair production cross sections at $\sqrt{s} = 500$ GeV (right) and $\sqrt{s} = 3$ TeV (left) for Dirac (ν_4) and Majorana (N_1) neutrinos. The Majorana neutrinos are analyzed at two different strengths of the Yukawa coupling a : $a = e$ and $a = g_W$. Figures from Ref. [131].

high center of mass energy. Analyses made include e^+e^- [131, 168], $\gamma\gamma$ [168] and muon colliders. Currently planned lepton colliders are *e.g.* ILC² and CLIC³.

In Ref. [131] the pair production of both Dirac $e^+e^- \rightarrow \nu'\bar{\nu}'$ and Majorana neutrinos $e^+e^- \rightarrow \nu_1\nu_1$ at lepton colliders are considered. There are two Majorana neutrinos (see Section 2.5.2), with the mass eigenvalues given in Eq. (2.82). It is assumed that the Majorana neutrinos mix with the known neutrinos in the same manner as the Dirac neutrinos do. In the analysis the focus is on the production of two ν_1 :s, since the final states $\nu_1\nu_2$ and $\nu_2\nu_2$ are suppressed by factors $\sin^2\theta$ and $\sin^4\theta$, respectively, with the mixing angle θ given in Eq. (2.83). These two final states suffer also from kinematic suppression, ν_2 being more massive than ν_1 .

For PMNS matrix entries U_{i4} , $U_{41} \sim \mathcal{O}(10^{-4} - 10^{-5})$, with $i = 1, 2, 3$, the following branching ratios are obtained:

$$\begin{aligned} \text{Br}(\nu_1 \rightarrow e^\mp W^\pm) &\approx 0.135, \\ \text{Br}(\nu_1 \rightarrow \mu^\mp W^\pm) &\approx 0.25, \\ \text{Br}(\nu_1 \rightarrow \tau^\mp W^\pm) &\approx 0.115. \end{aligned} \quad (4.15)$$

The cross sections computed for the Dirac case and the Majorana cases at coupling strengths of $a = e$ and $a = g_W$ are shown in Fig. 4.10 for two different center-of-mass energies. The low value of the Majorana cross section compared to the Dirac cross section stems from the fact that Majorana production is suppressed both kinematically and by the mixing angle θ , as noted above.

The cleanest signature of the fourth neutrino pairs is thought to be the muon channels. In the Majorana case a signal with two muons with the same sign does not have any background and the signal should be discernible from the background in the Dirac case, too, leading to the conclusion that the number of signal events with preferred topologies are sufficiently high to investigate the fourth family neutrino properties in detail.

²International Linear Collider, <http://www.linearcollider.org/>.

Electron-positron collider with a center of mass energy $\sqrt{s} = 500$ GeV with an upgrade possibility to 1 TeV, luminosity $10^{34} \text{ cm}^{-2}\text{s}^{-1}$, length approximately 31 km

³Compact Linear Collider, <http://cllc-study.org/>.

Electron-positron collider, $\sqrt{s} = 3$ TeV, luminosity $\sim 10^{35} \text{ cm}^{-2}\text{s}^{-1}$, length 48.3 km.

The possible discovery of the fourth generation fermions at CLIC has been analyzed in Ref. [168]

4.2.3 Existing experimental constraints

The existing constraints on fourth generation leptons mainly come from LEP II [166].

In the search for pair produced neutral heavy leptons two isolated leptons (e, μ, τ) of the same family are required, as are decay products of a W boson, *i.e.* $e^+e^- \rightarrow \ell'\bar{\ell}' \rightarrow \ell^+\ell^-W^+W^-$. When the final state leptons are electrons or muons, the events are further required to have :

- two isolated leptons of the same family with a total energy less than $0.7 \times E_{\text{beam}}$,
- the number of jets plus isolated leptons is at least 3,
- hadronic events with visible energy greater than 60 GeV and charged track multiplicity greater than 3.

If the neutrino decays to τ and W , the event selection depends on whether the τ decays leptonically or hadronically. In the case of the decay being leptonic, the above requirements are used, relaxing the first requirement so that the two isolated leptons are allowed to be one electron and one muon.

For cases where at least one τ decays hadronically, the requirements on the events are :

- the number of jets plus isolated leptons is at least 4,
- the polar angle of missing momentum is in the range $25^\circ < \theta_{\text{miss}} < 155^\circ$ and the fraction of visible energy in the forward-backward region ($\theta < 20^\circ$ and $\theta > 160^\circ$) is less than 40%,
- the electron and muon energies are less than 50 GeV,
- the angle between the most isolated track and the track nearest to it is greater than 50° , or the angle between the second most isolated track and the track nearest to it is at least 25° ,
- the transverse momenta of the two most isolated tracks is greater than 1.2 GeV, and at least one track has transverse momentum larger than 2.5 GeV.

The results of the LEP II analysis are shown in Table 4.3.

Neutral leptons			Charged leptons	
Decay mode	Dirac	Majorana	Decay mode	Dirac
$\nu' \rightarrow eW$	101.3	89.5	$\ell^\pm \rightarrow \nu W$	100.8
$\nu' \rightarrow \mu W$	101.5	90.7	$\ell^\pm \rightarrow \nu' W$	101.9
$\nu' \rightarrow \tau W$	90.3	80.5	stable	102.6

Table 4.3: *LEP II 95% C.L. lower mass limits in GeV for neutral heavy leptons and pair-produced charged heavy leptons of a sequential family. Values from Ref. [166].*

Stable neutrinos are furthermore constrained by the invisible width of the Z boson, requiring the possible fourth neutrino to be heavier than approximately 40 GeV.

LEP II bounds revisited

In a recent study the LEP II bounds on fourth generation Majorana masses are reanalyzed, for a scenario where one right-handed neutrino is included [169]. The two new neutrino states, ν'_1 and ν'_2 , have different mass eigenvalues and thus have different decay modes. The second of these, ν'_2 ,

ν'_1 decay mode	Bounds
$W\tau$	62.1
$W\mu$	79.9
We	81.8

Table 4.4: Bounds on ν'_1 mass in GeV for the various decay channels. Values from Ref. [169].

is by assumption heavy ($m_{\nu'_2} > m_{\nu'_1}$) and can decay either into ℓW , with $\ell = e, \mu, \tau$ or into $\nu'_1 Z$. The first of these modes is suppressed by the small mixing between the fourth generation with the others and the second mode dominates for most masses. For the lighter neutrino the only open channel is $\nu'_1 \rightarrow \ell W$.

The relative branching ratios of the channels depend on the unknown PMNS matrix elements. In the limit of complete mass degeneracy (pseudo-Dirac limit), there is phase space suppression of the first decay mode of ν'_2 and there may be model-dependent interference effects and other effects like displaced vertices. Therefore the authors have chosen to restrict their analysis to mass differences greater than 10 GeV. The results of the study are shown in Table 4.4. We see that the the LEP II bounds 4.3 are altered significantly.

A conclusion drawn is that if a fourth generation exists, relatively light right-handed neutrinos must exist in order to generate a sufficiently large neutrino mass and that the existence of these extra states modifies the search strategies for the fourth generation lepton sector.

4.3 Higgs searches

4.3.1 Higgs searches at Tevatron

A study made about ten years ago focused on the discovery of the Higgs boson at the upgraded Tevatron, taking into account the four-family model [170]. For a Higgs boson with mass in the range $175 < m_H < 300$ GeV, the ‘golden’ mode $H \rightarrow ZZ \rightarrow 4\ell$ (*cf.* Fig. E.7, Appendix E) is the most reliable one for the possible discovery of the Higgs boson. The discovery potential depends mainly on the available integrated luminosity. The cross section for this process depends on the Higgs boson mass, as shown in Fig. 4.11.

The main background from the pair production of Z bosons, namely $p\bar{p} \rightarrow ZZ X$, such that $Z \rightarrow \ell^+ \ell^-$ is reduced by the reconstruction of the four-lepton invariant mass distribution. This mode is thus esteemed to allow for :

$$\textbf{Tevatron} > 3\sigma \text{ observation of the Higgs possible for } 175 < m_H^{\text{SM4}} < 300 \text{ GeV.} \quad (4.16)$$

Recently the Tevatron experiments CDF and DØ have updated their analyses using data of 8.2 fb^{-1} from CDF and 8.1 fb^{-1} from DØ [171]. The collaborations searched for the Higgs boson in the decays $H \rightarrow W^+ W^-$ and $H \rightarrow ZZ$, using all the production processes of the SM, namely $gg \rightarrow H$, $q\bar{q} \rightarrow WH$, $q\bar{q} \rightarrow ZH$ and vector boson fusion.

Two four-generation scenarios are considered: a ‘low-mass’ scenario and a ‘high-mass’ scenario (see Fig. 4.12). In the former the authors fix the masses of the fourth generation leptons at $m_{\nu'} = 80$ GeV and $m_{\ell'} = 100$ GeV, in order to have maximum impact on Higgs decay ratios but to evade current experimental limits; in the latter they set $m_{\nu'} = m_{\ell'} = 1$ TeV, in which case the leptons of the fourth generation do not affect the branching ratios at all (they are kinematically inaccessible).

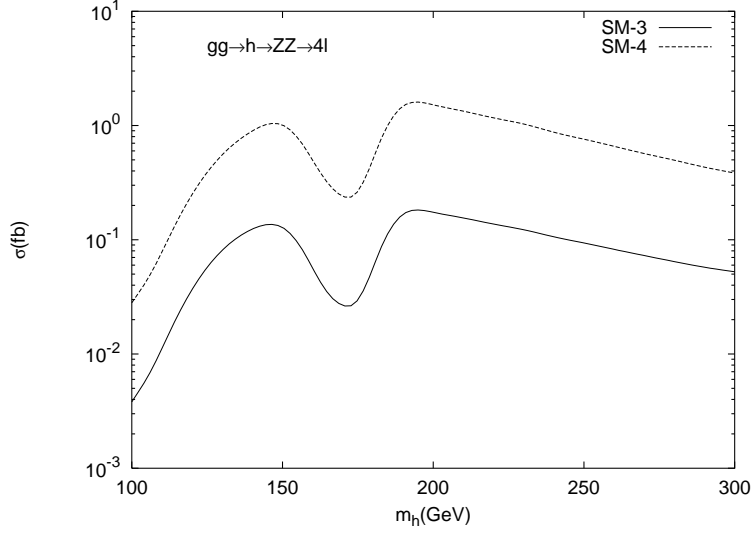


Figure 4.11: The cross section of the ‘golden’ mode $H \rightarrow ZZ \rightarrow 4\ell$ as a function of the Higgs mass for both three and four SM families. Figure from Ref. [170].

The masses of the fourth generation quarks are in both cases set so satisfy

$$\Delta m_{q'} \equiv m_{t'} - m_{u'} = 50 \text{ GeV} + 10 \ln \left(\frac{m_H}{115 \text{ GeV}} \right) \text{ GeV} . \quad (4.17)$$

The collaborations deem the uncertainties in the analyses to come from the total inelastic $p\bar{p}$ cross section used in luminosity measurements, SM diboson background production cross sections, and top pair and single production.

The result of the analysis is

$$\textbf{Tevatron (2011)} : \quad 124 < m_H^{\text{SM4}} < 286 \text{ GeV} \quad \text{excluded.} \quad (4.18)$$

The upper bound is at 300 GeV because searches with masses larger than this were not performed.

The validity of the exclusion (4.18) has since been questioned. In fact, arguments show [172] that (4.17) *overconstrains* the fourth generation parameter space and in fact, a better description of the parameter space might be [154]

$$\Delta m_{q'} \lesssim \left(1 + \frac{1}{5} \log \frac{m_H}{125 \text{ GeV}} - 15 s_{34}^2 \right) \times m_W , \quad (4.19)$$

where the mixing of the third and fourth generations has been taken into account in the inclusion of $s_{34} \equiv \sin \theta_{34} = |V_{t'b}|$.

4.3.2 Higgs searches at the LHC

The discovery potential of the LHC for the SM4 Higgs boson has been analyzed in Ref. [173]. The integrated luminosity needed at $\sqrt{s} = 14 \text{ TeV}$ is shown in Fig. 4.13 as a function of the Higgs mass, but also the collaborations themselves have published studies concerning the fourth generation:

The ATLAS collaboration has searched for the Higgs boson in the mass range 110–600 GeV in 35 to 40 pb^{-1} of data recorded in 2010 [174]. For the SM4 Higgs searches it was assumed that

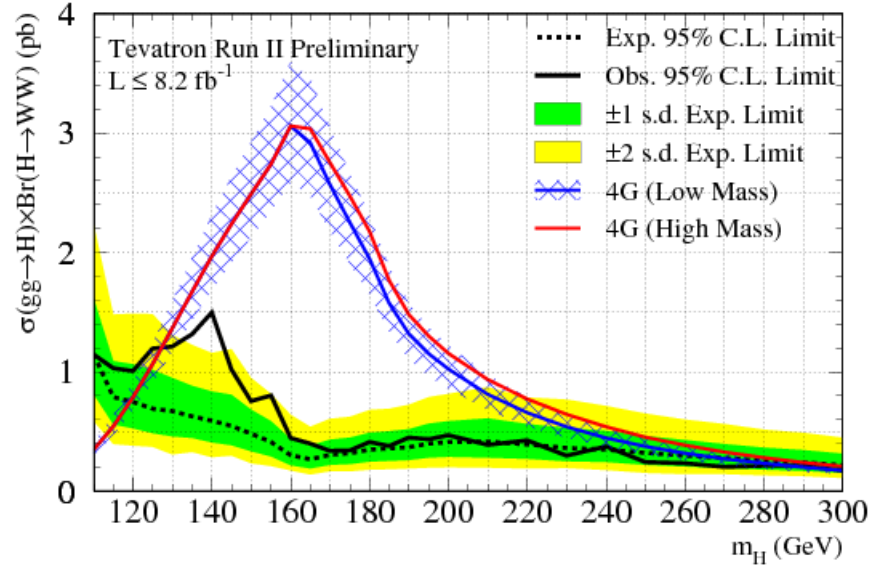


Figure 4.12: The Tevatron combined observed (solid black lines) and median expected (dashed black lines) 95% C.L. upper limits on $\sigma(gg \rightarrow H) \times \mathcal{B}(H \rightarrow W^+W^-)$. The shaded bands indicate the ± 1 standard deviation (s.d.) and ± 2 s.d. intervals on the distribution of the limits that are expected if a Higgs boson signal is not present. Also shown the prediction for a fourth-generation model in the low-mass and high-mass scenarios, 4G (Low mass) and 4G (High mass) respectively. The hatched areas indicate the theoretical uncertainty from PDF and scale uncertainties. The lighter curves show the high-mass theoretical prediction. Figure and caption from Ref. [171].

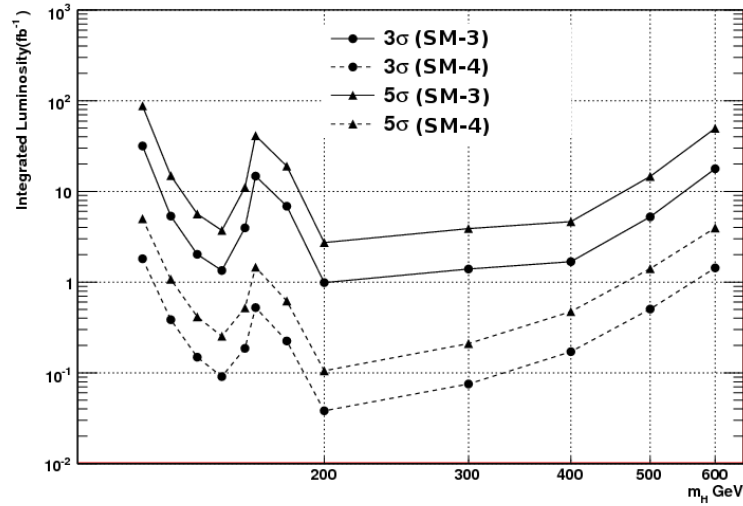


Figure 4.13: The integrated luminosity required at $\sqrt{s} = 14$ TeV for 3σ observation and 5σ discovery of the ‘golden mode’ $gg \rightarrow H \rightarrow ZZ \rightarrow 4\ell$ in the SM3 and SM4 cases. Figure from Ref. [173].

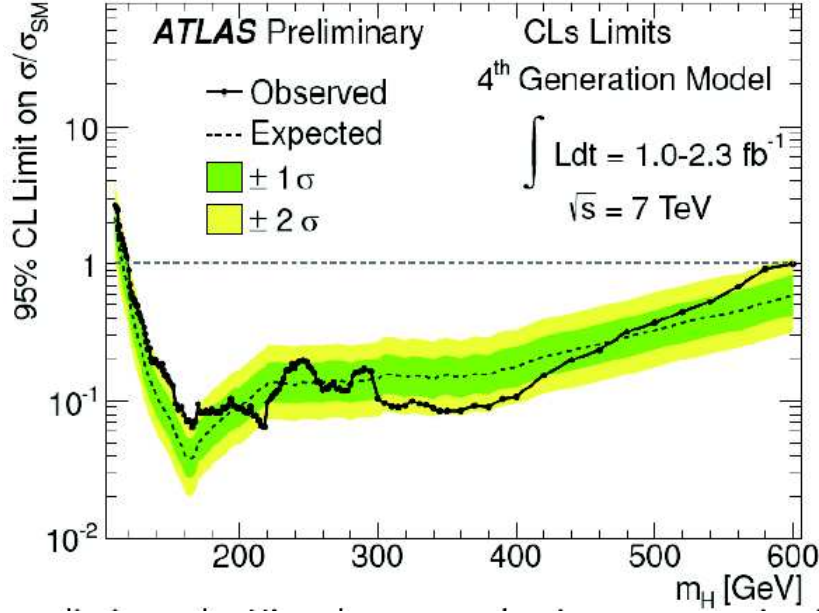


Figure 4.14: The combined upper limit on the Higgs boson production cross section in the framework of SM4. Figure from Ref. [175].

the fourth generation fermions are very heavy so that the possibility of the Higgs decaying into neutrinos is excluded. The results of the analysis is :

$$\text{ATLAS (2011)} : m_H^{\text{SM4}} = 140 - 185 \text{ GeV excluded.} \quad (4.20)$$

A few months later improved limits were reported [175]:

$$\text{ATLAS (Aug 2011)} : m_H^{\text{SM4}} < 600 \text{ GeV excluded,} \quad (4.21)$$

as is shown in Fig. 4.14.

Similarly, according to the results presented at the summer conferences of 2011 by the CMS collaboration [176]

$$\text{CMS (2011)} : m_H^{\text{SM4}} = 120 - 600 \text{ GeV excluded at 95\% C.L..} \quad (4.22)$$

The existence of a relatively light fourth family neutrino might require a reconsideration of the CMS and ATLAS experimental bounds (4.22), (4.20). The bounds would in this case be reduced from 120–600 GeV to 160–500 GeV because the opening of the $H \rightarrow \nu'\nu'$ modifies the situation [177].

However, as we will discuss in the next chapter, the statistics accumulated by the beginning of 2012 have been enough to exclude the four-family model reviewed in this section.

Chapter 5

Experimental exclusion of the minimal four-generation standard model

After the beginning of this work new results from experiments at CERN and Fermilab have been reported. In 2011 some excess could be seen in different channels somewhere around 150 GeV [178, 177, 171], however, at this stage only at $2.5\text{--}3\sigma$ significance. With the amount of data accumulated by July 2012, however, the LHC collaborations CMS [101] and ATLAS [100] measure a resonance at ~ 125 GeV at 5σ from the expected SM background [179]. Recent analyses done at Fermilab by CDF give similar hints [180]. This resonance is due to a bosonic particle, but whether it is SM-like or not is not yet known. The observed signal is not exactly equal to what would be expected from the standard model as such, but the deviation from the SM prediction is smaller than what is expected in the framework of four generations. This excess might signal new physics, or it might not – higher statistics is needed to get an answer.

The determination of the characteristics of this new particle, which is probably the Higgs, will require a lot more data, but already the mass and the decay rates observed serve to constrain beyond the BSM theories. Especially, it has been found that the standard model with a sequential fourth generation is excluded at 99.9% confidence level for a Higgs of mass 125 GeV [181].

Searches

The ATLAS, CMS, CDF and DØ collaborations have performed searches in five channels :

- $\gamma\gamma$, ZZ^* , WW^* from gluon fusion
- $b\bar{b}$ associated production
- $\gamma\gamma$ from vector boson fusion

These are shown in Figs. 5.1, 5.2. The LHC experiments have observed $\sim 5\sigma$ excess in the $\gamma\gamma$ and ZZ^* channels, whereas the Tevatron experiments have a significance of $\sim 3\sigma$ for $b\bar{b}$ associated production. The only one of the above channels where excess has not been seen is the WW^* one.

In the channel $H \rightarrow \gamma\gamma$ the signal is reported to have a statistical significance of more than 4 standard deviations [100, 101]. The total observed rate in this channel is somewhat higher than what is expected of the SM (with a factor 1.9 ± 0.5 for ATLAS and 1.56 ± 0.43 for CMS), lying within $\pm 2\sigma$ [179] from the SM expectation, but still not satisfied by SM4 either. In fact, the observed rate is at 4σ from SM4 [182]. An important thing to note about this channel is that it is actually *suppressed* in the four-generation model. Naively, the rate $H \rightarrow \gamma\gamma$ would be expected to

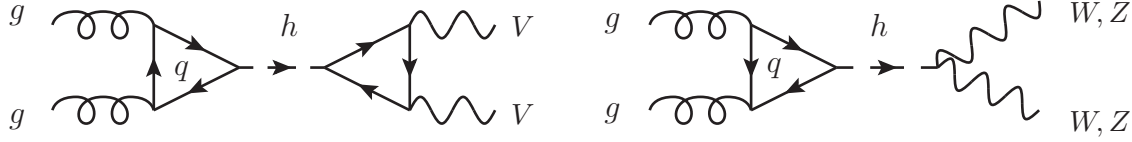


Figure 5.1: The channels $h \rightarrow VV$ with $VV = \gamma\gamma, WW^*, ZZ^*$ looked for at the LHC. On the left-hand side there is a fermion or a massive gauge boson running through the second loop. The Higgs does not have direct couplings to the photon, so the $h \rightarrow \gamma\gamma$ process can only proceed through loop processes (left).

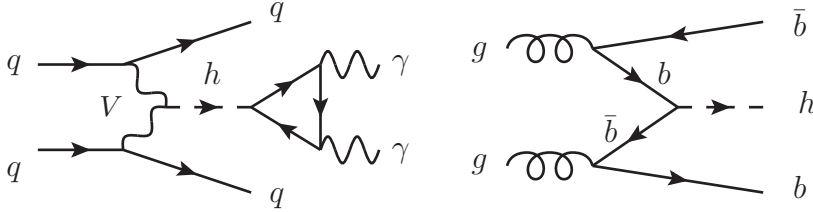


Figure 5.2: The channels $h \rightarrow \gamma\gamma$ from vector boson fusion $V = W, Z$ (left) and $b\bar{b}$ associated production (right).

be enhanced since Higgs production from gluon fusion has a larger cross section when the two new heavy quarks are included. But it turns out that when the full next-to-leading order corrections are taken into account, the rate of $H \rightarrow \gamma\gamma$ is suppressed by a large factor. This happens because the diagrams with a W in the loop have opposite sign from those with a quark in the loop, and when all fourth generation quarks are summed over in the loop, their contribution almost exactly cancels the W one. This cancellation is purely *accidental* (see for example [182]), and it also affects the $H \rightarrow W^+W^-, ZZ$ channels.

The same suppression does not take place for the double production of tau leptons: $H \rightarrow \tau\tau$ [183]. Therefore this channel should receive a significant enhancement from the aforementioned gluon fusion process, but so far this is not consistent with observations, giving a further argument against the four-generation scenario. The significance of this exclusion is at 4σ .

The CDF and DØ measurements of the ‘Higgs-strahlung’ process and the subsequent $H \rightarrow b\bar{b}$ decay (shown in Fig. 5.3) give a signal with a significance of 2.9 standard deviations [180]. The measured signal strength of $1.97^{+0.74}_{-0.68}$ is a little above the SM3 expectation, but way above the SM4 expectation, which is just 0.4 [182]. This Higgs-strahlung production mechanism is relevant for $m_H \sim 120$ GeV since in this mass range the background consisting of $b\bar{b}$ from gluon fusion is too large. In Higgs-strahlung from a W or Z the decay of the vector boson will help tag the $b\bar{b}$ pair. [128]

Summary: Why is the exclusion possible?

The measured signals serve to exclude the (minimal) four-generation standard model ¹ at the very high confidence level of 99.9% [181]. The exclusion is possible thanks to

¹We say *minimal* because an extended version of the SM4 will be considered in the following chapter.

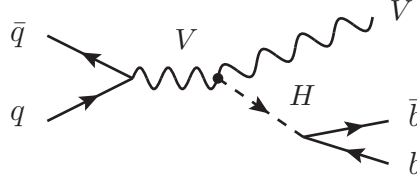


Figure 5.3: The diagram of the ‘Higgs-strahlung’ process with subsequent $H \rightarrow b\bar{b}$ decay.

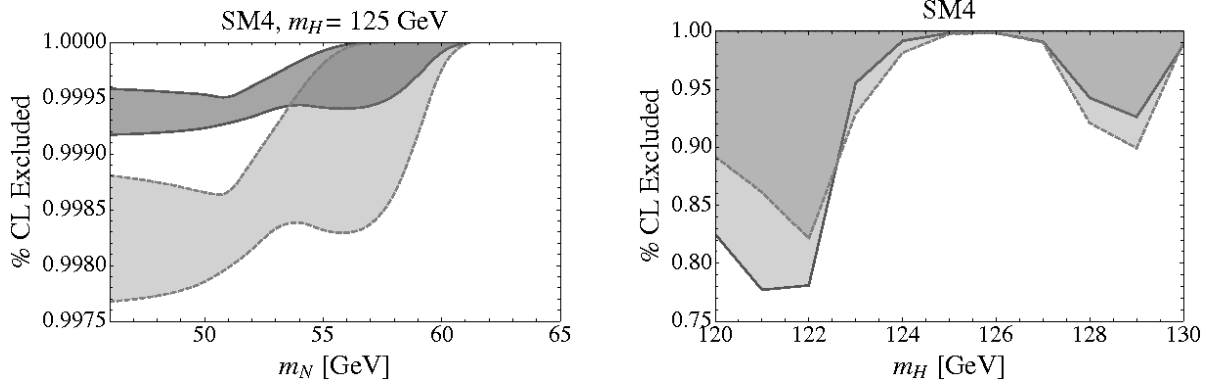


Figure 5.4: Constraints on the SM4 derived from scanning over the fourth generation fermion masses as described in the text. The darker region within the solid borders (light region within the dashed borders) shows the level of exclusion with (without) the $\gamma\gamma jj$ mode. Left: the exclusion limit as a function of the neutrino mass (the other fourth generation fermion masses are scanned) for fixed $m_h = 125$ GeV. Right: the exclusion limit as a function of m_h , with all fourth generation masses varied. Figure and caption from [181].

- $gg \rightarrow h$ production rate is *enhanced* by a factor $\mathcal{O}(10)$,
- the channel $h \rightarrow \gamma\gamma$ *suppressed* by a factor $\mathcal{O}(100)$,
- at tree level the corrections from the fourth generation to $\Gamma(h \rightarrow b\bar{b})$ and $\Gamma(h \rightarrow ZZ^*)$ are small,
- enhancement of $H \rightarrow \tau\tau$ not seen in experiments

The authors of [181] deduce constraints on the SM4 by minimizing χ^2 (A.1) in two different settings, depending on the treatment of the mass of the fourth generation neutrino (see Fig. 5.4). They find that for $124 \text{ GeV} \leq m_h \leq 127 \text{ GeV}$ the SM4 is excluded at a confidence level of more than 95% and that for the specific mass $m_h = 125 \text{ GeV}$ the exclusion is at 99.9% C.L.

A similar result is obtained in another study, where the authors develop a new method for the calculation of probabilities in order to evaluate the SM3 and SM4 fits [183]. The new method is necessary because the SM3 and SM4 are not *nested*, meaning that the SM3 cannot be obtained as a special case of SM4 with some parameters fixed. This non-nestedness implies that the usual formulae for computing probabilities in likelihood ratio tests does not work. Hence a new C++ framework is developed for this study, where the goodnesses of the SM3 and SM4 fits are evaluated. The χ^2 -distributions for the two scenarios are shown in Fig. 5.5. The figures show that both in

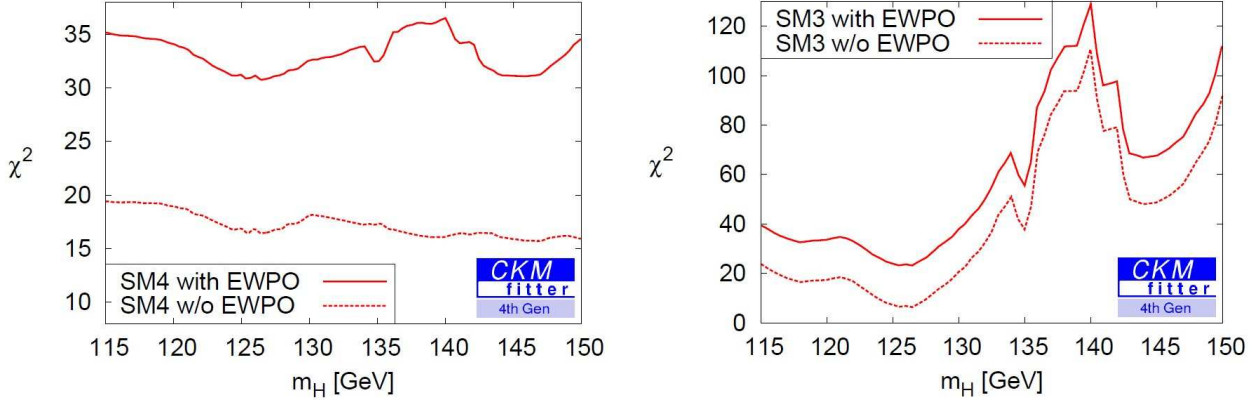


Figure 5.5: The minimum χ^2 value of the SM4 (left) and SM3 (right) as a function of the Higgs mass m_H . The solid line shows the results of the combined analysis of signal strengths and EWPOs. For the dashed line only the signal strengths were included in the fit. Figures and caption from [183].

the three and four-generation cases there is a minimum at the experimentally measured value of $m_H = 126.5$ GeV. As noted already in Section 1.2.3, some of the electroweak precision observables (EWPOs) alter the global fits. For the case of SM3, the minimum at the ‘correct’ value of 126.5 seems to be a global minimum, whereas in the SM4 case there are two minima, at 126.5 GeV and 147 GeV, both at almost the same χ^2 -value. These SM4 minima occur at $\Delta\chi^2 \approx +8$ with respect to the SM3 and are thus clearly worse. Also, the fact that the fits predicts a second minimum at 147 GeV, which is nowhere near the measured value, is in disfavor of SM4, since it shows that the SM4 has some severe difficulties in describing the data.

The exclusion was shown to have reached over 5σ confidence level [184] a few days prior to the submittance of this thesis. When both EWPD and the recent Higgs signal strengths from both the LHC and the Tevatron are taken into account, likelihood-ratio tests are used to compare the SM and SM4. (As noted above, the comparison cannot be made analytically but rather using numerical simulations.) The LHC data alone is not sufficient for a 5σ exclusion, giving a statistical significance of ‘only’ 4.8σ , but when Tevatron data is included the significance rises to 5.3σ . The SM4 seems to be most decisively ruled out.

Higgs mass impact on fourth generation neutrino

The observed signal at ~ 125 GeV constrains the neutrino sector of the fourth generation. If the channel $H \rightarrow \nu'\bar{\nu}'$ were open, and the Higgs light $m_H \lesssim 160$ GeV, then the Higgs width would be very small $\Gamma_H \lesssim 1$ GeV. In this case the neutrino channel would dominate over the other Higgs decay modes [182]. For the neutrino channel to be kinematically accessible, it is of course required that

$$m_{\nu'} \lesssim \frac{1}{2}m_H. \quad (5.1)$$

However, the experiments (ATLAS and CMS, see above) have reported excess in the diphoton channel, quite the opposite of suppression. In this case the neutrino channel cannot be open, so in fact the relation (5.1) is not satisfied and as a consequence the neutrino is heavier than ~ 62.5 GeV. [182]

Part III

The two Higgs doublet model

Chapter 6

Theory of the two Higgs doublet model

After the beginning of this work the minimal four-generation standard model has been excluded by experiments (see the previous chapter). The use of the word ‘minimal’ here refers to the fact that, in the SM4 we have (as is the case of SM3) just included *one* Higgs doublet in the scalar sector of the theory. It might well be that there exist more than one scalar doublet in nature; at present we do not know. In the rest of this report we will consider the impact of adding another scalar doublet to the four-generation standard model considered previously.

6.1 Why add another doublet?

In this report we have discussed the number of fermion families in the standard model. An interesting thing to note is that even though we know that there are at least three fermion families and two left-handed $SU(2)$ doublets in each family, the SM still has just one scalar doublet (the ‘standard’ Higgs doublet). However, there is no reason for there to be just one Higgs doublet, and on the contrary there are some arguments that favor several such doublets. Motivation for models including *two* Higgs doublets (2HDM:s) instead of one include [185]

- *Supersymmetry (SUSY)*
Supersymmetry requires at least two Higgs doublets, because scalars come in chiral multiplets and the complex conjugates come in multiplets of opposite chirality – hence there must be at least two Higgs doublets.
- *Cancellation of anomalies*
In the SM the fermion families need to be complete in order for anomalies to be cancelled. In SUSY, the introduction of a single Higgsino (the supersymmetric partner of the Higgs) introduces anomalies. These are cancelled when one introduces a second doublet.
- *Axion models*
According to axion models in QCD possible CP violating terms (that are experimentally known to be very small) in \mathcal{L}_{QCD} may be rotated away if the Lagrangian exhibits a global $U(1)$ symmetry. Such a symmetry exists only if there are two Higgs doublets.
- *Baryon asymmetry of the Universe* The baryon asymmetry of the Universe is not properly described by the standard model. 2HDMs, however, may explain this asymmetry thanks to the flexibility of the scalar mass spectrum as well as additional new sources of CP violation.

A very important parameter giving information about the scalar sector is the ρ parameter (2.62)

$$\rho = \frac{\sum_{i=1}^n \{I_i(I_i + 1) - \frac{1}{4}Y_i^2\} v_i}{\sum_{i=1}^n \frac{1}{2}Y_i^2 v_i}, \quad (6.1)$$

whose experimental value is known to be very close to one (2.63). Eq. 6.1 shows that both $SU(2)$ singlets with $Y = 0$ and doublets with $Y = \pm 1$ give $\rho = 1$ because in both these cases $I(I+1) = \frac{3}{4}Y$.

6.2 The scalar potential and the field content

Complex scalar doublets have four degrees of freedom so with two (Higgs) doublets Φ_1, Φ_2 there are eight. Three of these are just Goldstone bosons that give masses to the W^\pm and Z and the remaining five are the physical scalars – the Higgs fields. Of these five there is a charged scalar (with two physical states), two neutral ones and a pseudoscalar (see *e.g.* [128]):

$$(h^0, H^0, A^0, H^\pm) \quad (6.2)$$

with masses (m_h, m_H, m_A, m_\pm) . Here h^0, H^0, H^\pm are the scalars (CP-even particles) and A^0 is the pseudoscalar (CP-odd).

Whereas the SM Higgs sector has only one free parameter (the Higgs mass) 2HDMs contain several free parameters and the vacuum structure is much richer. The most general scalar potential contains several parameters and it has CP-conserving, CP-violating and charge-violating minima. The potential reads [185]

$$\begin{aligned} V = & m_{11}^2 \Phi_1^\dagger \Phi_1 + m_{22}^2 \Phi_2^\dagger \Phi_2 - m_{12}^2 (\Phi_1^\dagger \Phi_2 + \Phi_2^\dagger \Phi_1) + \frac{\lambda_1}{2} (\Phi_1^\dagger \Phi_1)^2 + \frac{\lambda_2}{2} (\Phi_2^\dagger \Phi_2)^2 \\ & + \lambda_3 \Phi_1^\dagger \Phi_1 \Phi_2^\dagger \Phi_2 + \lambda_4 \Phi_1^\dagger \Phi_2 \Phi_2^\dagger \Phi_1 + \frac{\lambda_5}{2} \left[(\Phi_1^\dagger \Phi_2)^2 + (\Phi_2^\dagger \Phi_1)^2 \right], \end{aligned} \quad (6.3)$$

for Φ_1, Φ_2 the two doublets of hypercharge +1. All the parameters of the potential are real. The large Yukawa couplings of the fourth generation fields can destabilize the potential (6.3) due to the possibly very large radiative corrections that they bring [186]. A way to deal with this problem is to assume that the effective potential of the model is stabilized by some new effect near the TeV scale, and that (6.3) is valid below this scale.

A region of parameter space minimizing the potential (6.3) gives the vacuum expectation values

$$\langle \Phi_1 \rangle_0 = \frac{1}{\sqrt{2}} \begin{pmatrix} 0 \\ v_1 \end{pmatrix}, \quad \langle \Phi_2 \rangle_0 = \frac{1}{\sqrt{2}} \begin{pmatrix} 0 \\ v_2 \end{pmatrix}. \quad (6.4)$$

For the vacuum (6.4) the fields have the following mass terms in the Lagrangian

$$\mathcal{L}_{\phi^\pm}^{\text{mass}} = [m_{12}^2 - (\lambda_4 + \lambda_5)v_1 v_2] \begin{pmatrix} \phi_1^- & \phi_2^- \end{pmatrix} \begin{pmatrix} \frac{v_2}{v_1} & -1 \\ -1 & \frac{v_1}{v_2} \end{pmatrix} \begin{pmatrix} \phi_1^+ \\ \phi_2^+ \end{pmatrix}, \quad (6.5)$$

$$\mathcal{L}_\eta^{\text{mass}} = \frac{m_A^2}{v_1^2 + v_2^2} \begin{pmatrix} \eta_1 & \eta_2 \end{pmatrix} \begin{pmatrix} v_2^2 & -v_1 v_2 \\ -v_1 v_2 & v_1^2 \end{pmatrix} \begin{pmatrix} \eta_1 \\ \eta_2 \end{pmatrix}, \quad (6.6)$$

$$\mathcal{L}_\rho^{\text{mass}} = - \begin{pmatrix} \rho_1 & \rho_2 \end{pmatrix} \begin{pmatrix} m_{12}^2 \frac{v_2}{v_1} + \lambda_1 v_1^2 & -m_{12}^2 + \lambda_{345} v_1 v_2 \\ -m_{12}^2 + \lambda_{345} v_1 v_2 & m_{12}^2 \frac{v_1}{v_2} + \lambda_2 v_2^2 \end{pmatrix} \begin{pmatrix} \rho_1 \\ \rho_2 \end{pmatrix}, \quad (6.7)$$

for $\lambda_{345} = \lambda_3 + \lambda_4 + \lambda_5$ and when the doublet Φ_i is written

$$\Phi_i = \begin{pmatrix} \phi_i^+ \\ \frac{v_i + \rho_a + i\eta_i}{\sqrt{2}} \end{pmatrix}, \quad i = 1, 2, \quad (6.8)$$

with charged scalar ϕ^\pm , pseudoscalar η and neutral scalar ρ . The mass-squared matrices of Eqs. (6.5), (6.6) each have a zero eigenvalue, corresponding to the massless Goldstones that give the masses to the W^\pm and Z , respectively. Besides the zero eigenvalues these matrices also give the physical masses for the charged and pseudoscalar Higgses:

$$m_\pm^2 = [m_{12}^2/(v_1 v_2) - \lambda_4 - \lambda_5] (v_1^2 + v_2^2) \quad (6.9)$$

$$m_A^2 = [m_{12}^2/(v_1 v_2) - 2\lambda_5] (v_1^2 + v_2^2) \quad (6.10)$$

The mass matrices of Eqs. (6.5), (6.6), (6.7) can be diagonalized, but in general not simultaneously. We will discuss this in the next section. Two important parameters in the study of 2HDMs are α and β , the angles that diagonalize the mass-squared matrices of the pseudoscalar and charged scalar sector and the neutral scalar sector, respectively. The angle β is defined using the VEVs of the two doublets Φ_1, Φ_2

$$\tan \beta \equiv \frac{v_2}{v_1}. \quad (6.11)$$

6.3 Flavor conservation

As already mentioned, the mass-squared matrices of the various Higgs fields may in general not be diagonalized simultaneously. This gives rise to tree-level flavor-changing neutral currents (FCNC). Since FCNCs have not been observed in nature their existence poses a problem for such models with several scalar multiplets. In order to illustrate this let us consider the Lagrangian describing the mass of down-type quarks [185]

$$\mathcal{L}_Y^d = y_{ij}^{(1)} \bar{\psi}_i \psi_j \Phi_1 + y_{ij}^{(2)} \bar{\psi}_i \psi_j \Phi_2, \quad (6.12)$$

where i, j are a family indices. The corresponding mass matrix reads

$$M_{ij}^d = y_{ij}^{(1)} \frac{v_1}{\sqrt{2}} + y_{ij}^{(2)} \frac{v_2}{\sqrt{2}}. \quad (6.13)$$

In the SM, with just one Higgs multiplet, the diagonalization of the mass matrix M implies the diagonalization of the Yukawa couplings y . This is not the case of Eq. (6.13), however, where $y^{(1)}$ and $y^{(2)}$ usually do not have the same set of eigenvectors, and so in general the Yukawa interactions (6.12) will have FCNCs at the tree level (*e.g.* couplings $\bar{d}s\phi$). Getting rid of these is customarily done by introducing some additional, continuous or discrete symmetries. [185]

There are different ways to introduce the symmetries that hinder the FCNCs. One option is to introduce a discrete symmetry

$$\Phi_1 \longrightarrow -\Phi_1, \quad (6.14)$$

which is done for example in the so-called *type I 2HDM*, where Φ_1 is chosen to couple to all fields of the theory, and Φ_2 to none.

Another option is to have transformations

$$\Phi_1 \longrightarrow -\Phi_1, \quad d_R^i \longrightarrow -d_R^i, \quad (6.15)$$

ξ_h^u	$\cos \alpha / \sin \beta$	ξ_H^u	$\sin \alpha / \sin \beta$	ξ_A^u	$\cot \beta$
ξ_h^d	$-\sin \alpha / \cos \beta$	ξ_H^d	$\cos \alpha / \cos \beta$	ξ_A^d	$\tan \beta$
ξ_h^ℓ	$-\sin \alpha / \cos \beta$	ξ_H^ℓ	$\cos \alpha / \cos \beta$	ξ_A^ℓ	$\tan \beta$

Table 6.1: Yukawa couplings of u, d, ℓ to the neutral Higgs bosons h, H, A in the type II 2HDM. The couplings to the charged Higgs bosons are obtained from Eq. (6.16). Values from Ref. [185].

as may be done in the *type II 2HDM*, where the right-handed down-type quarks couple to Φ_1 and the right-handed up-type quarks couple to Φ_2 . In this report we will concentrate on the model of the second type, which is in fact the one that has been studied the most extensively in the literature since it is the structure that is present in supersymmetric models. The non-supersymmetric case differs from the SUSY one in a few important aspects [185]:

- there is no strict upper limit on the mass of the lightest Higgs,
- the scalar self-couplings are arbitrary,
- the angle α that diagonalizes the mass-squared matrix of the pseudoscalar and charged scalar sector is arbitrary,
- decays $H^\pm \rightarrow A^0 W^\pm$ are usually allowed.

6.4 Yukawa couplings of the type II 2HDM

In the type II 2HDM the Yukawa terms in the SM Lagrangian may be written as [185]

$$\begin{aligned} \mathcal{L}_{\text{Yukawa}}^{\text{2HDM}} = & - \sum_{f=u,d,\ell} \frac{m_f}{v} \left(\xi_h^f \bar{f} f h + \xi_H^f \bar{f} f H + i \xi_A^f \bar{f} \gamma_5 f A \right) \\ & - \left\{ \frac{\sqrt{2} V_{ud}}{v} \bar{u} \left(m_u \xi_A^u P_L + m_d \xi_A^d P_R \right) d H^+ + \frac{\sqrt{2} m_\ell}{v} \xi_A^\ell \bar{\nu}_L \ell_R H^+ + \text{h.c.} \right\}, \quad (6.16) \end{aligned}$$

where the f are fermion fields with Yukawa couplings ξ^f as in Table 6.1, $P_{L,R}$ are the projection operators on left and right-handed helicities, respectively.

The couplings of the neutral, scalar Higgses h, H to the massive vector bosons Z and W are proportional to the SM coupling of the single Higgs, namely

$$g(hWW, hZZ)|_{\text{2HDM}} = \sin(\beta - \alpha) \cdot g(hWW, hZZ)|_{\text{SM}} \quad (6.17)$$

$$g(HWW, HZZ)|_{\text{2HDM}} = \cos(\alpha - \beta) \cdot g(HWW, HZZ)|_{\text{SM}}. \quad (6.18)$$

The coupling of the pseudoscalar A to the vector bosons is zero.

Chapter 7

4F2HDM phenomenology

When the second scalar doublet is added to the theory this necessarily affects the production and decay of the Higgs particles. Already the field content is modified, there are several Higgses, not just one. Also, the couplings of these many scalars are different from the minimal case of the SM. The production and decay probabilities are, as normally done in QFTs, computed from the amplitudes of the relevant processes, and these depend on the properties of and the couplings between the fields participating in the process. What is then experimentally measured in the detectors of particle colliders are the decay products, and the rates at which different decays are observed. Since these differ from model to model the decays, especially through the measured branching ratios, give information about the properties of the decaying particle and allows to distinguish between various models. That is why we in this section concentrate on the (production and) decay of the fourth generation particles and the Higgses of the type-II 2HDM, the model of interest to us.

7.1 Higgs production and decay in the 2HDM-II

An important thing to note about the branching ratios of the extended Higgs sector is that they will not only depend on the masses but also on the two new parameters α, β that are introduced in the theory when another scalar doublet is added [128]. Since these two parameters are unknown, their values must be fixed in order to get concrete predictions. This implies that comprehensive analyses are difficult and more specifically that any plot of the branching ratios is necessarily incomplete.

The impact of a fourth generation on SM Higgs production was discussed in Section 3.2. As noted before, the dominant production mechanism at hadron colliders is gluon fusion (see Fig. 3.5). In the standard model, the largest contribution comes from a top quark loop, whereas in SM4 the three heavy quarks t, t', b' give the largest contribution. In both these cases the largest contribution comes from the quarks having the largest Yukawa couplings. Since the bottom quark is quite a bit lighter than the top quark, its effect on the gluon fusion process is negligible with respect to the top. In the four-fermion 2HDM (4F2HDM) model the bottom quark contribution to the loop diagram 3.5 may for the 2HDM-II be sizeable and even dominate over t in a region of parameter space.

As the Yukawa couplings of the various Higgses differ, we will present their production and decays separately. We will only consider the two lightest particles h^0 and A^0 since these are the ones that are most likely to be discovered at particle colliders, and h^0 has perhaps already been found (see Chapter 5).

7.1.1 Production and decay of the neutral pseudoscalar A^0

The ratio of the 4F2HDM $gg \rightarrow A$ cross section to that of the SM3 is (compare with Eq. (3.26) for the ratio of SM4 to SM3) [128] :

$$\frac{\sigma[gg \rightarrow A^0]_{4F2H}}{\sigma[gg \rightarrow h^0]_{SM3}} = \frac{\left| \sum_{Q=t',b',t} \xi_A^Q \mathcal{I}_A(\tau_Q) \right|^2}{|\mathcal{I}_S(\tau_t)|^2}, \quad (7.1)$$

where the form factors are given in Appendix F.

In the enhancement (7.1) we see the Yukawa couplings ξ (Table 6.1) appearing. In particular this means that when $\tan \beta$ is large the affect of a b quark in the loop of the gluon fusion process may be relatively large, and has to be taken into account in the sum in the denominator of (7.1).

The decay of A^0 to the fourth generation neutrinos ν', \mathcal{N}' with masses (2.81) it of great interest because, as we will shortly see, this is the dominant decay channel in a large part of the parameter space. The decay has the tree-level width [128] :

$$\Gamma(A^0 \rightarrow \nu' \bar{\nu}', \mathcal{N}' \bar{\mathcal{N}}') = \frac{M_{\nu', \mathcal{N}'}^2 M_A |\xi_A^{\nu'}|^2}{4\pi v^2 (1 + \tan^2 \theta)^2} \left(1 - \frac{4M_{\nu', \mathcal{N}'}^2}{M_A^2} \right)^{\frac{3}{2}}, \quad (7.2)$$

where θ is given in (2.84) and the channel is open when the neutrinos have masses smaller than half the A^0 mass. Fourth generation fermions are also present in the loops of $A^0 \rightarrow gg, \gamma\gamma, \gamma Z$ [128]:

$$\Gamma(A^0 \rightarrow gg)_{4F2H} = \frac{\alpha_s^2 M_A^3}{32\pi^3 v^2} \left| \sum_{Q=t',b',t} \xi_A^Q \mathcal{I}_A(\tau_Q) \right|^2, \quad (7.3)$$

$$\Gamma(A^0 \rightarrow \gamma\gamma)_{4F2H} = \frac{\alpha^2 M_A^3}{64\pi^3 v^2} \left| \sum_f N_c^f e_f^2 \xi_A^f \mathcal{I}_A(\tau_f) \right|^2, \quad (7.4)$$

$$\Gamma(A^0 \rightarrow \gamma Z)_{4F2H} = \frac{\alpha M_A^3 m_W^2}{32\pi^4 v^4} \left(1 - \frac{m_Z^2}{M_A^2} \right)^3 \left| \sum_f \xi_A^f N_c^f \frac{e_f c_f}{c_W} \tilde{\mathcal{I}}_A(\tau_f, \lambda_f) \right|^2. \quad (7.5)$$

Here e_f is the charge of the fermion f and the expressions for c_f and $\tilde{\mathcal{I}}_A(\tau_f, \lambda_f)$ are given in (F.3) and (F.4), respectively. The widths (7.3) – (7.5) are larger than in SM3 because the form factors \mathcal{I} (F.1) and $\tilde{\mathcal{I}}$ (F.4) are positive. Since there are no cubic $A^0 VV^*$ vertices with $V = W, Z$ in the Lagrangian (6.16) these decays are not considered here. The lack of these diboson decays especially implies that the existing limits on the Higgs mass would be significantly weakened. [128]

The various partial decay widths allow for a computation of the A^0 branching fractions, which have been calculated up to NLO in QCD corrections in Ref. [128]. The results are shown in Fig. 7.1 for fixed values of $\tan \beta = \tan \theta = 1$, varying m_A in the range 100–1000 GeV, and for fixed $m_A = 126$ GeV (in accordance with the reported signal, see Chapter 5) but varying $\tan \beta, \tan \theta$ in Fig. 7.2. In this analysis $\tan \theta$ was let to vary in the interval (2.85). We recall from the definition of the neutrino mixing parameter θ given in Eq. (2.84) and the mass eigenvalues (2.81), that the value $\tan \theta = 1$ corresponds to two degenerate states of a purely Dirac neutrino. In the case of such degeneracy the decay rates of $A^0 \rightarrow \nu' \bar{\nu}'$ and $A^0 \rightarrow \mathcal{N}' \bar{\mathcal{N}}'$ are equal (see Eq. (7.2)).

In the low mass range of $m_A \lesssim 2m_t$ the branching ratios in Fig. 7.1 show that the ‘invisible’ channel $A^0 \rightarrow \nu' \bar{\nu}', \mathcal{N}' \bar{\mathcal{N}}'$ (shown in the graph as $\nu_4 \bar{\nu}_4, \mathcal{N}_4 \bar{\mathcal{N}}_4$) suppresses the other channels for $(\tan \beta, \tan \theta) = (1, 1)$. The decay is invisible if the neutrinos have long enough lifetimes to escape the detector before decaying. The suppression might be as strong as a factor $\mathcal{O}(50 - 100)$ in

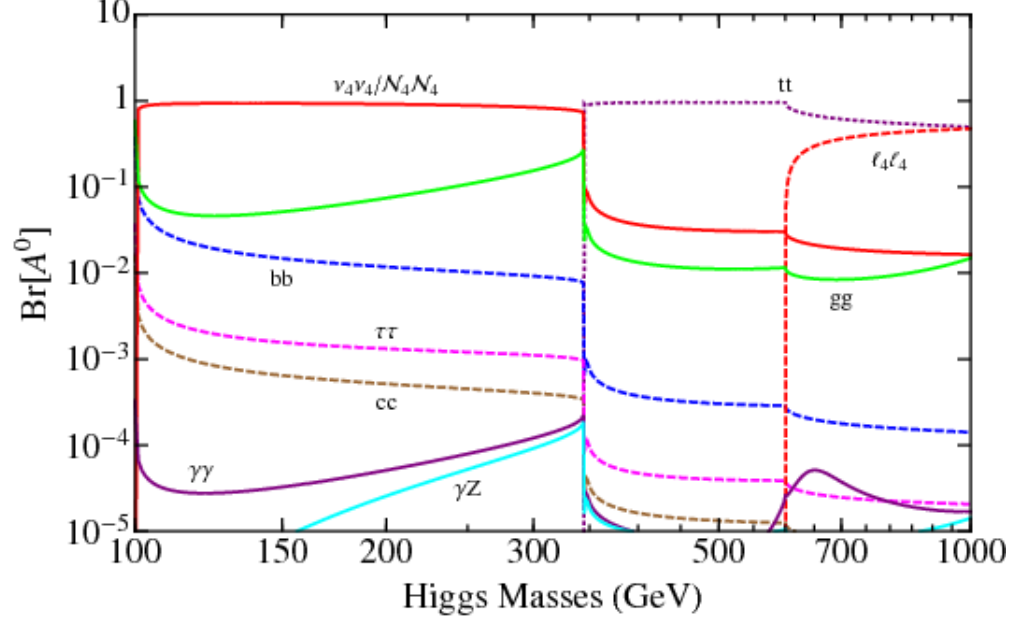


Figure 7.1: Decay branching ratios of the CP-odd Higgs boson A^0 as functions of its mass M_A for the 4F2HDM-II. The other input parameters are fixed as $(\tan \beta, \tan \theta) = (1, 1)$. Figure and caption from [128].

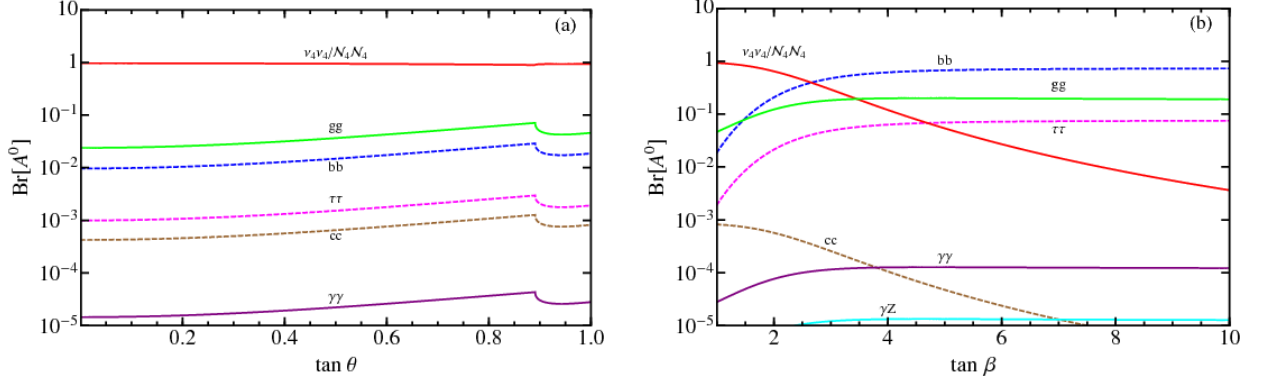


Figure 7.2: Decay branching ratios of the CP-odd Higgs boson A^0 with mass $M_A = 126$ GeV for the 4F2HDM-II. Plot-(a): $\text{Br}[A^0]$ as a function of the fourth-family neutrino mixing angle $\tan \theta$, with fixed $\tan \beta = 1$. Plot-(b): $\text{Br}[A^0]$ as a function of $\tan \beta$, with fixed $\tan \theta = 1$. Figure and caption from [128].

comparison to $\text{BR}(H \rightarrow \gamma\gamma)$ of SM3 [128]. This invisible channel seems to be dominant at all values of $\tan\theta$ considered as well as for moderate values $\tan\beta \lesssim 2$. Therefore the diphoton channel is the good one for discovery in the light-mass range, the range in which a new particle has recently been seen (see Chapter 5). The type-II 2HDM with four generations can explain the observed excess in this signal. The lack of $A^0 VV^*$ vertices implying the lack of significant $\text{BR}(A^0 \rightarrow VV^*)$ is also in accordance with the data, lacking a signal in the $H \rightarrow WW^*$ channel. [128]

7.1.2 Production and decay of the light neutral Higgs h^0

The case of the light, neutral scalar is more complicated than the previous considerations, because h^0 mixes with the other neutral scalar, the heavier H^0 . Hence there is one more free parameter, and that is the $h^0 - H^0$ mixing angle α . There are also two more tree-level decay channels to consider, namely the ones into the massive gauge bosons, since h^0 has couplings $h^0 VV^*$ (where $V = W, Z$) of strength (6.17).

As in the case of A^0 also h^0 production is enhanced by the fourth generation quarks, which have Yukawa couplings as given in the first row of Table 6.1. For a SM Higgs of the mass of h^0 , the ratio of the 4F2HDM gluon fusion cross section to that of the SM3 has an expression analogous to that of Eq. (7.1) in the case of the pseudoscalar [128]:

$$\frac{\sigma[gg \rightarrow h^0]_{4\text{F2H}}}{\sigma[gg \rightarrow h^0]_{\text{SM3}}} = \frac{\left| \sum_{Q=t',b',t} \xi_h^Q \mathcal{I}_S(\tau_Q) \right|^2}{|\mathcal{I}_S(\tau_t)|^2}, \quad (7.6)$$

The ratio (7.6) is moderate due to the couplings ξ_h (Table 6.1) and if the fourth generation quarks are very heavy with respect to h^0 ($m_h^2 \ll 2m_{q'}^2$) then the ratio is approximately the same as for SM4, that is, approximately nine.

The CP-even light, neutral Higgs has similar couplings as the single scalar boson of the SM. The usual tree-level SM decay widths to fermions and massive gauge bosons are just scaled by factors [128]:

$$\Gamma(h^0 \rightarrow f\bar{f})|_{4\text{F2HDM}} = |\xi_h^f|^2 \Gamma(h^0 \rightarrow f\bar{f})|_{\text{SM3}}, \quad (7.7)$$

$$\Gamma(h^0 \rightarrow VV^*)|_{4\text{F2HDM}} = \sin^2(\beta - \alpha) \Gamma(h^0 \rightarrow VV^*)|_{\text{SM3}}, \quad (7.8)$$

where the factors $|\xi_h^f|^2, \sin^2(\beta - \alpha)$ follow from Eqs. (6.16), (6.17), respectively.

The decays proceeding through loops are :

$$\Gamma(h^0 \rightarrow gg)_{4\text{F2H}} = \frac{\alpha_s^2 M_h^3}{8\pi^3 v^2} \left| \sum_{Q=t,t_4,b_4} \xi_h^Q \mathcal{I}_S(\tau_Q) \right|^2, \quad (7.9)$$

$$\Gamma(h^0 \rightarrow \gamma\gamma)_{4\text{F2H}} = \frac{\alpha^2 M_h^3}{16\pi^3 v^2} \left| \sum_{f=t,t_4,b_4,\ell_4} N_c^f e_f^2 \xi_h^f \mathcal{I}_S(\tau_f) + \frac{1}{2} \sin(\beta - \alpha) \mathcal{I}_W(\tau_W) \right|^2, \quad (7.10)$$

$$\Gamma(h^0 \rightarrow \gamma Z^0)_{4\text{F2H}} = \frac{\alpha M_h^3 m_W^2}{128\pi^4 v^4} \left(1 - \frac{m_Z^2}{M_h^2} \right)^3 \times \left| \sum_{f=t,t',b',\ell_4} \xi_h^f N_c^f \frac{e_f c_f}{c_W} \mathcal{A}_f^H(\tau_f, \lambda_f) + \sin(\beta - \alpha) \mathcal{A}_W^H(\tau_W, \lambda_W) \right|^2. \quad (7.11)$$

As before, the form factors are given in Appendix F. In the decays where the loop couples to the electromagnetic field, that is, when the decay products include at least one photon (7.10), (7.11), it

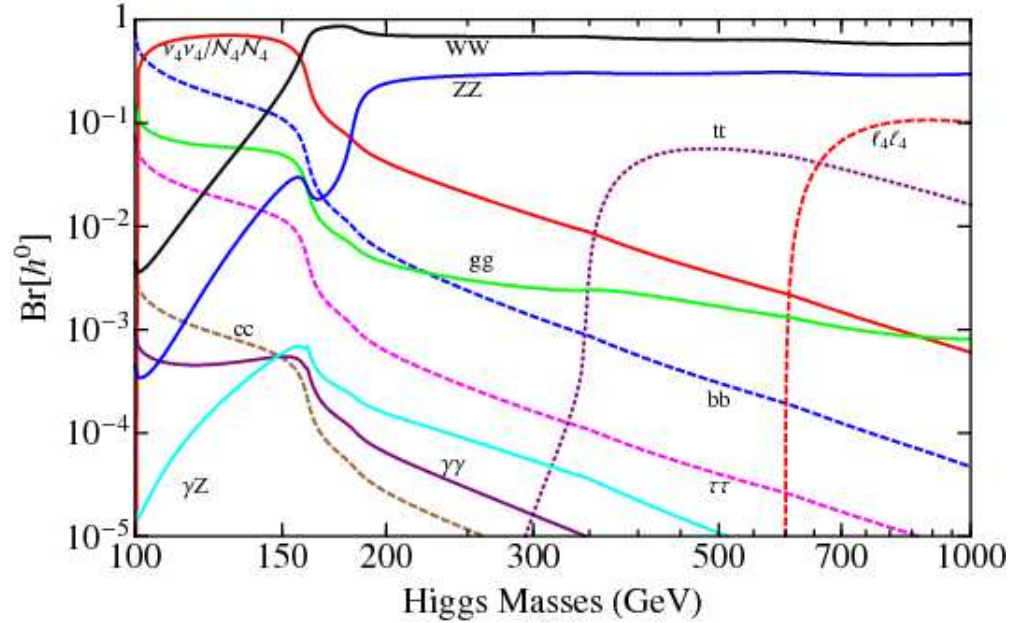


Figure 7.3: Decay branching ratios of CP-even Higgs boson h^0 in the 4F2HDM-II for the mass-range $m_h = 100 - 1000$ GeV and sample input $(\tan \beta, \tan \alpha) = (1, -3)$. Figure and caption from [128].

is also possible to have the charged Higgs H^\pm running through the loop. If the charged H^\pm is very heavy, as would seem fit from flavor physics constraints [128], then its contribution to the widths (7.10), (7.11) is negligible.

All branching ratios $\text{BR}[h^0]$ are shown in Fig. 7.3 as a function of m_h for fixed α, β . For a very light h^0 , with a mass smaller than twice the W mass, the dominant decay mode is the invisible $\nu'\nu', \mathcal{N}'\mathcal{N}'$. When the massive gauge bosons become kinematically accessible they take over.

In Fig. 7.4 the branching ratios for a Higgs of mass $m_h = 126$ GeV are shown on the left-hand side as a function of $\tan \beta$ for fixed $\tan \theta = 1$ and on the right-hand side as a function of $\tan \theta$ for fixed $\tan \beta = 1$. The branching ratios do not have a strong $\tan \theta$ dependence, whereas they do vary as functions of $\tan \beta$. As for the pseudoscalar A^0 , the invisible channel of the fourth generation neutrinos has the largest BR when $\tan \beta \lesssim 2$. The recent data suggesting $m_h \simeq 125$ GeV with a slight enhancement in the diphoton channel may well be explained by the results of this analysis of Ref. [128] presented here thanks to the enhanced $gg \rightarrow h^0$ cross section and the suppression of the diphoton channel.

7.1.3 The charged Higgs

The heavy neutral Higgs is often taken to be so heavy that its effect in most cases is negligible. Its interactions are similar to those of the light h^0 . The charged Higgs may also be heavy, but due to its electric charge its interactions with other particles differ from those of A^0, h^0 and H^0 , so we will very briefly consider its decays here.

If the charged Higgs is not so heavy that it is integrated out of the dynamics then it may decay

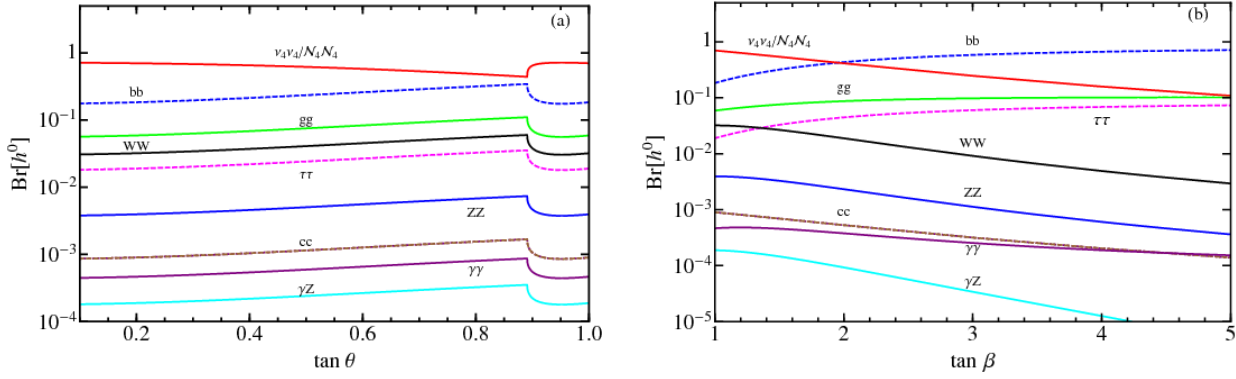


Figure 7.4: Decay branching ratios of CP-even Higgs boson h^0 with mass $m_h = 126$ GeV. Plot-(a): $Br[h^0]$ versus $\tan \theta$ with $\tan \beta = 1$. Plot-(b): $Br[h^0]$ versus $\tan \beta$, with $\tan \theta = 1$. In both plots $\tan \alpha = -3.0$ is fixed. Figure and caption from [128].

into third and fourth generation particles, h^0 and massive gauge bosons [187]:

$$\begin{aligned}
 H^+ &\longrightarrow tb, \\
 H^+ &\longrightarrow t'b, \\
 H^+ &\longrightarrow hW^+, \\
 H^+ &\longrightarrow \tau\nu_\tau \quad \text{and} \quad H^+ \longrightarrow \ell'\nu_\tau.
 \end{aligned} \tag{7.12}$$

H^\pm will rarely decay into particles of the first two generations, since these are so very light. Quite generally, the decays of H^0, H^\pm (and also A^0) are very parameter-dependent in the 4F2HDM [186].

7.2 Searches for the 4F2HDM at the LHC

The addition of another scalar doublet affects the phenomenology of the fourth generation, and especially it allows for new decays of the fourth generation quarks. In Ref. [188] it was found that the new channels

$$\begin{aligned} t' &\longrightarrow h^0 t, & b' &\longrightarrow h^0 b, \\ t' &\longrightarrow H^+ b, & b' &\longrightarrow H^- t, \\ t' &\longrightarrow W^+ b', & b' &\longrightarrow W^- t', \end{aligned} \quad (7.13)$$

are allowed by electroweak precision data and that they may even be the dominant decay channels of the fourth generation up-type quark. The second of these may be kinematically inaccessible if the charged Higgs is very heavy. The last one is forbidden in the SM [188, 187]. The presence of these new channels affect the existing bounds on t', b' (relaxing them) and in general the experimental searches have to be changed somewhat in order to better take into account the possible new signals.

7.2.1 Fourth generation quarks masses

The extension of the Higgs sector introduces new interactions to the fourth generation quarks and makes their decays more complex than in SM4. As already noted H^0 is often taken to be very heavy and integrated out of the interactions. This leaves the two light neutral Higgses h^0 and A^0 that we have focused on in the last chapters as well as the charged H^\pm .

The decays (7.13) give rise to new collider signals such as [187]

$$q\bar{q} \longrightarrow t'\bar{t}' \longrightarrow 6W + 2b, \quad (7.14)$$

$$q\bar{q} \longrightarrow t'\bar{t}' \longrightarrow 2W + 6b, \quad (7.15)$$

and quite generally one has event topologies

$$t'\bar{t}', b'\bar{b}' \longrightarrow n_W W + n_b b, \quad (7.16)$$

where n_W (n_b) is the number of W 's (b quarks). In a recent analysis the discovery potential of such channels was studied and the statistical significance of the signals in (7.14), (7.15) are shown in Table 7.1). The statistical significance is S/\sqrt{B} , with S the signal and B the background. Three different masses are considered for t' : 350, 400 and 450 GeV and the parameters $\tan\beta = 1$ and $V_{34} = 0.1$ are fixed. A result of the analysis is that existing limits on the t', b' masses need to be reanalysed, taking into account the new decays (7.16). For the minimal four-generation model SM4 it is estimated that the mass limit on t' should be ~ 350 GeV instead of the $\sim 450 - 557$ GeV in (4.12).

Mass splittings

It has already been noted that comprehensive studies of all of the parameter space of 2HDMs are difficult. Even more so when a fourth generation of fermions are added to the field content. As scanning the allowed regions of all parameters is challenging, it is necessary to fix some of these in order to be able to extract information about the other, free parameters. This is what was done in Ref. [186], where the fourth generation masses were left free while the other unknown variables were given fixed values, because a lot of information can be gained already from the knowledge of the masses.

Process	S/\sqrt{B}
$2W+6b \ m_{t'} = 350 \text{ GeV}$	5.66
$2W+6b \ m_{t'} = 400 \text{ GeV}$	4.55
$2W+6b \ m_{t'} = 450 \text{ GeV}$	2.93
$6W+2b \ m_{t'} = 350 \text{ GeV} \ 6$	4.65
$6W+2b \ m_{t'} = 400 \text{ GeV} \ 4$	3.43
$6W+2b \ m_{t'} = 450 \text{ GeV}$	2.32

Table 7.1: The statistical significance $\frac{S}{\sqrt{B}}$ for each of the new signatures (7.14), (7.15) for three different values of $m_{t'}$ at the LHC (7 TeV) with $\int Ldt = 1 \text{ fb}^{-1}$. Table values from [187].

In the study [186] the scalar potential used is (6.3), without the term $\propto m_{12}$. This potential is used to make a sampling of the four-generation parameter space. The samples are compared to the EWPD and then the most likely mass spectrum for t', b', ℓ' and ν' is deduced. This is done by computing

$$\sigma(gg \rightarrow h^0) \cdot \frac{\Gamma(h^0 \rightarrow \gamma\gamma, VV^*)}{\Gamma_{4F2HDM}(\text{tot})} \quad (7.17)$$

for each scanned value of α (the $h^0 - H^0$ mixing angle) and extracting a χ^2 . Each sample is then weighted according to its χ^2 value. The constraints that are used are :

- mass of the lightest scalar $m_h = 124.5 \text{ GeV}$,
- tree-level unitarity,
- perturbativity (quartic Higgs couplings have to be smaller than 4π),
- absence of runaway directions,
- oblique electroweak parameters.

Constraints coming from decays of the other Higgses H^0, H^\pm, A^0 are *not* taken into account, because these depend to a very high degree on the parametrization that is used. In this way the most probable parameter space of $m_{\nu'}$ vs. $m_{\ell'}$ and $m_{b'}$ vs. $m_{t'}$ are obtained (see Fig. 7.5 right and left, respectively). (In Fig. 7.5 $m_{\nu'}$ is denoted by $m(\nu_4)$, $m_{\ell'}$ by $m(\tau_4)$, $m_{b'}$ by $m(b_4)$ and $m_{t'}$ by $m(t_4)$.)

The sampling of the parameter space shows that the quark and lepton mass splittings are smaller than m_W in 99% and 65% of the samples, respectively. The fourth generation doublets have normal mass hierarchies with a probability of 59% in the quark sector, 72% in the lepton sector. The relation of $\Delta q = m_{t'} - m_{b'}$ to $\Delta \ell = m_{\ell'} - m_{\nu'}$ is shown on the left-hand side of Fig. 7.6. This figure also shows that the data prefers a low value for $\tan \beta$ (see the right-hand side of Fig. 7.6). The sampling results in $\tan \beta < 1$ 46% of the time.

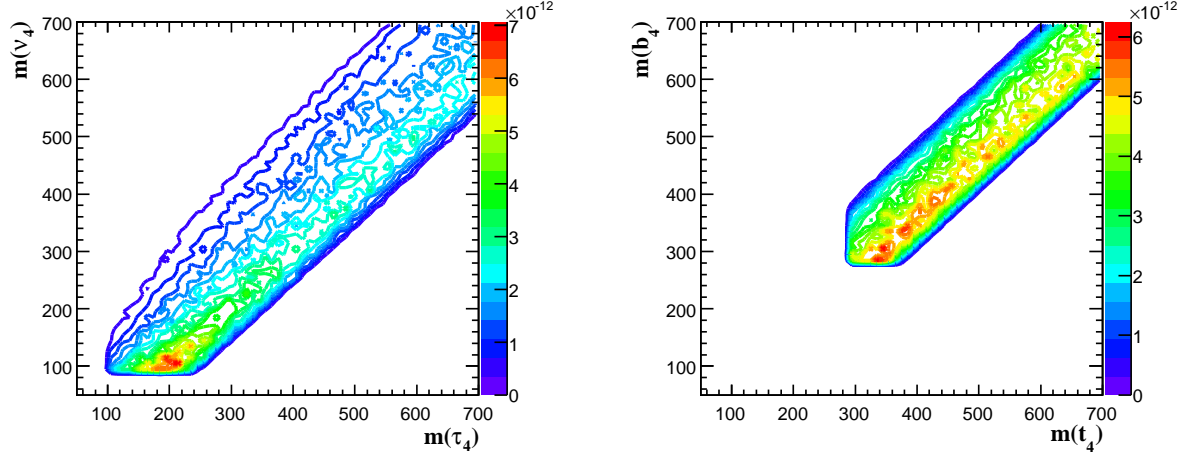


Figure 7.5: Contour plots of the probability densities in 4F2HDM with the mass of the lightest CP -even state $m_h = 124.5$ GeV. Left: $m_{\nu'} \equiv m(\nu_4)$ vs. $m_{\ell'} \equiv m(\tau_4)$; Right: $m_{b'} \equiv m(b_4)$ vs. $m_{t'} \equiv m(t_4)$; All scales are in GeV; probability densities have been normalized and each bin is $10 \text{ GeV} \times 10 \text{ GeV}$. Figure and caption from Ref. [186].

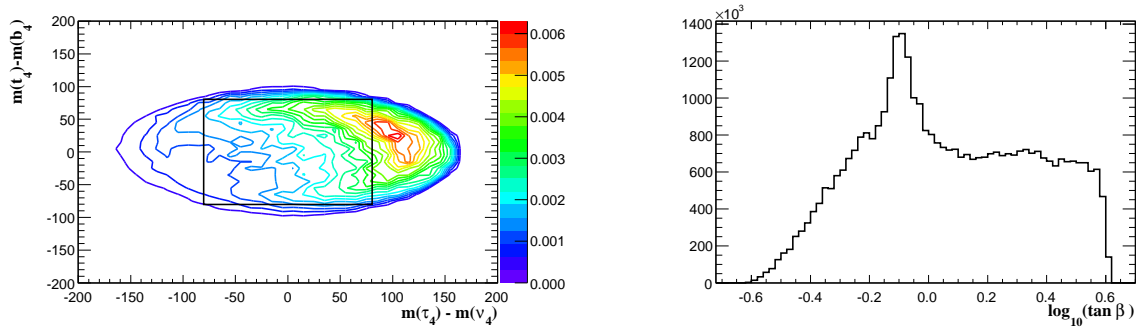


Figure 7.6: Left: Contour plots of the probability densities in 4F2HDM with the mass of the lightest CP -even state $m_h = 124.5$ GeV. Quark mass splitting vs. lepton mass splitting. The box marks the area where the magnitude of the mass splittings is less than m_W . All scales are in GeV; probability densities have been normalized and each bin is $10 \text{ GeV} \times 10 \text{ GeV}$. Right: The probability density function for $\log_{10}(\tan \beta)$ in 2HD4G with the mass of the lightest CP -even state $m_h = 124.5$ GeV. Figure and caption from Ref. [186].

Chapter 8

Conclusions

In this thesis we have reviewed particle physics models with four generations of elementary particles. The motivation for studying such extensions of the standard model (SM) comes from the SM lacking explanations for a number of phenomena observed in nature. Some of these issues are of fundamental nature, such as the baryon asymmetry of the universe or the reason for family replication and the number of families. Other issues are of specific experimental nature: measurements whose results cannot be accommodated in the SM (see Section 1.2.3 for details). An appealing feature of the four-family models is that they agree with electroweak precision data and flavor observables. For certain observables, the agreement is even better in the four-generation scenario than it is in the SM.

Also, the nature of electroweak symmetry breaking and the origin of mass have been uncertain for a long time, but at the moment the physics community is living exciting times, as a resonance has just been observed (see Chapter 5). This resonance is presumably the much sought-after Higgs particle. Its characteristics are not yet known, so whether it is standard model-like is not clear. The few pieces of information that lead to the discovery already suffice, however, to severely constrain models that incorporate new physics beyond the SM. Specifically, since the beginning of this work, the model which has been a major part of this work – the SM with four generations of elementary particles but just one scalar doublet (SM4) – has been excluded with a very high level of certainty (see Chapter 5). This is exciting in the sense that the SM4 is now the first of the popular new physics-models whose minimal version has been ruled out. (Some BSM models incorporate new physics at such scales that it is questionable whether they can be verified or excluded in the foreseeable future.) Just a few days before this thesis was submitted, the experimental exclusion of the SM4 was shown to have reached the very decisive statistical significance of 5.3σ (see Chapter 5 and Ref. [184]). This is possible thanks to the non-decoupling property of the fourth generation: the loop corrections from the fourth generation do not tend towards zero when the masses of the particles are increased.

Pushing the extension further, following the exclusion of the minimal version, a perhaps ‘next-to-minimal’ model is one in which a scalar doublet is added to the SM along with the sequential fourth family. This four-fermion two Higgs doublet model (4F2HDM), which is phenomenologically richer than the minimal one, can accommodate the new data from the LHC. The experimental exclusion of the SM4 relies in part on the enhancement of Higgs production through gluon fusion in SM4 as opposed to the SM. In the two doublet model the light, neutral Higgses dominantly decay into the fourth generation neutrinos in a large region of parameter space. (This decay, of course, requires that the neutrinos be kinematically accessible to the Higgses.)

Interestingly, these decays are invisible if the lifetime of the fourth generation neutrinos is larger than the scale of the detector. The other, subdominant channels then get event rates that could

match the observations. The partial decay widths depend on the parameters of the model, and in the 4F2HDM notably upon the parameters $\tan\beta$ (giving the ratio of vacuum expectation values of the two scalar doublets) and $\tan\theta$ (the neutrino mixing angle) and since the values of these are as yet unknown, no quantitative predictions can be made. Quite generally, given the number of free parameters in the models with two Higgs doublets, it is difficult to perform comprehensive analyses covering the whole of the possible parameter space.

Precision measurements of the recently observed resonance – most likely the Higgs – are currently being performed and more statistics will be accumulated in the near future. Hopefully, the new data may soon give answers to some of the questions mentioned in this thesis.

Appendices

Appendix A

Definitions of electroweak observables

The following definitions are found for example in Ref. [189].

- **The parameter χ^2** is often used as a measure of the deviation from the central values of the tree level bounds of the global SM fit [111]

$$\frac{\chi^2}{\#(\text{d.o.f.})} \equiv \frac{1}{n} \sum_{i=ud,us,ub,cd,cs,cb} \left(\frac{|V_{\text{CKM}4,i}| - |V_i|}{\Delta V_i} \right)^2, \quad (\text{A.1})$$

where n is the number of considered degrees of freedom (d.o.f.).

- **For the Z -pole measurements** there are several observables that can be considered. The one of interest to us is the observable $\sin 2\beta$:

$$\beta = \arg \left(\frac{V_{cd}V_{cb}^*}{V_{td}V_{tb}^*} \right), \quad (\text{A.2})$$

where V_{ij} are the matrix elements of the CKM matrix.

- **The front-back asymmetry $A_{FB}^{q\bar{q}}$** for a quark of flavor q is defined as

$$A_{FB}^{q\bar{q}} = \frac{\sigma_F^q - \sigma_B^q}{\sigma_F^q + \sigma_B^q}, \quad (\text{A.3})$$

where the cross-sections are integrated over the full forward (F) and backward (B) hemispheres, ‘forward’ (‘backward’) meaning that the quark, rather than the antiquark, is produced at positive (negative) $\cos \theta$.

- **The left-right forward-backward asymmetry** of a given event :

$$A_{LRFB} = \frac{(\sigma_F - \sigma_B)_L - (\sigma_F - \sigma_B)_R}{(\sigma_F + \sigma_B)_L + (\sigma_F + \sigma_B)_R} \times \frac{1}{\langle |\mathcal{P}| \rangle}, \quad (\text{A.4})$$

where the subscripts L, R define the helicities (left, right) of the initial-state particle and the beam polarization \mathcal{P} is taken as positive for right-handed beam helicity, negative for left and $\langle |\mathcal{P}| \rangle$ is the average of the absolute value of the polarization of the beam.

- **The asymmetry parameter \mathcal{A}_f** is defined for a fermion f and it is given by a relation between the couplings of left (L) and right (R) handed helicity states: g_{Lf} and g_{Rf} the couplings of the left and right-handed ones, respectively, or equally well by a relation between the axial (A) and vectorial (V) couplings $g_{Vf} = g_{Lf} + g_{Rf}$ and $g_{Af} = g_{Lf} - g_{Rf}$:

$$\mathcal{A}_f = \frac{g_{Lf}^2 - g_{Rf}^2}{g_{Lf}^2 + g_{Rf}^2} = \frac{2g_{Vf}g_{Af}}{g_{Vf}^2 + g_{Af}^2} . \quad (\text{A.5})$$

- **The average charge of all particles in a jet**, called ‘jet charge’, gives information about the charge of the original quark. The jet charge can be defined as

$$Q_h = \frac{\sum_i q_i p_{||i}^\kappa}{\sum_i p_{||i}^\kappa} , \quad (\text{A.6})$$

where the sum is over all charged particles in the hemisphere with charge q_i and longitudinal momentum with respect to the thrust axis $p_{||i}$ and κ is a parameter (usually fixed to have a value between 0.3 and 1). Jet events are divided into two hemispheres by the plane perpendicular to the thrust axis. The jet charge in the forward (backward) hemisphere is denoted by Q_F (Q_B). Therefore $Q_{FB} = Q_F - Q_B$ can be thought of as the forward-backward charge flow, which gives an effective observable, allowing for a derivation of the average charge asymmetry.

- **The b -quark partial width of the Z -pole**, normalized to the total hadronic width of the Z -peak, is

$$R_b = \frac{\Gamma_{b\bar{b}}}{\Gamma_{\text{had}}} , \quad (\text{A.7})$$

where $\Gamma_{b\bar{b}}$ is the width of the $Z \rightarrow b\bar{b}$ decay and

$$\Gamma_{\text{had}} = \sum_{q \neq t} \Gamma_{q\bar{q}} \quad (\text{A.8})$$

is the hadronic width of the Z -pole (the top quark is excluded in the sum (A.8) because it is kinematically inaccessible: $m_t > m_Z$).

- **The value for the effective leptonic mixing angle $\sin^2 \theta_{\text{eff}}^\ell$** , is derived from the experimental observables A_f , given in Eq. (A.5) and

$$A_{LR} = \frac{2(1 - 4\sin^2 \theta_{\text{eff}}^f)}{1 + (1 - 4\sin^2 \theta_{\text{eff}}^f)^2} \quad (\text{A.9})$$

provided that the ratio of the vectorial to axial coupling of the given type of fermion is

$$\frac{g_{Vf}}{g_{Af}} = 1 - \frac{2Q_f}{T_3^f} \sin^2 \theta_{\text{eff}}^f = 1 - 4|Q_f| \sin^2 \theta_{\text{eff}}^f . \quad (\text{A.10})$$

Appendix B

The Goldstone model

In this section we first review the Goldstone model, a field theory invariant under global $U(1)$ transformations. This model necessarily leads to massless bosons – not photons – which are not observed in nature, making them an undesirable and *unphysical* feature of the model. These bosons are absent when *spontaneous symmetry breaking* is applied to a theory that is invariant under a *local* symmetry transformation, *i.e.*, to a gauge theory. In a gauge theory these so-called *Nambu-Goldstone* or *Goldstone bosons* have an interpretation as the longitudinal modes of the vector fields, making the vector fields behave as if they were *massive*. We will follow the presentations given in Refs. [190, 102, 191].

Non-invariance of the ground state

Consider a system whose Lagrangian density \mathcal{L} possesses a particular symmetry, meaning that it is invariant under the corresponding group of symmetry transformations. When classifying the energy levels of the system, there are two distinct cases: A given energy level can be *non-degenerate* making the corresponding energy eigenstate *unique*. In this case the eigenstate is invariant under the symmetry group of \mathcal{L} . On the other hand the energy level might be *degenerate* and the corresponding energy eigenstates are not invariant and transform linearly amongst themselves under the symmetry transformations of \mathcal{L} . A particular eigenstate is the state of lowest energy, *the vacuum*. A non-degenerate vacuum is unique and possesses the symmetries of \mathcal{L} ; on the other hand, when it is degenerate there is no unique state to represent the vacuum. A vacuum may then be arbitrarily chosen and due to degeneracy it will not be invariant under the symmetries of \mathcal{L} , it is *asymmetric*. This is called *spontaneous symmetry breaking*.

Non-invariance in the Hamiltonian formalism

Whenever an interaction possesses some symmetry a given problem is often simplified considerably. Exact symmetries (such as electric charge conservation) are fairly rare in nature, and one often assumes the system to be such that it is just a small piece of the Hamiltonian \mathcal{H} or Lagrangian \mathcal{L} density that violates a particular symmetry whereas the rest of \mathcal{H} or \mathcal{L} is invariant. (This is the case in the SM: strong interactions conserve parity, isospin and strangeness, but at the same time electromagnetic interactions violate isospin and weak interactions violate isospin, parity and strangeness, so a hierarchy of forces arise.)

Let a system be described by such a Hamiltonian that can be written in parts as

$$\mathcal{H} = \mathcal{H}_0 + \lambda \mathcal{H}_1 , \tag{B.1}$$

where \mathcal{H}_0 is invariant under some group of transformations whereas \mathcal{H}_1 is not and λ is a parameter. When there is an element U of the symmetry group that leaves the Hamiltonian \mathcal{H}_0 invariant, then

$$U\mathcal{H}_0U^\dagger = \mathcal{H}_0 , \quad (\text{B.2})$$

and U connects states that form an irreducible representation of the group

$$U|A\rangle = |B\rangle . \quad (\text{B.3})$$

It follows that the energies of states related in the way of (B.3) are equal :

$$E_A = \langle A|\mathcal{H}_0|A\rangle = \langle B|\mathcal{H}_0|B\rangle = E_B . \quad (\text{B.4})$$

This is just a statement of the degeneracy of the states $|A\rangle$ and $|B\rangle$, and so *the symmetry of the Hamiltonian is manifest in the degeneracy of the energy eigenstates that correspond to the irreducible representations of the symmetry group.*

When the formalism of creation and annihilation operators is used, the states $|A\rangle$ and $|B\rangle$ can be related to the ground state $|0\rangle$ through some creation operators ϕ_A and ϕ_B

$$|A\rangle = \phi_A|0\rangle , \quad |B\rangle = \phi_B|0\rangle \quad (\text{B.5})$$

which satisfy

$$U\phi_AU^\dagger = \phi_B . \quad (\text{B.6})$$

Hence Eq. (B.3) is satisfied only if

$$U|0\rangle = |0\rangle . \quad (\text{B.7})$$

When Eq. (B.7) is not satisfied the equality in Eq. (B.3) is violated and the symmetry consequence of the degenerate energy levels no longer holds. This situation is often referred to as a *spontaneous symmetry breakdown*. The Hamiltonian (or Lagrangian) is still invariant under the symmetry transformation even though the symmetry is no longer manifest in the degenerate energy levels.

Goldstone's theorem

Let us consider the Lagrangian density of a complex scalar field $\phi(x)$:

$$\mathcal{L} = (\partial_\mu\phi^*)(\partial^\mu\phi) - \mu^2\phi\phi^* - \lambda(\phi\phi^*)^2 , \quad (\text{B.8})$$

called the *Goldstone Lagrangian* density. This density is invariant under the $U(1)$ group of *global* transformations

$$\phi(x) \longrightarrow \phi'(x) = e^{-i\alpha}\phi(x) , \quad (\text{B.9})$$

with α an arbitrary parameter that does not depend on the spacetime coordinates x . The kinetic term in (B.8) is positive and vanishes only if $\phi(x)$ is constant. The ground state of the system is obtained at the minimum of the ‘potential’

$$V(\phi) \equiv \mu^2\phi\phi^* + \lambda(\phi\phi^*)^2 . \quad (\text{B.10})$$

As $V(\phi)$ depends on ϕ and ϕ^* only through $\phi\phi^* = |\phi|^2$ we can ease the notation by defining

$$\rho \equiv \phi\phi^* , \quad (\text{B.11})$$

so that (B.10) becomes a functional of ρ

$$V(\phi) \rightarrow V(\rho) = \mu^2 \rho + \lambda \rho^2 . \quad (\text{B.12})$$

The potential has a minimum only if $\lambda > 0$, which we therefore take to be true. Interpreting μ^2 as a conventional mass term > 0 , the potential has a symmetric ground state at $\phi = 0$. This ground state is unique and symmetric under (B.9). On the other hand, if $\mu^2 < 0$ the minimum is at

$$\rho = -\frac{\mu^2}{2\lambda} , \quad (\text{B.13})$$

which implies that there exists a whole ring of radius $|\phi| = \sqrt{\rho}$ in the complex ϕ plane whose points give the minimum of the potential V . Defining

$$v \equiv \sqrt{\frac{-\mu^2}{\lambda}} , \quad (\text{B.14})$$

the ring of minima is at

$$|\phi| = \frac{v}{\sqrt{2}} . \quad (\text{B.15})$$

The point $\phi = 0$ is now unstable, whereas the number of stable points satisfying Eq. (B.15) is infinite. Each of the points in the ground state can be reached from another ground state point by a $U(1)$ transformation. For a point on the real axis

$$\phi(x) = \frac{1}{\sqrt{2}} [v + \xi(x) + i\chi(x)] , \quad (\text{B.16})$$

with $\xi, \chi \in \Re$ and $\xi = \chi = 0$ in the ground state. Substituting this into the Godstone Lagrangian (B.8) and ignoring constant terms gives

$$\mathcal{L} = \frac{1}{2}(\partial_\mu \xi)^2 + \frac{1}{2}(\partial_\mu \chi)^2 - \lambda v^2 \xi^2 - \lambda v \xi(\xi^2 + \chi^2) - \frac{1}{4}\lambda(\xi^2 + \chi^2)^2 . \quad (\text{B.17})$$

Interpreting the Lagrangian (B.17) as one describing a quantum field theory with two basic fields ξ and χ , we see that there is no mass term for the field χ , but that there is a mass term of the usual form $-\frac{1}{2}m_\xi^2 \xi^2$ for ξ with

$$m_\xi^2 = 2\lambda v^2 . \quad (\text{B.18})$$

What has happened is that starting with an \mathcal{L} , constructed from a complex scalar field $\phi(x)$, invariant under $U(1)$ and with $\mu^2 < 0$ we have ended with two fields: a massless field χ and a field ξ whose mass (B.18) has been generated ‘spontaneously’.

When the Lagrangian (B.8) is generalized from one to n real scalar fields ϕ_j :

$$\mathcal{L} = \sum_j \left\{ \frac{1}{2}(\partial_\mu \phi_j)(\partial^\mu \phi_j) - \frac{1}{2}\mu^2 \phi_j \phi_j - \lambda(\phi_j \phi_j)^2 \right\} \quad (\text{B.19})$$

its symmetry group is the n -dimensional orthogonal group $O(n)$ with $\frac{1}{2}n(n-1)$ generators. The symmetry group mixes the fields with each other. The ground state is again the ‘ring’ at $\sum_j \phi_j \phi_j = -\mu^2/4\lambda$ when $\mu^2 < 0$. Thinking of the fields ϕ_j as components of a vector Φ , then the ground state fixes the length of this vector but leaves its direction arbitrary. Therefore one is free to choose just one of the components of Φ to be nonzero, say the n th one. All other vacua can then be obtained from this chosen one by an $O(n)$ transformation. (Physically, the various equivalent ground states

differ according to the number of Goldstone bosons (of zero energy and momentum) that they contain.) The difference to the previously considered case is that the chosen a vacuum state

$$\Phi_{vac} = \begin{pmatrix} 0 \\ 0 \\ \vdots \\ 0 \\ v \end{pmatrix} \quad (\text{B.20})$$

is now invariant under a nontrivial subgroup of $O(n)$, namely under $O(n-1)$, that mixes the $n-1$ first components amongst themselves but does not touch the n th component. The group $O(n-1)$ has $\frac{1}{2}(n-1)(n-2)$ generators. Thus the difference in the number of generators between the *original* group $O(n)$ and the *residual* group $O(n-1)$ equals $n-1$. These correspond to the $n-1$ ‘broken generators’ of the original symmetry group, playing the role of the Goldstone bosons or the longitudinal polarizations of vector bosons.

Repeating the calculation of Eqs. (B.16)–(B.18) one sees that there is still just one massive field and that the $n-1$ other fields, called ‘Goldstones’, remain massless. The above considered cases are examples of the *Goldstone theorem* [192] (also [193, 60, 61]) viable for any symmetry group:

*For every broken generator in a spontaneous symmetry breaking
there exists a massless scalar boson.*

Appendix C

Mathematical description of neutrino oscillations

Neutrino flavor change is the process $\nu_\alpha \rightarrow \nu_\beta$, such that $\alpha \neq \beta$, *i. e.* a neutrino with flavor α becomes one with a different flavor, β . This quantum mechanical phenomenon happens both for neutrinos propagating in vacuum and in matter. In most experiments neutrinos are produced by charged current weak interactions. A neutrino beam is a superposition of various particle eigenstates, which evolve differently as the beam propagates and the probability of finding different eigenstates in the beam varies with time. This phenomenon, which is a consequence of neutrino mixing, is called *neutrino oscillation*.

Let us consider charged current interactions, resulting in charged antileptons $\bar{\ell}$ and neutrinos ν_ℓ . The neutrinos participating in weak interactions are in the *interaction basis*, which is different from the *mass eigenstates* [194]. A physically observable state in the interaction basis is generally a superposition of the mass states ν_α with masses m_α :

$$|\nu_\ell\rangle = \sum_{\alpha} U_{\ell\alpha} |\nu_\alpha\rangle , \quad (\text{C.1})$$

where $U \in U(N)$ is the amplitude of the process (see also Section 2.5.2). Let us for simplicity assume that all neutrinos in the beam have the same three-momentum \mathbf{p} . Since the masses of the components differ the energies of the various components cannot be equal, as follows from

$$E_\alpha^2 = \mathbf{p}^2 + m_\alpha^2 \quad , \quad \mathbf{p}_\alpha = \mathbf{p} \quad \forall \alpha . \quad (\text{C.2})$$

The evolution of states is given by standard quantum mechanics (see *e.g.* [195]), so that at a time t the beam has evolved from the initial state at $t = 0$ to

$$|\nu_\ell(t)\rangle = \sum_{\alpha} e^{-i\hat{H}_\alpha t} U_{\ell\alpha} |\nu_\alpha\rangle = \sum_{\alpha} e^{-iE_\alpha t} U_{\ell\alpha} |\nu_\alpha\rangle , \quad (\text{C.3})$$

with $|\nu_\alpha\rangle \equiv |\nu_\alpha(t = 0)\rangle$. This result (C.3) holds under the assumption that neutrinos are stable particles.

As already noted in (C.2), the different E_α 's are not equal. The superposition (C.3) is different from (C.1). The amplitude of a state $\nu_{\ell'}$ in the state $|\nu_\ell(t)\rangle$ is

$$\langle \nu_{\ell'} | \nu_\ell(t) \rangle = \sum_{\alpha, \beta} \langle \nu_\beta | U_{\beta\ell'}^\dagger e^{-iE_\alpha t} U_{\ell\alpha} | \nu_\alpha \rangle \quad (\text{C.4})$$

and the probability of finding the state $\nu_{\ell'}$ is

$$\begin{aligned} P_{\nu_{\ell}\nu_{\ell'}}(t) &= |\langle \nu_{\ell'} | \nu_{\ell}(t) \rangle|^2 \\ &= \sum_{\alpha, \beta} |U_{\ell\alpha} U_{\ell'\alpha}^* U_{\ell\beta}^* U_{\ell'\beta}| \cos [(E_{\alpha} - E_{\beta})t - \varphi_{\ell\ell'\alpha\beta}] , \end{aligned} \quad (\text{C.5})$$

where we have used the fact that the mass eigenstates are orthonormal, $\langle \nu_{\ell'} | \nu_{\ell} \rangle = \delta_{\ell'\ell}$ and $\varphi_{\ell\ell'\alpha\beta}$ is defined as

$$\varphi_{\ell\ell'\alpha\beta} = \arg(U_{\ell\alpha} U_{\ell'\alpha}^* U_{\ell\beta}^* U_{\ell'\beta}) . \quad (\text{C.6})$$

Neutrinos are usually ultrarelativistic, so

$$E_{\alpha} \simeq |\mathbf{p}| + \frac{m_{\alpha}^2}{2|\mathbf{p}|} . \quad (\text{C.7})$$

In the ultrarelativistic limit t may be replaced by the distance traveled at that time, say x (since $v \simeq c = 1$), giving the probability (C.5)

$$P_{\nu_{\ell}\nu_{\ell'}}(t) = \sum_{\alpha, \beta} |U_{\ell\alpha} U_{\ell'\alpha}^* U_{\ell\beta}^* U_{\ell'\beta}| \cos \left(\frac{2\pi x}{L_{\alpha\beta}} - \varphi_{\ell\ell'\alpha\beta} \right) , \quad (\text{C.8})$$

with

$$L_{\alpha\beta} \equiv \frac{4\pi|\mathbf{p}|}{\Delta m_{\alpha\beta}^2} \quad (\text{C.9})$$

and

$$\Delta m_{\alpha\beta}^2 \equiv m_{\alpha}^2 - m_{\beta}^2 . \quad (\text{C.10})$$

The *oscillation lengths* $|L_{\alpha\beta}|$ give a distance scale over which the effects of oscillation are discernible. For all distances $x \neq n \cdot L_{\alpha\beta}$, $n \in \mathbb{Z}$, the effects of oscillation are nontrivial.

Experimental values

In order to cite values given in the literature [55] for the above parameters we need to specify the otherwise completely arbitrary numbering of the neutrinos, ν_i . We choose to identify $|\Delta m_{21}^2|$ with the smaller of the neutrino mass differences squared and for convenience that $m_1 < m_2$ so that $\Delta m_{21}^2 > 0$. Which other mass difference is chosen as the second independent parameter does not really matter, since in fact $|\Delta m_{21}^2| \ll |\Delta m_{31(32)}^2|$, $|\Delta m_{21}^2|/|\Delta m_{31(32)}^2| \approx 0.03$ and $\Delta m_{31}^2 \simeq \Delta m_{32}^2$ (for motivation, see Ref. [55]). The current values of the parameters are shown in Table C.1, where the upper (lower) row corresponds to normal (inverted) neutrino mass hierarchy, where ‘normal’ and ‘inverted’ mass hierarchies correspond to $|\Delta m_{31}^2| > |\Delta m_{32}^2|$ and $|\Delta m_{32}^2| > |\Delta m_{31}^2|$, respectively.

Parameter	Best fit $\pm 1\sigma$
Δm_{21}^2 $[10^{-5}\text{eV}^2]$	$7.59_{-0.18}^{+0.20}$
Δm_{31}^2 $[10^{-3}\text{eV}^2]$	2.4 ± 0.09 $-(2.34_{-0.09}^{+0.10})$

Table C.1: Values of neutrino mixing parameters $\Delta m_{\alpha\beta}^2$. For Δm_{31}^2 the upper (lower) row corresponds to normal (inverted) neutrino mass hierarchy. Values from Ref. [129]

Appendix D

Oblique electroweak parameters

While the $SU(2) \times U(1)_Y$ gauge theory of electroweak interactions is widely accepted the mechanism responsible for the breaking $SU(2)_L \times U(1)_Y \rightarrow U(1)_Q$, called the Higgs sector, is still a mystery. There is a multitude of alternative models (several Higgs doublets, technicolor *etc.*), but none of the particles predicted by these models have yet been discovered directly ¹, so it is important to make use of *indirect information* from current measurements. The most important constraints come from the measurement of weak interaction parameters, which are typically measured at a very high precision: typically to a part per mil [196].

The most general Higgs models allow for large deviations from the SM predictions. In the 70's it was noted that in the SM there is a ‘natural’ tree-level quantity called the ρ -parameter (2.62) that can be used to restrict models that break the electroweak symmetry. The theoretically predicted value for the ρ -parameter is unity (2.63) in the SM, a value that is in agreement with experiment (the deviation is smaller than 1%), so it is reasonable to assume that the corrections to this relation arise from radiative corrections only [137]. The radiative corrections are sensitive to new particles going through the loops.

Later it was noted that the effects of vacuum-polarization diagrams, as in Fig. D.1, so-called *oblique corrections*, could also be used as a tool to scrutinize new-physics models in a general way [197] and this idea was incorporated into a complete theory of weak radiative corrections [198, 199, 200].

In many studies about the fourth generation these oblique corrections are used to constrain the parameter space of the SM4. A possible fourth generation affects many amplitudes through loop diagrams, and for the Z and W bosons the effects of new heavy quarks and leptons enter *only* through vacuum-polarization diagrams. In this section we will consider the physics of these diagrams in some detail, following the presentation given in Ref. [137]

Vacuum polarizations affect the gauge interactions indirectly by modifying the gauge boson propagators. This is why they are called ‘oblique’ corrections as opposed to ‘direct’ vertex and box corrections, which directly affect the form of the interaction. The vacuum polarization amplitudes are defined as $\Pi_{XY}(q^2)$, with $(XY) = (11), (22), (33), (3Q)$ and (QQ) , by

$$ig^{\mu\nu}\Pi_{XY}(q^2) + (q^\mu q^\nu \text{ terms}) \equiv \int d^4x e^{-iqx} \langle J_X^\mu(x) J_Y^\nu(0) \rangle . \quad (\text{D.1})$$

¹At the time of finishing this report, in July 2012, a resonance has been seen at ~ 125 GeV by the ATLAS [100] and CMS [101] collaborations at the LHC and also by D0 and CDF at the Tevatron [180]. The observed decays hint at this being the Higgs boson.

$$\begin{aligned}
\gamma \text{ --- } \text{---} \bullet \text{---} \gamma &= ie^2 \Pi_{QQ} g^{\mu\nu} + \dots \\
Z \text{ --- } \text{---} \bullet \text{---} \gamma &= i \frac{e^2}{cs} (\Pi_{3Q} - s^2 \Pi_{QQ}) g^{\mu\nu} + \dots \\
Z \text{ --- } \text{---} \bullet \text{---} Z &= i \frac{e^2}{c^2 s^2} (\Pi_{33} - 2s^2 \Pi_{3Q} + s^4 \Pi_{QQ}) g^{\mu\nu} + \dots \\
W \text{ --- } \text{---} \bullet \text{---} W &= i \frac{e^2}{s^2} \Pi_{11} g^{\mu\nu} + \dots
\end{aligned}$$

Figure D.1: Definition of basic electroweak vacuum polarization amplitudes, as given in Ref. [137]. The notation used is explained in Eqs. (D.1)–(D.5).

Here J_Q^μ , J_3^μ and $J_\pm^\mu = J_1^\mu \pm iJ_2^\mu$ denote the electromagnetic (index Q) and weak isospin currents (indices 1,2,3). In the formalism where the currents J interact with the gauge field, the coupling of the J 's to the electroweak gauge bosons has the form

$$\frac{e}{\sqrt{2}s_W} (W_\mu^+ J_+^\mu + W_\mu^- J_-^\mu) + \frac{e}{s_W c_W} Z_\mu (J_3^\mu - s_W^2 J_Q^\mu) + e A_\mu J_Q^\mu, \quad (\text{D.2})$$

where

$$s_W \equiv \sin \theta_W \quad \text{and} \quad c_W \equiv \cos \theta_W, \quad (\text{D.3})$$

and θ_W the weak mixing angle. It is useful to define another quantity, $\Pi'_{XY}(q^2)$ by

$$\Pi_{XY}(q^2) \equiv \Pi_{XY}(0) + q^2 \Pi'_{XY}(q^2), \quad (\text{D.4})$$

so that the first term $\Pi_{XY}(0)$, which is regular at $q = 0$, does not depend on q and is therefore also regular in the limit when the four-momentum is very large – it is ultraviolet (UV) finite.

Let us also define a shorthand notation for the combinations of Π 's that give the one-particle irreducible (1PI) self energies of the photon (A), the W , the Z and the 1PI photon- Z mixing, shown in the second line Fig. D.1 (recall from Section 2.4 that A and Z have the same basis so they mix)

$$\begin{aligned}
\Pi_{AA} &= e^2 \Pi_{QQ}, \quad \Pi_{ZA} = \frac{e^2}{sc} (\Pi_{3Q} - s^2 \Pi_{QQ}), \\
\Pi_{ZZ} &= \frac{e^2}{s^2 c^2} (\Pi_{33} - 2s^2 \Pi_{3Q} + s^4 \Pi_{QQ}), \\
\Pi_{WW} &= \frac{e^2}{s^2} \Pi_{11}.
\end{aligned} \quad (\text{D.5})$$

If the physics included in the vacuum polarization diagrams is associated with new, heavy particles of mass greater than m_Z , the vacuum polarization amplitudes will have rapidly converging Taylor series expansions in q^2 , where q is the four-momentum flowing through a given diagram.

Now we are ready to define the three ultraviolet-finite *oblique parameters* S , T and U by

$$\begin{aligned}
\alpha S &\equiv 4e^2 [\Pi'_{33}(0) - \Pi'_{3Q}(0)], \\
\alpha T &\equiv \frac{e^2}{s^2 c^2 m_Z^2} [\Pi_{11}(0) - \Pi_{33}(0)], \\
\alpha U &\equiv 4e^2 [\Pi'_{11}(0) - \Pi'_{33}(0)].
\end{aligned} \quad (\text{D.6})$$

Several different notations for these parameters appear in the literature. The above parameters are written in terms of e , θ_W and m_Z since these are some of the most accurately measured parameters of electroweak interactions and serve as good reference points. Of the three listed in (D.6), the S and T parameters divide the contribution of electroweak radiative corrections into pieces which have a distinct physical significance:

S is isospin-symmetric and gives a part of the momentum dependence of Π_{33} , the part that is ultraviolet finite,

T obtains contributions only from effects that violate a global $SU(2)$ symmetry called a *custodial symmetry*.

In fact S can be pictured as measuring the total size of the new sector while T measures the total isospin-breaking induced by this new sector. U is often predicted to be very small.

Provided that the mass scale of new physics is high and that the main contribution from it mostly comes from virtual loops to the electroweak observables, then the three oblique parameters provide a *representation of the discrepancies expected from nonstandard physics*. All neutral-current and low-energy observables depend only on S and T , whereas the only accurately measured weak interaction observable that depends on U is m_W .

The use of S, T, U is convenient as it allows for the predictions from various models to be compared with electroweak precision data. For a given model, the prediction of any electroweak observable O is [172]

$$O = O_{\text{SM,ref}}(M_{H,\text{ref}}, m_{t,\text{ref}}) + c_S S + c_T T + c_U U , \quad (\text{D.7})$$

where $O_{\text{SM,ref}}$ is the SM prediction of the observable in the SM and c_S , c_T , c_U are constants. The SM reference depends on M_H and m_t , which take fixed values, and includes all known higher-order electroweak corrections. The parameters c_S , c_T , c_U can be found in the literature [55] for the full set of electroweak observables. Because these have been measured with such high precision, the oblique parameters of various BSM models are restricted by the relation (D.7).

As can be seen from (D.7), S, T and U all vanish in the SM. As our interest in this report is in the physics of SM4 we note that each extra fermion doublet that is put into the theory contributes *additively* to both S and T , because the contribution from a fermion doublet (u, d) is [137]

$$S(x_u, x_d) = \frac{N_c}{6\pi} \left[1 - Y \log \left(\frac{x_u}{x_d} \right) \right] , \quad (\text{D.8})$$

$$T(x_u, x_d) = \frac{N_c}{16\pi s_W^2 (1 - s_W^2)} \left[x_u + x_d - \frac{2x_u x_d}{x_u - x_d} \log \left(\frac{x_u}{x_d} \right) \right] , \quad (\text{D.9})$$

$$U(x_u, x_d) = \frac{N_c}{6\pi} \left[-\frac{5x_u^2 - 22x_u x_d + 5x_d^2}{3(x_u - x_d)^2} + \frac{x_u^3 - 3x_u^2 x_d - 3x_u x_d^2 + x_d^3}{(x_u - x_d)^3} \log \left(\frac{x_u}{x_d} \right) \right] , \quad (\text{D.10})$$

where $x_f \equiv m_f^2/m_Z^2$, N_c is the number of colors ($N_c=3$ for quarks and $N_c=1$ for leptons) and Y is the hypercharge of the doublet. The total contribution to the S, T, U parameters from a fourth generation is obtained when both quark and lepton doublets are taken into account in the relations (D.8)–(D.10) and the mixing with the third family (which is assumed dominant – mixings to the

two first generations is assumed negligible) is included, too [86]:

$$\Delta S_4 = S(x_{t'}, x_{b'}) + S(x_{\ell'}, x_{\nu'}) , \quad (\text{D.11})$$

$$\Delta T_4 = -s_{34}^2 T(x_t, x_b) + s_{34}^2 T(x_{t'}, x_b) + s_{34}^2 T(x_t, x_{b'}) + c_{34}^2 T(x_{t'}, x_{b'}) + T(x_{\ell'}, x_{\nu'}) , \quad (\text{D.12})$$

$$\Delta U_4 = -s_{34}^2 U(x_t, x_b) + s_{34}^2 U(x_{t'}, x_b) + s_{34}^2 U(x_t, x_{b'}) + c_{34}^2 U(x_{t'}, x_{b'}) + U(x_{\ell'}, x_{\nu'}) , \quad (\text{D.13})$$

where s_{34} and c_{34} are the sine and the cosine, respectively, of the mixing angle θ_{34} and mixing in the lepton sector has been neglected.

Positive S and T , as would be expected by a fourth family according to the above, are not excluded experimentally since the values currently given in the literature are [55]

$$\begin{aligned} S &= 0.01 \pm 0.10 \text{ } (-0.8) \\ T &= 0.03 \pm 0.11 \text{ } (+0.09) \\ U &= 0.09 \pm 0.10 \text{ } (+0.01) \end{aligned} \quad (\text{D.14})$$

The central values assume $M_H = 117$ GeV and in the parenthesis give the difference to assuming $M_H = 300$ GeV. The SM parameters can be determined with no M_H dependence, whereas U has some, if little, dependence on the Higgs boson mass. However, not all of the parameters S, T, M_H can be obtained simultaneously, because the Higgs boson loops have a resemblance to oblique effects.

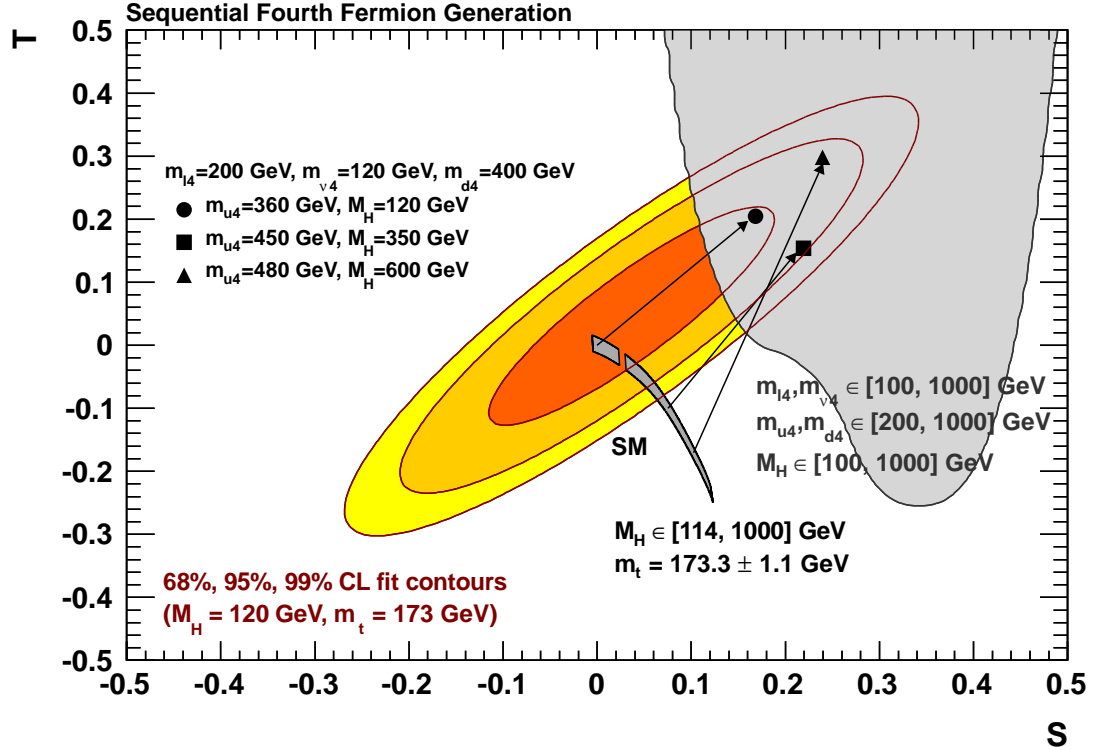


Figure D.2: Oblique parameters in a model with a fourth fermion generation. Shown are the S , T fit results (leaving U free) compared with the prediction from the SM (dark grey) and the sequential fourth generation model with vanishing flavour mixing (light grey). The symbols illustrate the predictions for three example settings of the parameters m_{u4} , m_{d4} , $m_{\nu'}$, $m_{\ell'}$ and M_H . (The notation used in the definition of the y -axis is $\nu_4 = \nu'$, $l_4 = \ell'$.) The light grey area is obtained by varying the free mass parameters in the ranges indicated in the figure. Figure and caption from [172].

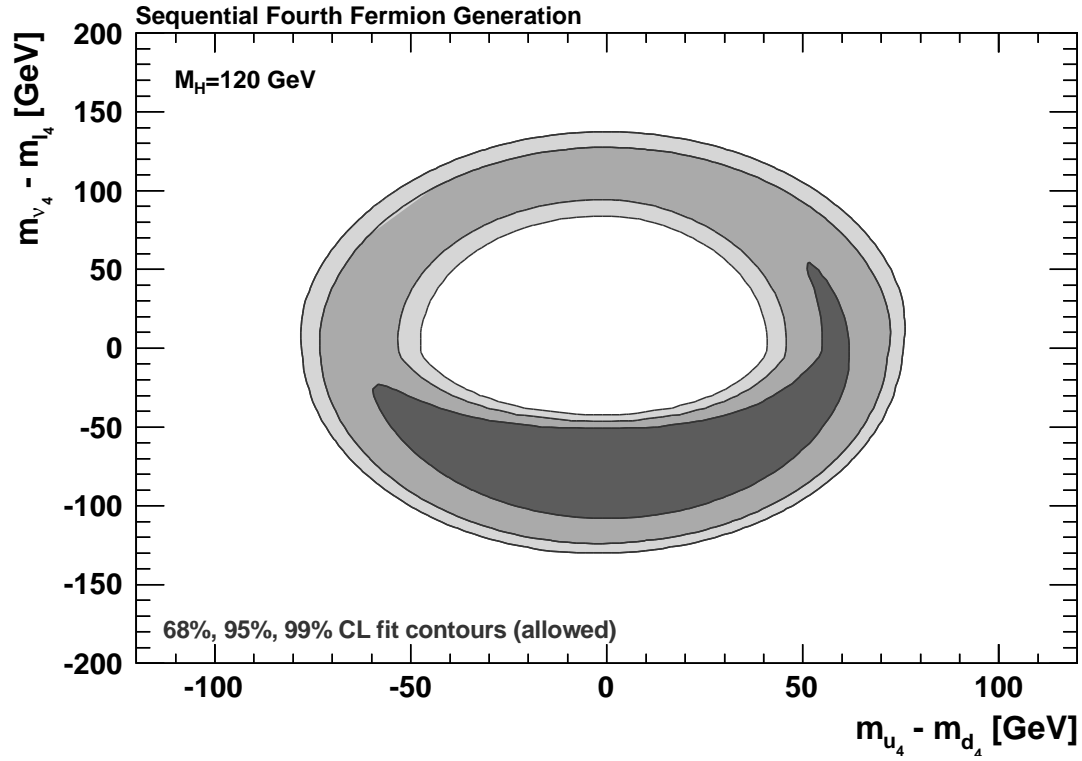


Figure D.3: Constraints in a model with a fourth fermion generation from fits of the oblique parameters to the electroweak precision data. Shown are the 68%, 95% and 99% CL allowed fit contours in the $(m_{\ell'} - m_{\nu'}, m_{\ell'} - m_{\nu'})$ plane as derived from the fit for $M_H = 120$. Figure from [172].

Appendix E

Feynman diagrams for production of fourth family particles

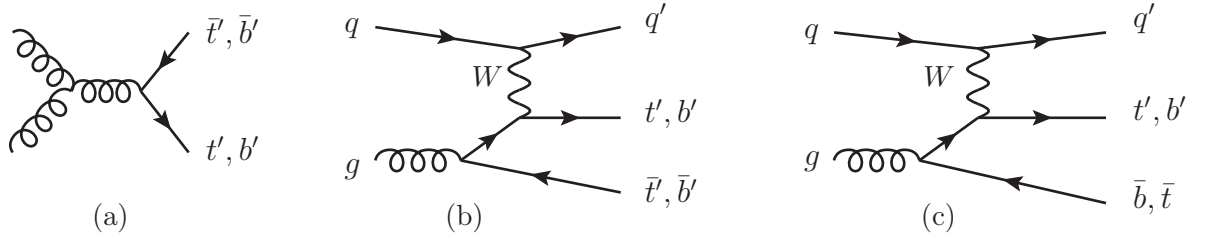


Figure E.1: Production of fourth generation quarks. (a) Strong pair production of heavy quarks at leading order, (b) $2 \rightarrow 3$ Born diagrams contributing to $t' \bar{b}'$ and $\bar{t}' b'$ and (c) $t' \bar{b}$ and $\bar{t} b'$ t -channel electroweak production. The amplitude of (c) is suppressed if the 3–4 CKM mixing is small. Diagrams as in [154].

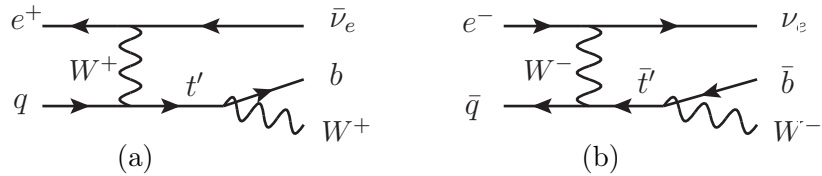


Figure E.2: The diagrams for single production of fourth family t' (a) and \bar{t}' (b) quarks in ep collisions, as given in Ref. [152].

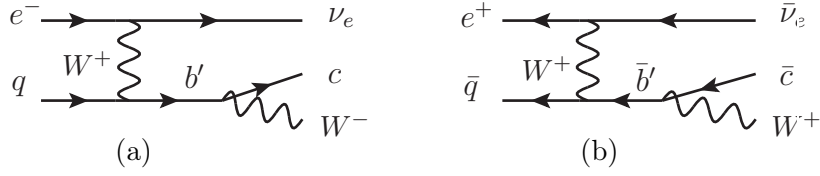


Figure E.3: The diagrams for single production of fourth family b' (a) and \bar{b}' (b) quarks in ep collisions, as given in Ref. [156].

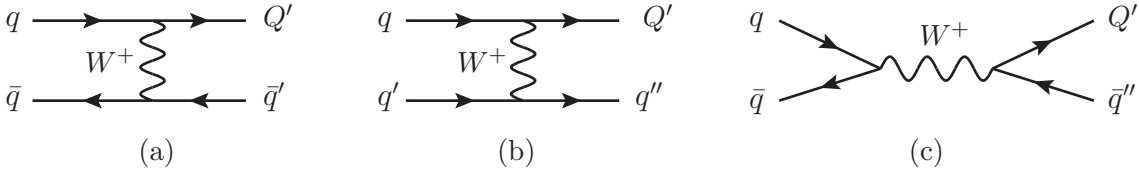


Figure E.4: The diagrams for single production of fourth family quarks Q in pp collisions. Diagrams as in Ref. [153].

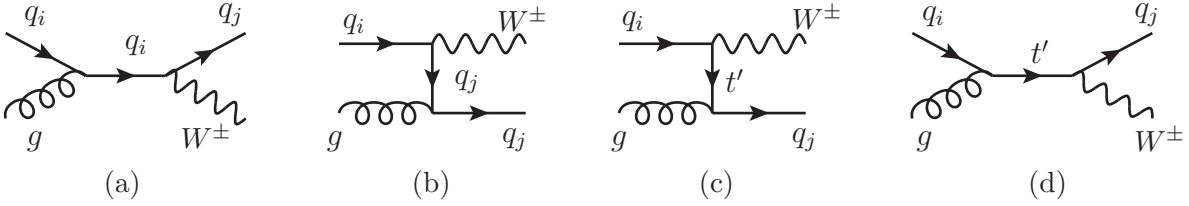


Figure E.5: The diagrams for $qq_i \rightarrow W^+ q_j$ subprocesses including $t' qg$ anomalous vertices. q_i is a quark from the proton and q_j is a quark of any flavor depending on the charged current interaction. For $W^- \bar{q}_j$ final states one may change the direction of the current lines and replace the outgoing quarks with incoming antiquarks. Diagrams and caption from Ref. [158].

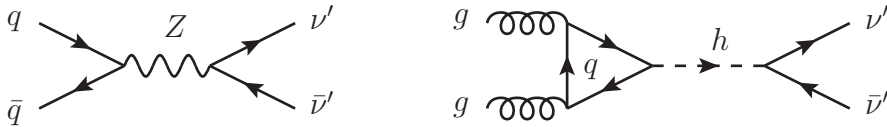


Figure E.6: The ν' pair production of via neutral current (left) and Higgs interaction (right). Diagrams as in Ref. [148].

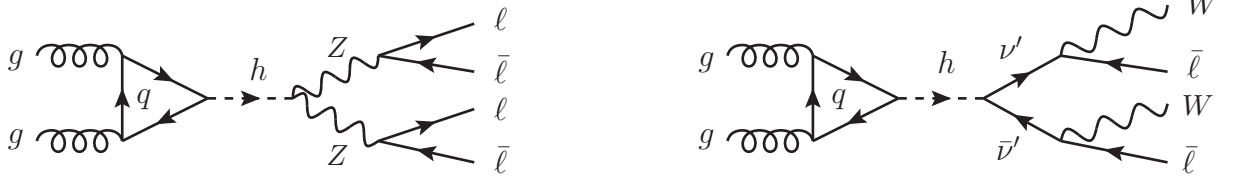


Figure E.7: The ‘golden’ (left) and ‘silver’ (right) modes for the discovery of a heavy Higgs boson. For the golden mode $\ell = e, \mu$ while for the silver mode $\ell = \mu$ only. Diagrams as in Ref. [167].

Appendix F

Form factors for A^0, h^0 branching ratios

In this Appendix we give the form factors of the Higgs branching ratios presented in Chapter 7. The formulas are from Ref. [128].

The pseudoscalar A^0

The functions appearing in Eq. 7.1 are the following:

$$\mathcal{I}_S(\tau) = \frac{1}{\tau^2} [\tau + (\tau-1)f(\tau)], \quad \mathcal{I}_A(\tau) = \frac{1}{\tau} f(\tau). \quad (\text{F.1})$$

These are the form factors for the CP-even (subscript S) and CP-odd (subscript A) Higgses, respectively. Eqs. (F.1) depend on the function $f(\tau)$, which is (written in different manner than in (3.22)) reads :

$$f(\tau) = \begin{cases} \arcsin^2 \sqrt{\tau}, & \tau \leq 1, \\ -\frac{1}{4} \left[\ln \frac{1+\sqrt{1-\tau^{-1}}}{1-\sqrt{1-\tau^{-1}}} - i\pi \right]^2, & \tau > 1, \end{cases} \quad (\text{F.2})$$

where $\tau \equiv m_A^2/(4m_f^2)$.

The parameter c_f and function $\tilde{\mathcal{I}}_A(\tau_f, \lambda_f)$ appearing in the width of $A^0 \rightarrow \gamma Z$ (7.5) are :

$$c_f \equiv 2T_{3f} - 4e_f s_W^2, \quad (\text{F.3})$$

$$\tilde{\mathcal{I}}_A(\tau_f, \lambda_f) = \frac{f(\tau_f) - f(\lambda_f)}{2(\tau_f - \lambda_f)}, \quad (\text{F.4})$$

where s_W, c_W are given in (D.3) and $\lambda_f \equiv m_Z^2/(4m_f^2)$.

The light scalar h^0

The form factors of Eqs. (7.9) – (7.11) are :

$$\mathcal{I}_W(\tau) = -\frac{1}{\tau^2} \left[2\tau^2 + 3\tau + 3(2\tau - 1)f(\tau) \right] , \quad (\text{F.5})$$

$$\mathcal{A}_f^H(\tau, \lambda) = I_1(\tau, \lambda) - I_2(\tau, \lambda) , \quad (\text{F.6})$$

$$\mathcal{A}_W^H(\tau, \lambda) = c_W \left\{ 4 \left(3 - \frac{s_W^2}{c_W^2} \right) I_2(\tau, \lambda) + \left[(1 + 2\tau) \frac{s_W^2}{c_W^2} - (5 + 2\tau) \right] I_1(\tau, \lambda) \right\} , \quad (\text{F.7})$$

$$I_1(\tau, \lambda) = \frac{1}{2(\lambda - \tau)} + \frac{f(\tau) - f(\lambda)}{2(\lambda - \tau)^2} + \frac{\lambda [g(\tau) - g(\lambda)]}{(\tau - \lambda)^2} , \quad (\text{F.8})$$

$$I_2(\tau, \lambda) = \frac{f(\tau) - f(\lambda)}{2(\tau - \lambda)} , \quad (\text{F.9})$$

where s_W, c_W are given in (D.3), $f(\tau)$ in (F.2) and the function $g(\tau)$ is :

$$g(\tau) = \begin{cases} \sqrt{\tau^{-1} - 1} \arcsin \sqrt{\tau} , & \tau \leq 1 , \\ \frac{\sqrt{1 - \tau^{-1}}}{2} \left[\ln \frac{1 + \sqrt{1 - \tau^{-1}}}{1 - \sqrt{1 - \tau^{-1}}} - i\pi \right] , & \tau > 1 . \end{cases} \quad (\text{F.10})$$

Bibliography

- [1] Hideki Yukawa. On the interaction of elementary particles. *Proc. Phys. Math. Soc. Jap.*, 17:48–57, 1935.
- [2] W. Pauli. Letter to Lise Meitner on December 4. For a copy of the letter, see the Pauli letters collection: <http://cdsweb.cern.ch/record/83282/files/> , 1930.
- [3] Seth H. Neddermeyer and Carl D. Anderson. Note on the nature of cosmic-ray particles. *Phys. Rev.*, 51(10):884–886, May 1937.
- [4] J. C. Street and E. C. Stevenson. New evidence for the existence of a particle of mass intermediate between the proton and electron. *Phys. Rev.*, 52(9):1003–1004, Nov 1937.
- [5] Rabi, I. I. 1937. Cited in e.g. Cahn, R. N. and Goldhaber, G. *The Experimental Foundations of Particle Physics*. Cambridge University Press, 1989.
- [6] C. M. G. Lattes, H. Muirhead, G. P. S. Occhialini, and C. F. Powell. Processes involving charged mesons. *Nature*, 159:694–697, 1947.
- [7] C. M. G. Lattes, G. P. S. Occhialini, and C. F. Powell. Observations on the tracks of slow mesons in photographic emulsions. 1. *Nature*, 160:453–456, 1947.
- [8] C. M. G. Lattes, G. P. S. Occhialini, and C. F. Powell. Observations on the tracks of slow mesons in photographic emulsions. 2. *Nature*, 160:486–492, 1947.
- [9] G. D. Rochester and C. C. Butler. Evidence for the existence of new unstable elementary particles. *Nature*, 160:855–857, December 1947.
- [10] J. Steinberger, W. K. H. Panofsky, and J. Steller. Evidence for the production of neutral mesons by photons. *Phys. Rev.*, 78:802–805, 1950.
- [11] Jagdish Mehra and Helmut Rechenberg. *The historical development of quantum theory*. Springer Verlag New York, Inc., 2001.
- [12] L. Leprince-Ringuet and M. L’héritier. Existence probable d’une particule de masse 990 m0 dans le rayonnement cosmique. *Comptes Rendus Acad. Sciences de Paris*, page 618, séance du 13 Dec 1944.
- [13] R. Brown, U. Camerini, P.H. Fowler, H. Muirhead, and D. M. Ritson. Observations with electron-sensitive plates exposed to cosmic radiation. *Nature*, 163:82–87, January 1949.
- [14] T. Nakano and K. Nishijima. Charge Independence for V -particles. *Prog. Theor. Phys.*, 10:581–582, 1953.
- [15] M. Gell-Mann. Isotopic Spin and New Unstable Particles. *Phys. Rev.*, 92:833–834, 1953.
- [16] Murray Gell-Mann. A Schematic Model of Baryons and Mesons. *Phys. Lett.*, 8:214–215, 1964.
- [17] George Zweig. CERN report 8182 / Th.401. Unpublished, 1964.
- [18] O. W. Greenberg. Spin and Unitary Spin Independence in a Paraquark Model of Baryons and Mesons. *Phys. Rev. Lett.*, 13:598–602, 1964.
- [19] M. Y. Han and Yoichiro Nambu. Three-triplet model with double $SU(3)$ symmetry. *Phys. Rev.*, 139:B1006–B1010, 1965.

- [20] G. Danby et al. Observation of High-Energy Neutrino Reactions and the Existence of Two Kinds of Neutrinos. *Phys. Rev. Lett.*, 9:36–44, 1962.
- [21] J. D. Bjorken and S. L. Glashow. Elementary Particles and SU(4). *Phys. Lett.*, 11:255–257, 1964.
- [22] S. L. Glashow, J. Iliopoulos, and L. Maiani. Weak interactions with lepton-hadron symmetry. *Phys. Rev. D*, 2(7):1285–1292, Oct 1970.
- [23] Nicola Cabibbo. Unitary symmetry and leptonic decays. *Phys. Rev. Lett.*, 10(12):531–533, Jun 1963.
- [24] J. J. Aubert, U. Becker, P. J. Biggs, J. Burger, M. Chen, G. Everhart, P. Goldhagen, J. Leong, T. McCarriston, T. G. Rhoades, M. Rohde, Samuel C. C. Ting, Sau Lan Wu, and Y. Y. Lee. Experimental observation of a heavy particle j . *Phys. Rev. Lett.*, 33(23):1404–1406, Dec 1974.
- [25] J. E. Augustin et al. Discovery of a narrow resonance in $e + e^-$ annihilation. *Phys. Rev. Lett.*, 33(23):1406–1408, Dec 1974.
- [26] Samuel C. C. Ting. The discovery of the j particle: A personal recollection. *Rev. Mod. Phys.*, 49(2):235–249, Apr 1977.
- [27] Burton Richter. From the psi to charm: The experiments of 1975 and 1976. *Rev. Mod. Phys.*, 49(2):251–266, Apr 1977.
- [28] A. Salam. in Elementary Particle Theory, edited by N. Svartholm, Almqvist and Wiksell. *Nobel Symposium*, page 367, 1968.
- [29] Gerard 't Hooft. Renormalization of massless yang-mills fields. *Nucl. Phys.*, B33:173–199, 1971.
- [30] Gerard 't Hooft. Renormalizable lagrangians for massive yang-mills fields. *Nucl. Phys.*, B35:167–188, 1971.
- [31] Steven Weinberg. A Model of Leptons. *Phys. Rev. Lett.*, 19:1264–1266, 1967.
- [32] H. Fritzsch, Murray Gell-Mann, and H. Leutwyler. Advantages of the Color Octet Gluon Picture. *Phys. Lett.*, B47:365–368, 1973.
- [33] H. David Politzer. Reliable perturbative results for strong interactions. *Phys. Rev. Lett.*, 30:1346–1349, 1973.
- [34] H. David Politzer. Asymptotic Freedom: An Approach to Strong Interactions. *Phys. Rept.*, 14:129–180, 1974.
- [35] David J. Gross and Frank Wilczek. Ultraviolet behavior of non-abelian gauge theories. *Phys. Rev. Lett.*, 30(26):1343–1346, Jun 1973.
- [36] D. J. Gross and Frank Wilczek. Asymptotically Free Gauge Theories. 1. *Phys. Rev.*, D8:3633–3652, 1973.
- [37] D. J. Gross and Frank Wilczek. Asymptotically free gauge theories. 2. *Phys. Rev.*, D9:980–993, 1974.
- [38] M. L. Perl et al. Evidence for anomalous lepton production in $e^+ - e^-$ annihilation. *Phys. Rev. Lett.*, 35(22):1489–1492, Dec 1975.
- [39] S. W. Herb et al. Observation of a dimuon resonance at 9.5 gev in 400-gev proton-nucleus collisions. *Phys. Rev. Lett.*, 39(5):252–255, Aug 1977.
- [40] Christoph Berger et al. Observation of a Narrow Resonance Formed in $e^+ e^-$ Annihilation at 9.46-GeV. *Phys. Lett.*, B76:243–245, 1978.
- [41] S. Abachi et al. Observation of the top quark. *Phys. Rev. Lett.*, 74(14):2632–2637, Apr 1995.
- [42] F. Abe et al. Observation of top quark production in pp collisions with the collider detector at fermilab. *Phys. Rev. Lett.*, 74(14):2626–2631, Apr 1995.
- [43] K. Kodama et al. Observation of tau-neutrino interactions. *Phys. Lett.*, B504:218–224, 2001, hep-ex/0012035.

- [44] Amitava Datta and Sreerup Raychaudhuri. Quark masses and mixing angles in a four-generation model with a naturally heavy neutrino. *Phys. Rev. D*, 49(9):4762–4772, May 1994.
- [45] Michael S. Chanowitz. Bounding CKM Mixing with a Fourth Family. *Phys. Rev.*, D79:113008, 2009, 0904.3570.
- [46] S. L. Glashow. Partial Symmetries of Weak Interactions. *Nucl. Phys.*, 22:579–588, 1961.
- [47] Michael S. Chanowitz. Electroweak data and the higgs boson mass: A case for new physics. *Phys. Rev. D*, 66(7):073002, Oct 2002.
- [48] P.Q. Hung and Chi Xiong. Dynamical Electroweak Symmetry Breaking with a Heavy Fourth Generation. *Nucl.Phys.*, B848:288–302, 2011, 1012.4479. * Temporary entry *.
- [49] G. S. Abrams et al. Measurements of z-boson resonance parameters in $e+e-$ annihilation. *Phys. Rev. Lett.*, 63(20):2173–2176, Nov 1989.
- [50] G. S. Abrams et al. Initial measurements of z-boson resonance parameters in $e+e-$ annihilation. *Phys. Rev. Lett.*, 63(7):724–727, Aug 1989.
- [51] P. A. Aarnio et al. Measurement of the Mass and Width of the Z0 Particle from Multi - Hadronic Final States Produced in $e+ e-$ Annihilations. *Phys. Lett.*, B231:539, 1989.
- [52] B. Adeva et al. A Determination of the Properties of the Neutral Intermediate Vector Boson Z0. *Phys. Lett.*, B231:509, 1989.
- [53] M. Z. Akrawy et al. Measurement of the Z0 Mass and Width with the OPAL Detector at LEP. *Phys. Lett.*, B231:530, 1989.
- [54] D. Decamp et al. Determination of the Number of Light Neutrino Species. *Phys. Lett.*, B231:519, 1989.
- [55] K. Nakamura et al. (Particle Data Group). *JPG*, 37(075021), 2010.
- [56] Saleh Sultansoy. The Naturalness of the Fourth SM Family. *Balk. Phys. Lett.*, 17:353–358, 2009, 0905.2874.
- [57] Wei-Shu Hou. CP Violation and Baryogenesis from New Heavy Quarks. *Chin. J. Phys.*, 47:134, 2009, 0803.1234.
- [58] B. Holdom et al. Four Statements about the Fourth Generation. *PMC Phys.*, A3:4, 2009, 0904.4698.
- [59] J. Beringer et al. (Particle Data Group). 2012 review of particle physics. *Phys. Rev.*, D86(010001), 2012.
- [60] Yoichiro Nambu and G. Jona-Lasinio. Dynamical model of elementary particles based on an analogy with superconductivity. II. *Phys. Rev.*, 124:246–254, 1961.
- [61] Yoichiro Nambu and G. Jona-Lasinio. Dynamical model of elementary particles based on an analogy with superconductivity. I. *Phys. Rev.*, 122:345–358, 1961.
- [62] Pierre Binetruy. *Supersymmetry: Theory, Experiment, and Cosmology*. Oxford Graduate Series. Oxford University Press, 2006.
- [63] B. Holdom. The discovery of the fourth family at the LHC: What if? *JHEP*, 08:076, 2006, hep-ph/0606146.
- [64] Haim Harari, Herve Haut, and Jacques Weyers. Quark Masses and Cabibbo Angles. *Phys. Lett.*, B78:459, 1978.
- [65] Saleh Sultansoy. Flavor Democracy in Particle Physics. *AIP Conf. Proc.*, 899:49–52, 2007, hep-ph/0610279.
- [66] Amitava Datta. Flavor democracy calls for the fourth generation. *Pramana*, 40:L503–L509, 1993, hep-ph/9207248.

- [67] S. Atag et al. Fourth SM family, breaking of mass democracy, and the CKM mixings. *Phys. Rev. D*, 54(9):5745–5749, Nov 1996.
- [68] A. K. Ciftci, R. Ciftci, and S. Sultansoy. Fourth standard model family neutrino at future linear colliders. *Phys. Rev. D*, 72(5):053006, Sep 2005.
- [69] Michael S. Chanowitz. $Z \rightarrow b\bar{b}$ Decay Asymmetry: Lose-Lose for the Standard Model. *Phys. Rev. Lett.*, 87(23):231802, Nov 2001.
- [70] Enrico Lunghi and Amarjit Soni. Footprints of the Beyond in flavor physics: Possible role of the Top Two Higgs Doublet Model. *JHEP*, 09:053, 2007, 0707.0212.
- [71] Enrico Lunghi and Amarjit Soni. Possible Indications of New Physics in B(d)-mixing and in $\sin(2\beta)$ Determinations. *Phys. Lett.*, B666:162–165, 2008, 0803.4340.
- [72] Amarjit Soni, Ashutosh Kumar Alok, Anjan Giri, Rukmani Mohanta, and Soumitra Nandi. The Fourth family: A Natural explanation for the observed pattern of anomalies in B^- CP asymmetries. *Phys. Lett.*, B683:302–305, 2010, 0807.1971.
- [73] D. Asner et al. Averages of b-hadron, c-hadron, and tau-lepton Properties. 2010, 1010.1589.
- [74] J. Charles et al. CP violation and the CKM matrix: Assessing the impact of the asymmetric B factories. *Eur. Phys. J.*, C41:1–131, 2005, hep-ph/0406184.
- [75] Heavy flavor averaging group (HFAG): <http://www.slac.stanford.edu/xorg/hfag/>.
- [76] M. Bona et al. First Evidence of New Physics in $b \longleftrightarrow s$ Transitions. *PMC Phys.*, A3:6, 2009, 0803.0659.
- [77] Alexander Lenz and Ulrich Nierste. Theoretical update of B(s - anti-B(s) mixing. *JHEP*, 06:072, 2007, hep-ph/0612167.
- [78] T. Aaltonen et al. First Flavor-Tagged Determination of Bounds on Mixing-Induced CP Violation in $B^0 \rightarrow J/\psi\phi$ Decays. *Phys. Rev. Lett.*, 100:161802, 2008, 0712.2397.
- [79] V.M. Abazov et al. Measurement of $B^0 \rightarrow J/\psi\phi$ mixing parameters from the flavor-tagged decay $B^0 \rightarrow J/\psi\phi$. *Phys. Rev. Lett.*, 101:241801, 2008, 0802.2255.
- [80] The four LEP experiments ALEPH, DELPHI, L3 and OPAL. LEP Electroweak Working Group, Status of May 2001.
- [81] Precision electroweak measurements on the Z resonance. *Phys. Rept.*, 427:257–454, 2006, hep-ex/0509008.
- [82] The four LEP experiments ALEPH, DELPHI, L3 and OPAL. LEP Electroweak Working Group, Status of July 2010.
- [83] Michael S. Chanowitz, M.A. Furman, and I. Hinchliffe. Weak Interactions of Ultraheavy Fermions. 2. *Nucl. Phys.*, B153:402, 1979.
- [84] Benjamin W. Lee, C. Quigg, and H. B. Thacker. Weak Interactions at Very High-Energies: The Role of the Higgs Boson Mass. *Phys. Rev.*, D16:1519, 1977.
- [85] Abdelhak Djouadi. The Anatomy of electro-weak symmetry breaking. I: The Higgs boson in the standard model. *Phys. Rept.*, 457:1–216, 2008, hep-ph/0503172.
- [86] Amol Dighe, Diptimoy Ghosh, Rohini M. Godbole, and Arun Prasath. Large mass splittings for fourth generation fermions allowed by LHC Higgs exclusion. *Phys. Rev.*, D85:114035, 2012, 1204.3550.
- [87] Frank Wilczek. Quantum chromodynamics (QCD): The modern theory of the strong interaction. *Ann. Rev. Nucl. Part. Sci.*, 32:177–209, 1982.
- [88] Peter W. Higgs. Broken symmetries, massless particles and gauge fields. *Phys. Lett.*, 12:132–133, 1964.
- [89] Peter W. Higgs. Broken symmetries and the masses of gauge bosons. *Phys. Rev. Lett.*, 13:508–509, 1964.

- [90] F. Englert and R. Brout. Broken symmetry and the mass of gauge vector mesons. *Phys. Rev. Lett.*, 13:321–322, 1964.
- [91] D. Bailin and A. Love. *Introduction to quantum field theory*. Graduate student series in physics. Institute of physics publishing Bristol and Philadelphia, revised edition, 1986.
- [92] L.D. Faddeev and V.N. Popov. Feynman Diagrams for the Yang-Mills Field. *Phys.Lett.*, B25:29–30, 1967.
- [93] Vincent Rivasseau. Lecture notes - advanced quantum field theory. Ecole Normale Supérieure, Paris 75005, France, 2012.
- [94] Vincent Rivasesau. *From perturbative to constructive renormalization*. Princeton Series in Physics, 2nd edition, May 1991.
- [95] F.J. Dyson. Divergence of perturbation theory in quantum electrodynamics. *Phys.Rev.*, 85:631–632, 1952.
- [96] Michael E. Peskin and Daniel V. Schroeder. *An introduction to quantum field theory*. Westview Press Advanced book program, 1995.
- [97] Emmy Noether. Invariant Variation Problems. *Gott. Nachr.*, 1918:235–257, 1918, physics/0503066.
- [98] S. L. Glashow. . PhD thesis, Harvard University, 1958. Ph.D. thesis.
- [99] Chen-Ning Yang and Robert L. Mills. Conservation of Isotopic Spin and Isotopic Gauge Invariance. *Phys.Rev.*, 96:191–195, 1954.
- [100] Georges Aad et al. Observation of a new particle in the search for the Standard Model Higgs boson with the ATLAS detector at the LHC. 2012, 1207.7214.
- [101] Serguei Chatrchyan et al. Observation of a new boson at a mass of 125 GeV with the CMS experiment at the LHC. *Phys.Lett.B*, 2012, 1207.7235.
- [102] Ta-Pei Cheng and Ling-Fong Li. *Gauge theory of elementary particle physics*. Oxford Science Publications. Oxford University Press, 1984.
- [103] Philip W. Anderson. Plasmons, gauge invariance, and mass. *Phys. Rev.*, 130:439–442, 1963.
- [104] P. W. Anderson. Random-phase approximation in the theory of superconductivity. *Phys. Rev.*, 112:1900–1916, 1958.
- [105] Peter W. Higgs. Spontaneous Symmetry Breakdown without Massless Bosons. *Phys. Rev.*, 145:1156–1163, 1966.
- [106] Makoto Kobayashi and Toshihide Maskawa. CP Violation in the Renormalizable Theory of Weak Interaction. *Prog. Theor. Phys.*, 49:652–657, 1973.
- [107] Frederick J. Gilman and Yosef Nir. Quark mixing: The ckm picture. *Ann. Rev. Nucl. Part. Sci.*, 40:213–238, 1990.
- [108] M. L. Mehta. *Random matrices and the statistical theory of energy levels*. Academic Press, 1967.
- [109] Howard Georgi. *Lie algebras in particle physics*. Westview Press Advanced book program, 1999.
- [110] M. Battaglia et al. The CKM matrix and the unitarity triangle. Workshop, CERN, Geneva, Switzerland, 13-16 Feb 2002: Proceedings. 2003, hep-ph/0304132.
- [111] Markus Bobrowski, Alexander Lenz, Johann Riedl, and Jurgen Rohrwild. How much space is left for a new family of fermions? *Phys. Rev.*, D79:113006, 2009, 0902.4883.
- [112] J. Adam et al. New limit on the lepton-flavour violating decay $\mu \rightarrow e \gamma$. 2011, 1107.5547.
- [113] B. Pontecorvo. Mesonium and antimesonium. *Sov. Phys. JETP*, 6:429, 1957.
- [114] B. Pontecorvo. Neutrino experiments and the question of leptonic-charge conservation. *Sov. Phys. JETP*, 26:984–988, 1968.

- [115] Y. Katayama, K. Matumoto, S. Tanaka, and E. Yamada. Possible unified models of elementary particles with two neutrinos. *Prog. Theor. Phys.*, 28:675, 1962.
- [116] Ziro Maki, Masami Nakagawa, and Shoichi Sakata. Remarks on the unified model of elementary particles. *Prog. Theor. Phys.*, 28:870–880, 1962.
- [117] M. C. Gonzalez-Garcia. Global analysis of neutrino data. *Phys. Scripta*, T121:72–77, 2005, hep-ph/0410030.
- [118] Y. Suzuki. Super-Kamiokande: Present and future. *Nucl. Phys. Proc. Suppl.*, 137:5–14, 2004.
- [119] Y. Suzuki. Super-Kamiokande results on neutrino oscillations. *Phys. Scripta*, T121:23–28, 2005.
- [120] K. Eguchi et al. First results from KamLAND: Evidence for reactor anti- neutrino disappearance. *Phys. Rev. Lett.*, 90:021802, 2003, hep-ex/0212021.
- [121] F.P. An et al. Observation of electron-antineutrino disappearance at Daya Bay. *Phys.Rev.Lett.*, 108:171803, 2012, 1203.1669.
- [122] M. H. Ahn et al. Search for electron neutrino appearance in a 250-km long- baseline experiment. *Phys. Rev. Lett.*, 93:051801, 2004, hep-ex/0402017.
- [123] M. H. Ahn et al. Indications of Neutrino Oscillation in a 250 km Long- baseline Experiment. *Phys. Rev. Lett.*, 90:041801, 2003, hep-ex/0212007.
- [124] A. A. Aguilar-Arevalo et al. Event Excess in the MiniBooNE Search for $\bar{\nu}_\mu \rightarrow \bar{\nu}_e$ Oscillations. *Phys. Rev. Lett.*, 105:181801, 2010, 1007.1150.
- [125] Stuart Raby and Richard Slansky. Neutrino Masses - How to add them to the Standard Model. *Los Alamos Science*, (25), 1997.
- [126] Ettore Majorana. Theory of the Symmetry of Electrons and Positrons. *Nuovo Cim.*, 14:171–184, 1937.
- [127] Chung Wook Kim and Aihud Pevsner. *Neutrinos in Physics and Astrophysics*, volume 8. Harwood Academic Publisher, Contemporary Concepts in Physics, 1993.
- [128] Ning Chen and Hong-Jian He. LHC Signatures of Two-Higgs-Doublets with Fourth Family. *JHEP*, 1204:062, 2012, 1202.3072.
- [129] Thomas Schwetz, Mariam Tortola, and J. W. F. Valle. Global neutrino data and recent reactor fluxes: status of three-flavour oscillation parameters. *New J. Phys.*, 13:063004, 2011, 1103.0734.
- [130] B. Holdom. t' at the LHC: The physics of discovery. *JHEP*, 03:063, 2007, hep-ph/0702037.
- [131] A. K. Ciftci, R. Ciftci, and S. Sultansoy. The fourth SM family neutrino at future linear colliders. *Phys. Rev.*, D72:053006, 2005, hep-ph/0505120.
- [132] Graham D. Kribs, Tilman Plehn, Michael Spannowsky, and Timothy M. P. Tait. Four generations and Higgs physics. *Phys. Rev.*, D76:075016, 2007, 0706.3718.
- [133] Michael S. Chanowitz, M. A. Furman, and I. Hinchliffe. Weak Interactions of Ultraheavy Fermions. 2. *Nucl. Phys.*, B153:402, 1979.
- [134] Michael S. Chanowitz, M. A. Furman, and I. Hinchliffe. Weak Interactions of Ultraheavy Fermions. *Phys. Lett.*, B78:285, 1978.
- [135] M. J. G. Veltman. Limit on Mass Differences in the Weinberg Model. *Nucl. Phys.*, B123:89, 1977.
- [136] Michael E. Peskin and Tatsu Takeuchi. A New constraint on a strongly interacting Higgs sector. *Phys. Rev. Lett.*, 65:964–967, 1990.
- [137] Michael E. Peskin and Tatsu Takeuchi. Estimation of oblique electroweak corrections. *Phys. Rev. D*, 46(1):381–409, Jul 1992.
- [138] Johana A. Herrera, Richard H. Benavides, and William A. Ponce. Flavor changing neutral currents with a fourth family of quarks. *Phys. Rev.*, D78:073008, 2008, 0810.3871.

- [139] Michael S. Chanowitz. Higgs Mass Constraints on a Fourth Family: Upper and Lower Limits on CKM Mixing. *Phys. Rev.*, D:035018, 2010, 1007.0043.
- [140] Wei-Shu Hou, Makiko Nagashima, and Andrea Soddu. Enhanced $K(L) \rightarrow \pi^0 \nu \text{ anti-}\nu$ from direct CP violation in $B \rightarrow K \pi$ with four generations. *Phys. Rev.*, D72:115007, 2005, hep-ph/0508237.
- [141] Wei-Shu Hou, Makiko Nagashima, and Andrea Soddu. Large time-dependent CP violation in B/s^0 system and finite $D^0 - \text{anti-}D^0$ mass difference in four generation standard model. *Phys. Rev.*, D76:016004, 2007, hep-ph/0610385.
- [142] Jens Erler and Paul Langacker. Precision Constraints on Extra Fermion Generations. *Phys. Rev. Lett.*, 105:031801, 2010, 1003.3211.
- [143] Wei-Shu Hou and Chien-Yi Ma. Flavor and CP Violation with Fourth Generations Revisited. *Phys. Rev.*, D82:036002, 2010, 1004.2186.
- [144] Ringaile Placakyte. Parton Distribution Functions. 2011, 1111.5452.
- [145] Vernon Barger and Roger Phillips. *Collider Physics*. Addison-Wesley Publishing Company, Frontiers in Physics, 1987.
- [146] X. Ruan and Z. Zhang. Impact on the Higgs Production Cross Section and Decay Branching Fractions of Heavy Quarks and Leptons in a Fourth Generation Model. 2011, 1105.1634.
- [147] T. Aaltonen et al. Combined Tevatron upper limit on $gg \rightarrow H \rightarrow W+W-$ and constraints on the Higgs boson mass in fourth-generation fermion models. *Phys. Rev.*, D82:011102, 2010, 1005.3216.
- [148] T. Cuhadar-Donszelmann, Muge Karagoz, V. E. Ozcan, S. Sultansoy, and G. Unel. Fourth Family Neutrinos and the Higgs Boson. *JHEP*, 10:074, 2008, 0806.4003.
- [149] V. A. Novikov, L. B. Okun, Alexandre N. Rozanov, and M. I. Vysotsky. Mass of the Higgs versus fourth generation masses. *JETP Lett.*, 76:127–130, 2002, hep-ph/0203132.
- [150] Hong-Jian He, Nir Polonsky, and Shu fang Su. Extra families, Higgs spectrum and oblique corrections. *Phys. Rev.*, D64:053004, 2001, hep-ph/0102144.
- [151] David Atwood, Sudhir Kumar Gupta, and Amarjit Soni. Detecting Fourth Generation Quarks at Hadron Colliders. *JHEP*, 1206:105, 2012, 1104.3874.
- [152] O. Cakir, A. Senol, and A. T. Tasci. Single Production of Fourth Family t' Quarks at LHeC. *Europhys. Lett.*, 88:11002, 2009, 0905.4347.
- [153] O. Cakir, H. Duran Yildiz, R. Mehdiyev, and I. Turk Cakir. Single Production of Fourth Family Quarks at the LHC. *Eur. Phys. J.*, C56:537–543, 2008, 0801.0236.
- [154] Mathieu Buchkremer, Jean-Marc Gerard, and Fabio Maltoni. Closing in on a perturbative fourth generation. *JHEP*, 1206:135, 2012, 1204.5403.
- [155] M. Sahin, S. Sultansoy, and S. Turkoz. A Search for the Fourth SM Family: Tevatron still has a Chance. 2010, 1009.5405.
- [156] O. Cakir and V. Cetinkaya. Single Production of Fourth Family b' Quark at the Large Hadron electron Collider. *Mod. Phys. Lett.*, A25:2571–2577, 2010, 0912.2041.
- [157] J. B. Dainton, M. Klein, P. Newman, E. Perez, and F. Willeke. Deep inelastic electron nucleon scattering at the LHC. *JINST*, 1:P10001, 2006, hep-ex/0603016.
- [158] I. T. Cakir, H. Duran Yildiz, O. Cakir, and G. Unel. Anomalous resonant production of the fourth family up type quarks at the LHC. *Phys. Rev.*, D80:095009, 2009, 0908.0123.
- [159] David Cox. Search for a heavy top $t' \Rightarrow Wq$ in top events. 2009, 0910.3279.
- [160] Christian J. Flacco, Daniel Whiteson, and Matthew Kelly. Fourth generation quark mass limits in CKM-element space. 2011, 1101.4976.

- [161] Michael M.H. Luk. Searches For Fourth Generation Quarks With The CMS Detector. 2011, 1110.3246.
- [162] Serguei Chatrchyan et al. Search for heavy, top-like quark pair production in the dilepton final state in pp collisions at $\sqrt{s} = 7$ TeV. 2012, 1203.5410.
- [163] T. Aaltonen et al. Search for New Particles Leading to Z+jets Final States in p anti-p Collisions at $s^{*}(1/2) = 1.96$ -TeV. *Phys. Rev.*, D76:072006, 2007, 0706.3264.
- [164] Georges Aad et al. Search for down-type fourth generation quarks with the ATLAS detector in events with one lepton and hadronically decaying W bosons. *Phys.Rev.Lett.*, 109:032001, 2012, 1202.6540.
- [165] Serguei Chatrchyan et al. Search for heavy bottom-like quarks in 4.9 inverse femtobarns of pp collisions at $\sqrt{s} = 7$ TeV. *JHEP*, 1205:123, 2012, 1204.1088.
- [166] P. Achard et al. Search for heavy neutral and charged leptons in $e^+ e^-$ annihilation at LEP. *Phys. Lett.*, B517:75–85, 2001, hep-ex/0107015.
- [167] S. Sultansoy and G. Unel. ' Silver ' mode for the heavy Higgs search in the presence of a fourth SM family. 2007, 0707.3266.
- [168] R. Ciftci, A. K. Ciftci, E. Receptoglu, and S. Sultansoy. Fourth SM family manifestations at CLIC. *Turk. J. Phys.*, 27:179–186, 2003, hep-ph/0203083.
- [169] Linda M. Carpenter and Arvind Rajaraman. Revisiting Constraints on Fourth Generation Neutrino Masses. *Phys. Rev.*, D82:114019, 2010, 1005.0628.
- [170] O. Cakir and S. Sultansoy. The fourth SM family enhancement to the golden mode at the upgraded Tevatron. *Phys. Rev.*, D65:013009, 2002, hep-ph/0106312.
- [171] Doug Benjamin et al. Combined CDF and D0 upper limits on $gg \rightarrow H W^+ W^-$ and constraints on the Higgs boson mass in fourth-generation fermion models with up to 8.2 fb⁻¹ of data. 2011, 1108.3331.
- [172] M. Baak et al. Updated Status of the Global Electroweak Fit and Constraints on New Physics. 2011, 1107.0975.
- [173] N. Becerici Schmidt, S.A. Cetin, S. Istin, and S. Sultansoy. The Fourth Standart Model Family and the Competition in Standart Model Higgs Boson Search at Tevatron and LHC. *Eur.Phys.J.*, C66:119–126, 2010, 0908.2653.
- [174] Georges Aad et al. Limits on the production of the Standard Model Higgs Boson in pp collisions at $\sqrt{s} = 7$ TeV with the ATLAS detector. 2011, 1106.2748. * Temporary entry *.
- [175] A. Nisati. Higgs searches in ATLAS. *Talk given at the XXV International Symposium on Lepton Photon Interactions at High Energies, Mumbai, India*, 2011.
- [176] Andrey Korytov. Combined results on SM Higgs Search with the CMS Detector. *talk given at EPS 2011, Grenoble*, July 2011.
- [177] S. A. Cetin, T. Cuhadar-Donszelmann, M. Sahin, S. Sultansoy, and G. Unel. Impact of the relatively light fourth family neutrino on the Higgs boson search. 2011, 1108.4071.
- [178] Juste, A. for the ATLAS, CDF, CMS and D0 collaborations. Searches for the Higgs boson. *Plenary talk at DPF, Brown University, Providence*, 2011.
- [179] CMS Collaboration and ATLAS Collaboration. Cern experiments observe particle consistent with long-sought higgs boson. CERN Press Release PR17.12 04.07.2012.
- [180] Updated Combination of CDF and D0 Searches for Standard Model Higgs Boson Production with up to 10.0 fb⁻¹ of Data. 2012, 1207.0449.
- [181] Eric Kuflik, Yosef Nir, and Tomer Volansky. Implications of Higgs Searches on the Four Generation Standard Model. 2012, 1204.1975.
- [182] Abdelhak Djouadi and Alexander Lenz. Sealing the fate of a fourth generation of fermions. 2012, 1204.1252.

- [183] Otto Eberhardt, Alexander Lenz, Andreas Menzel, Ulrich Nierste, and Martin Wiebusch. Status of the fourth fermion generation before ICHEP2012: Higgs data and electroweak precision observables. 2012, 1207.0438.
- [184] Otto Eberhardt, Geoffrey Herbert, Heiko Lacker, Alexander Lenz, Andreas Menzel, et al. Impact of a Higgs boson at a mass of 126 GeV on the standard model with three and four fermion generations. 2012, 1209.1101.
- [185] G.C. Branco, P.M. Ferreira, L. Lavoura, M.N. Rebelo, Marc Sher, et al. Theory and phenomenology of two-Higgs-doublet models. *Phys.Rept.*, 516:1–102, 2012, 1106.0034.
- [186] Leo Bellantoni, Jens Erler, Jonathan J. Heckman, and Enrique Ramirez-Homs. Masses of a Fourth Generation with Two Higgs Doublets. 2012, 1205.5580.
- [187] Michael Geller, Shaouly Bar-Shalom, and Gad Eilam. The Need for New Search Strategies for Fourth Generation Quarks at the LHC. 2012, 1205.0575.
- [188] Shaouly Bar-Shalom, Soumitra Nandi, and Amarjit Soni. Two Higgs doublets with 4th generation fermions - models for TeV-scale compositeness. *Phys.Rev.*, D84:053009, 2011, 1105.6095.
- [189] Konstantin Matchev. TASI lectures on precision electroweak physics. pages 51–98, 2004, hep-ph/0402031.
- [190] F. Mandl and G. Shaw. *Quantum field theory*. John Wiley & Sons, The Atrium, Southern Gate, Chichester, West Sussex PO 19 8SQ, England, revised edition edition, 2005.
- [191] E. Leader and E. Predazzi. *An introduction to gauge theories and modern particle physics*, volume 1 of *Cambridge monographs on particle physics, nuclear physics and cosmology 3*. Cambridge University Press, 1996.
- [192] J. Goldstone. Field Theories with Superconductor Solutions. *Nuovo Cim.*, 19:154–164, 1961.
- [193] Jeffrey Goldstone, Abdus Salam, and Steven Weinberg. Broken Symmetries. *Phys. Rev.*, 127:965–970, 1962.
- [194] Pierre Binetruy. Lecture notes - Théories de jauge des interactions électrofaibles. Lectures given at the Ecole normale supérieure (Paris 75005, France), academic year 2011-2012.
- [195] J. J. Sakurai. *Modern Quantum Mechanics*. Addison-Wesley Publishing Company, revised edition, 1994.
- [196] ALEPH Collaboration et al. Precision Electroweak Measurements and Constraints on the Standard Model. 2010, 1012.2367.
- [197] M. E. Peskin, B W. Lynn, and R. G. Stuart. *in Physics at LEP, LEP Jamboree, CERN Report No. CERN-96-02*, 1986.
- [198] Dallas C. Kennedy. Renormalization of electroweak gauge interactions. Invited lectures given at 1991 Theoretical Advanced Studies Inst., Boulder, CO, Jun 2-28, 1991.
- [199] D. C. Kennedy and B. W. Lynn. Electroweak Radiative Corrections with an Effective Lagrangian: Four Fermion Processes. *Nucl. Phys.*, B322:1, 1989.
- [200] M. Kuroda, G. Moulataka, and D. Schildknecht. Direct one loop renormalization of SU(2)-L x U(1)-Y four fermion processes and running coupling constants. *Nucl. Phys.*, B350:25–72, 1991.